Journal of

CLINICAL PHYSIOLOGY and PATHOLOGY

2023 | Vol 2 | N 4 ISSN 2989-1116

Journal of International Society for Clinical Physiology & Pathology

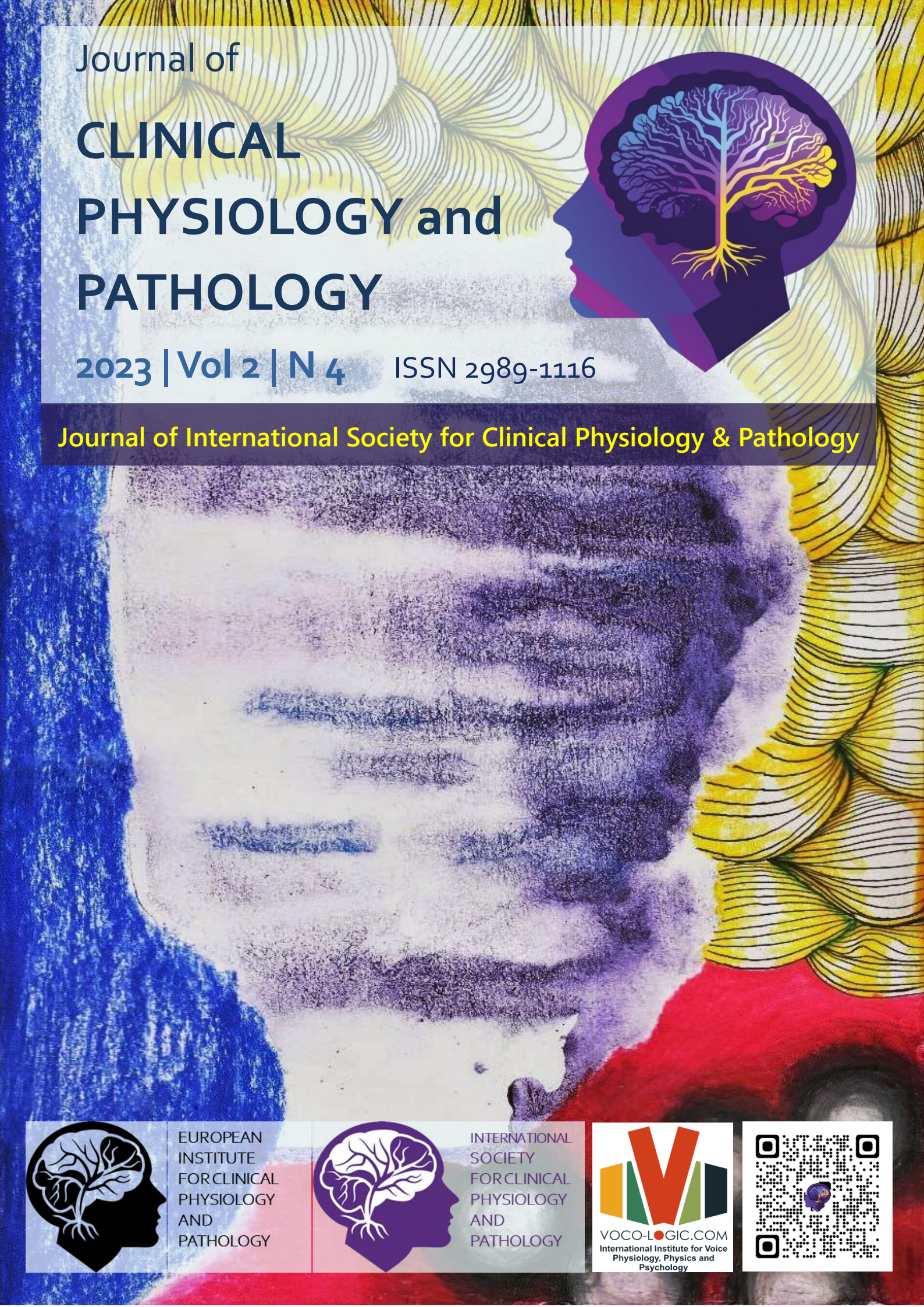

EUROPEAN INSTITUTE FOR CLINICAL PHYSIOLOGY AND PATHOLOGY

INTERNATIONAL SOCIETY FOR CLINICAL PHYSIOLOGY AND PATHOLOGY

VOCO-LOGIC.COM
International Institute for Voice Physiology, Physics and Psychology

Journal of CLINICAL PHYSIOLOGY and PATHOLOGY

2023 | Vol 2 | N 4 ISSN 2989-1116 (Online)

Journal of International Society for Clinical Physiology & Pathology

Medical & biological reviewed journal

The authors declare that they have no competing interests

Published materials conforms to internationally accepted ethical guidelines. Articles are checked in the "Anti-Plagiarism" system for the detection of borrowings.

Editor in chief: **Igor Kastyro** PhD, DSc, Professor,

Editorial staff managers: **Stepan Shilin, Nikita Kuznetsov, Adel Glukhova**

Founder and Publisher: **International Society for Clinical Physiology & Pathology**

ISSN 2989-1116 = Journal of Clinical Physiology and Pathology (Online)

COBISS.CG-ID 25476356

Website of ISCPP: https://iscpp.eu/

Website of JISCPP: https://journal.iscpp.eu/

Editor office address: 85347 Norveska, 5, Igalo, Herceg Novi, Montenegro

E-mail: journal@iscpp.eu

Contents

Article

Morphofunctional changes in brain and peripheral blood in aged Wistar rats due to AlCl3 exposure

Alexandra Sentyabreva[1,3*], Ekaterina Miroshnichenko[1,3], Ivan Tsvetkov[2], Anna Kosyreva[1,4]

[1] The laboratory of neuromorphology, Avtsyn Research Institute of Human Morphology of "Petrovsky National Research Centre of Surgery", Moscow, Russia;
[2] The laboratory of immunomorphology of inflammation, Avtsyn Research Institute of Human Morphology of "Petrovsky National Research Centre of Surgery", Moscow, Russia;
[3] The laboratory of cell technologies and tissue engineering, Research Institute of Molecular and Cellular Medicine, Peoples' Friendship University of Russia, Moscow, Russia;
[4] The laboratory of molecular pathophysiology, Research Institute of Molecular and Cellular Medicine, Peoples' Friendship University of Russia, Moscow, Russia;
* Correspondence:alexandraasentyabreva@gmail.com;
alexandraasentyabreva@gmail.com, https://orcid.org/0000-0001-5064-219x (A.S.);
katerinamir10011@gmail.com, https://orcid.org/0000-0002-0020-958X (E.M.);
davedm66@gmail.com, https://orcid.org/0000-0003-0946-1105 (I.Ts.);
kosyreva.a@list.ru, https://orcid.org/0000-0002-6182-1799 (A.K.).

Abstract: The purpose of the study: To examine morphofunctional changes of brain and peripheral blood in aged Wistar rats to observe adaptive reactions as a response on AlCl3 exposure.
Methods: The work was performed on male Wistar rats, 24 months of age. Animals consumed a solution of AlCl3 100 mg/kg per day for 60 days. Morphological changes of neurons and microglia, mRNA expression levels of pro- and anti-inflammatory cytokines, microglia activation markers, amyloid-related and hypoxia-related proteins, as well as monocyte and lymphocyte subpopulations in peripheral blood, were examined.
Results: AlCl3-treated old rats showed the increasing of hyperchromic neurons in 2 out of 3 examined regions of the hippocampus; morphological features of microglia cells' dystrophy; the upregulation of pro-inflammatory cytokine Il-18 and the downregulation of anti-inflammatory cytokine Il-10, as well as App, Bace1, and Hif-1a; the decreasing of percentage of B-cells, general CD3+ lymphocyte population, including CD4+ T-helpers and CD8+ cytotoxic cells, but the increasing of CD4+/CD8+ ratio in peripheral blood.
Conclusion: AlCl3-treated aged rats demonstrated systemic maladaptation to AlCl3 impact. Unlike adult rodents, aged ones have the background of inflammaging, as well as elderly people. The exposure of AlCl3 could potentially be a replacement of integral cellular and molecular processes accompanying age-related diseases, presenting in most elderly people, as an enhancer of inflammaging and hypoxia. These conditions make this model of neurodegeneration a reliable one to explore the initial mechanisms of such detrimental process, as well as prove aged rats more suitable subjects to perform future researches in this field.

Keywords: aging, inflammaging, neuroinflammation, neurodegeneration, cellular senescence, age-related diseases, animal models, Alzheimer's disease.

Citation: Sentyabreva A., Miroshnichenko E., Tsvetkov I., Kosyreva A. Morphofunctional changes in brain and peripheral blood in aged Wistar rats due to AlCl3 exposure. Journal of Clinical Physiology and Pathology (JISCPP) 2023; 2 (4): 4-13.

https://doi.org/10.59315/JISCPP.2023-2-4.4-13

Academic Editor: Igor Kastyro

Received: 02.10.23
Revised: 06.11.23
Accepted: 01.12.23
Published: 29.12.23

Publisher's Note: International Society for Clinical Physiology and Pathology (ISCPP) stays neutral with regard to jurisdictional claims in published maps and institutional affiliations.

1. Introduction

The stable growing of world's population as well as average lifespan, especially in developed countries, leads to the increasing of age-related diseases' incidence and prevalence, including ones leading to dementia. It is the most prevalent cause of disability globally [1] and its most common cause is neurodegenerative diseases such as Alzheimer's disease (AD). There were more than 55 million patients with dementia worldwide in 2019 [1], and this number will triple in next 30 years. It is a great burden for not only patients, their families, and healthcare workers. It also demands an annual global cost of just over 1 trillion USD on treatment and social support [1]. Among other reasons, this amount of costs is due the absence of any effective treatment for dementia. Existing and approved drugs can only faintly and briefly slow down the symptoms.

The development of new effective treatment approaches is hampered by insufficient data concerning the initial mechanisms of AD pathogenesis. Recent studies showed that it is quite complex process not limited by amyloid deposits alone [2], [3], and 3rd part clinical trial of Lecanemab, an amyloid-antibody based drug, showed questionable efficacy [4]. The role of inflammaging, or chronic age-related low-grade systemic inflammation is one of the most perspective and intensively studying hypotheses of neurodegeneration's initiation so far. It represents a manifestation of senescence-associated secretory phenotype (SASP), which is expressed by senescent cells of aged organisms [5]. Inflammaging is one of risk factors of other age-related diseases development

as well, including advanced stage of atherosclerosis, type 2 diabetes mellitus, metabolic syndrome, etc. At the same time, these very pathological conditions as well some others, like major depressive disorder [6], may contribute in enhancing of its pro-inflammatory background.

Sporadic form of AD, also known as late onset AD (LOAD), begins to manifest with mild cognitive impairment in people of age >60-65 years [7] and belongs to the group of age-related pathologies. However, its modeling is still being conducted mostly on adult rodents, and lots of studies are performed on various lines of transgenic mice, which pathological processes do not exactly correspond with ones leading to neurodegeneration on humans. Among vast variations of AD animal models there are one based on exposure of aluminum compounds. Al3+ ions are capable of increasing the production of reactive oxygen species (ROS). They involve in mitochondrial and DNA damage as well as promoting of pro-inflammatory mediators production and hypoxic condition establishing [8], [9]. All these events are typical for aging as well, which means that experiments on old animals can provide more relevant data due to the cellular senescence presence. Hence, the purpose of this work was to study morphofunctional changes in brain and peripheral blood in aged Wistar rats to observe their adaptive reactions on AlCl3 exposure.

2. Materials and Methods

2.1. Animals and neurodegeneration modelling

The work was performed on aged male Wistar rats 24 months old (n=20). Animals were divided randomly on 2 groups, 10 animals each. Animals were kept in plastic cages (60 x 38 x 18.5 cm) in social groups of 5 animals each with free access to food and water. The temperature in the vivarium room was maintained within 18-22°C, and air humidity was 50-65%. The study was approved by the Bioethical Commission of the Avtsyn Research Institute of Human Morphology of "Petrovsky National Research Centre of Surgery" (Protocol №36 (12) March 28, 2022). All experimental work involving animals was carried out according to directive 2010/63/EU of the European Parliament and of the Council of the EU on the protection of animals used for scientific purposes (Strasbourg, September 22, 2010).

Rats of the experimental group consumed aluminum chloride (AlCl3) in dosage of 100 mg/kg per day for 60 days with drinking water, as described before [10]. Animals of the control group consumed regular drinking water.

2.2. Samples obtaining and histological prepaprations

On the 61st day of the experiment, samples of peripheral blood were obtained under Zoletil (Vibrac Sante Animale) anaesthesia, then animals were euthanized by overdose (15 mg/kg) of Zoletil. The whole brains were fixed in 10% buffered formalin (BioVitrum, Russia) for 24 hours, then dissected at the level of 6.0 mm posterior relative to bregma (each sample of 5 mm thick) [11]. After that, the specimens were dehydrated with ethanol of ascending concentration, cleared with xylene, infiltrated with a histological wax, and embedded in paraffin blocks for further slicing (5 μm thick).

2.3. Morphological study

For morphological study, histological sections of brains were stained according to Nissl's method. The absolute number of neurons in the standard area of the visual field (25000 μm2) and the relative number of hyperchromic and morphologically altered neurons were evaluated on these sections in zones CA1, CA3, and the dentate gyrus of the hippocampus. The pictures were captured with the Leica microscope (DM 2500 Leica Microsystems) on magnification x400.

2.4. Immunohistochemical study

For ICH-P study, frontal histological sections of brains (6.0 mm posterior relative to bregma) were prepared as previously described [9]. Then they were stained with rabbit primary antibodies Iba1 (1:100; P4C288Ra01, Cloud Clone) and secondary HRP Donkey-anti-Rabbit antibody (1:500; 416035, Novex Life Technologies) with additional hematoxylin staining. The pictures were captured with the Leica microscope (DM 2500 Leica Microsystems) on magnification x1600.

2.5. qPCR-RT study

The expression mRNA was assayed by real-time qPCR in tissue fragments of the prefrontal cortex, preserved in IntactRNA solution (Eurogen, Russia) and stored on -20C until studied. The performed analysis included the detection and evaluation of expression levels of pro-inflammatory cytokines (Il-6, Il-18, and Tnf-a), anti-inflammatory cytokines (Il-10 and Tgf-b), microglia M1 (iNos) and M2 (Cd163+) activation markers, amyloid-related proteins (App and Bace1) and hy-

poxia marker Hif-1a. The levels of all aforementioned mRNA expression relative to GAPDH expression level as a reference were determined using a qPCRmix-HS SYBR (Eurogen, Russia) containing fluorescent intercalating dye SYBR Green I. Amplification with detection and digital analysis of fluorescence in real time was carried out on DT-96 Real-Time PCR Cycler (DNA-Technology JSC, Moscow, Russia) in a standard mode at 95°C for 5 minutes followed by 95°C for 15 seconds, 62°C for 10 seconds + reading and 72°C for 20 seconds ×45.

Table 1. Used primers' sequences (all picked up by on-line soft Primer-BLAST precisely for rat specie).

Primer	Forward sequence	Reverse sequence
GAPDH	GCGAGATCCCGCTAACATCA	CCCTTCCACGATGCCAAAGT
IL-18	GACAAAAGAAACCCGCCTG	ACATCCTTCCATCCTTCACAG
TNF-a	CCACCACGCTCTTCTGTCTA	GCTACGGGCTTGTCACTCG
IL-10	GCCCAGAAATCAAGGAGCAT	TGAGTGTCACGTAGGCTTCTA
TGF-β	CCGCAACAACGCAATCTATG	AGCCCTGTATTCCGTCTCCTT
iNOS	CGCTGGTTTGAAACTTCTCAG	GGCAAGCCATGTCTGTGAC
CD163	TCTTGTGGACTCTGAAGCGA	TCTTAAATGCCAACCCGAGG
APP	TGGATGATCTCCAACCGTG	CGTCGACAGGCTCAACTTC
BACE1	GGGCAGTAGTAATTTTGCAGT	TTCGGAGGTCTCGGTATGT
HIF-1a	TCACAGTCGGACAACCTCAC	TGCTGCAGTAACGTTCCAATTC

2.6. Flow cytometry

The relative numbers of lymphocytes various subpopulations and monocyte were counted using flow cytometry (Beckman Coulter, USA) in peripheral blood. The following antibodies (eBioscience, USA) were used for immune phenotypic analysis: anti-rat CD3-PE for total T-lymphocyte population, anti-rat CD4-FITC for CD3+CD4+ T-helpers, anti-rat CD8-PE-Cy5 for CD3+CD8+ for T-cytotoxic cells, anti-rat CD45R-FITC for CD45R+ B-cells, and anti-rat CD43-PE for CD43+ monocyte. Erythrocytes were lysed with the OptiLyse C solution (eBioscience, USA).

2.7. Statistical analysis.

The results were analyzed by Statistica 8.0 software (StatSoft, Inc.). The normality of data distribution was checked by using the Kolmogorov-Smirnov test. The Mann-Whitney test was used to establish the reliability of differences between groups by median. With $p<0.05$, it was considered as statistically significant.

3. Results

3.1. The percentage of altered hyperchromic neurons

The absolute numbers of neurons in zones CA1, CA3 and the dentate gyrus of the hippocampus were almost the same in both groups, whereas the relative numbers of altered hyperchromic neurons differed significantly. Rats that consumed AlCl3 have shown 2.1-fold number of hyperchromic neurons in CA3 hippocampal zone and 1.7-fold one in the dentate gyrus compared with control group animals (Fig. 1a,b).

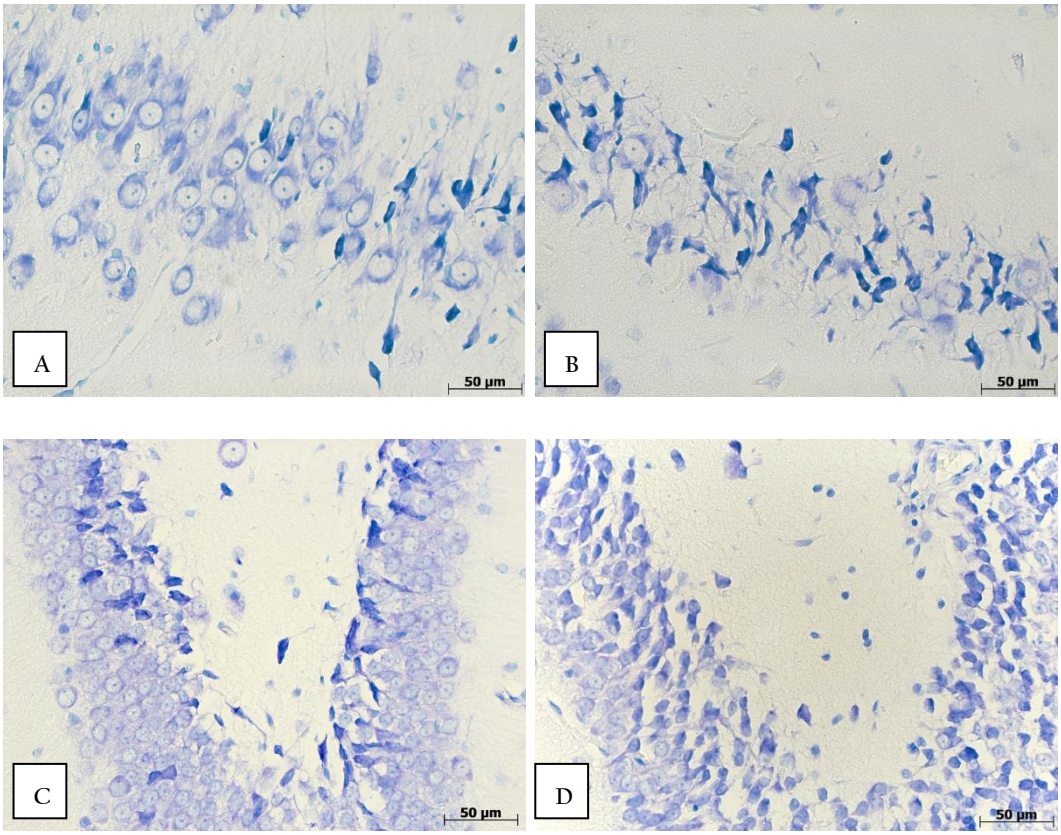

Figure 1a. CA3 zone(A, B) and the dentate gyrus (C, D) of the hippocampus in rats of control (A, C) and experimental (B, D) groups. Nissl's staining, x400.

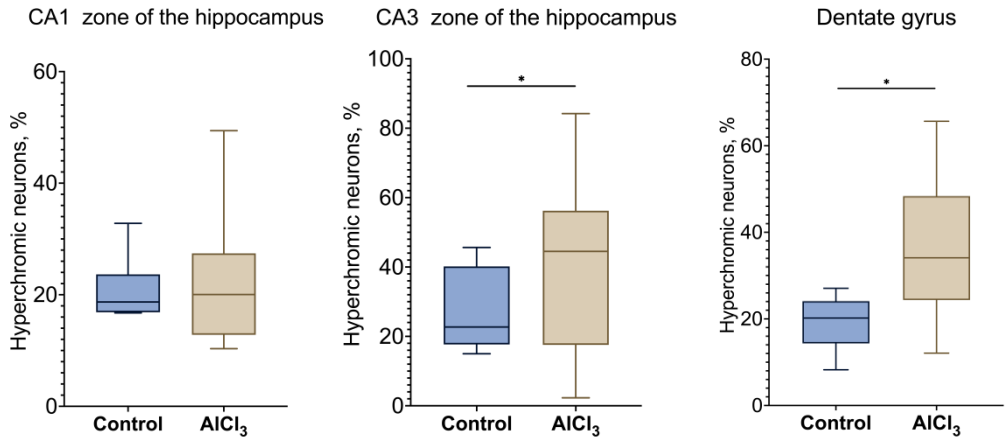

Figure 1b. The percentage of hyperchromic neurons in zones CA1, CA3, and the dentate gyrus of the hippocampus in rats of control and experimental groups.
The data displayed as: line – median, box – 25-75 quartiles, whiskers – non-outlier range;
* - $p<0.05$. The Mann-Whitney test comparisons.

3.2. Morphological features of microglia

Identified by ICH staining with anti-Iba1 antibody, in rats of control group microglia cells had an increased size (›30 µm with a reference of 15-30 µm) and spheroidal swelling, hypertrophic, beaded, and tortuous processes. At the same time, there were microglia of an increased size concurrently with beaded, tortuous, and fragmented, but not thickened processes in group of AlCl3-consumed rats (Fig. 2).

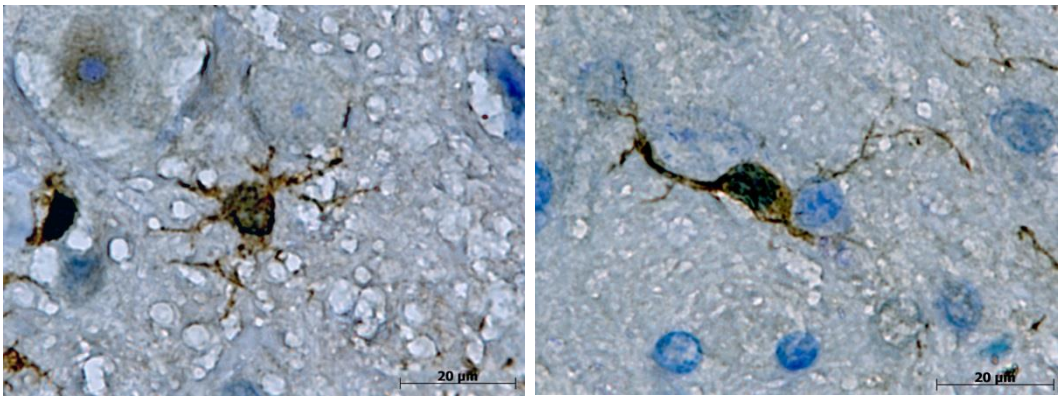

Figure 2. Morphological characteristics of microglia cells with thin and short processes in both Adult-C (A) and Adult-AlCl3 (B) groups, enlarged microglia with spheroidal swelling, hypertrophic, beaded, and tortuous processes in Old-C rats (C), and microglia of an increased size with beaded, tortuous, and fragmented, but not thickened processes in Old-AlCl3 rats (D). Iba-1 antibody + HRP secondary antibody IHC and hematoxylin staining, x1600.

3.3. qPCR-RT examination of the prefrontal cortex

The result of qPCR-RT of prefrontal cortex tissue fragments demonstrated the statistically significant difference between groups due to Il-18 expression level – it was in 2.8 times less in experimental group rats than in control ones. However, no reliable distinctions were detected in pro-inflammatory cytokine Tnf-α expression levels, as well as in anti-inflammatory Tgf-β ones (Fig. 3). The expression of anti-inflammatory cytokine Il-10 was not detected at all.

The levels of expression of M1 activated microglia marker iNos and M2 activated microglia marker Cd163 were also similar in both groups despite the statistically insignificant tendencies of upregulation of iNos expression and downregulation of Cd163+ one in rats of experimental groups relative to control rodents (Fig. 3).

At the same time, amyloid precursor protein (App) expression was 1.8 times less in rats of experimental group than in control one. Like App, Beta-site APP-cleaving enzyme 1 (Bace1) expression changed in similar way and was downregulated in 2.4 times in rats consumed AlCl3 compared with control group animals. Also, hypoxia-inducible factor 1-alpha (Hif-1a), which displays a presence of a hypoxic condition always appearing alongside inflammation, was downregulated in 4.2 times in experimental group animals in comparison with control ones (Fig. 3.).

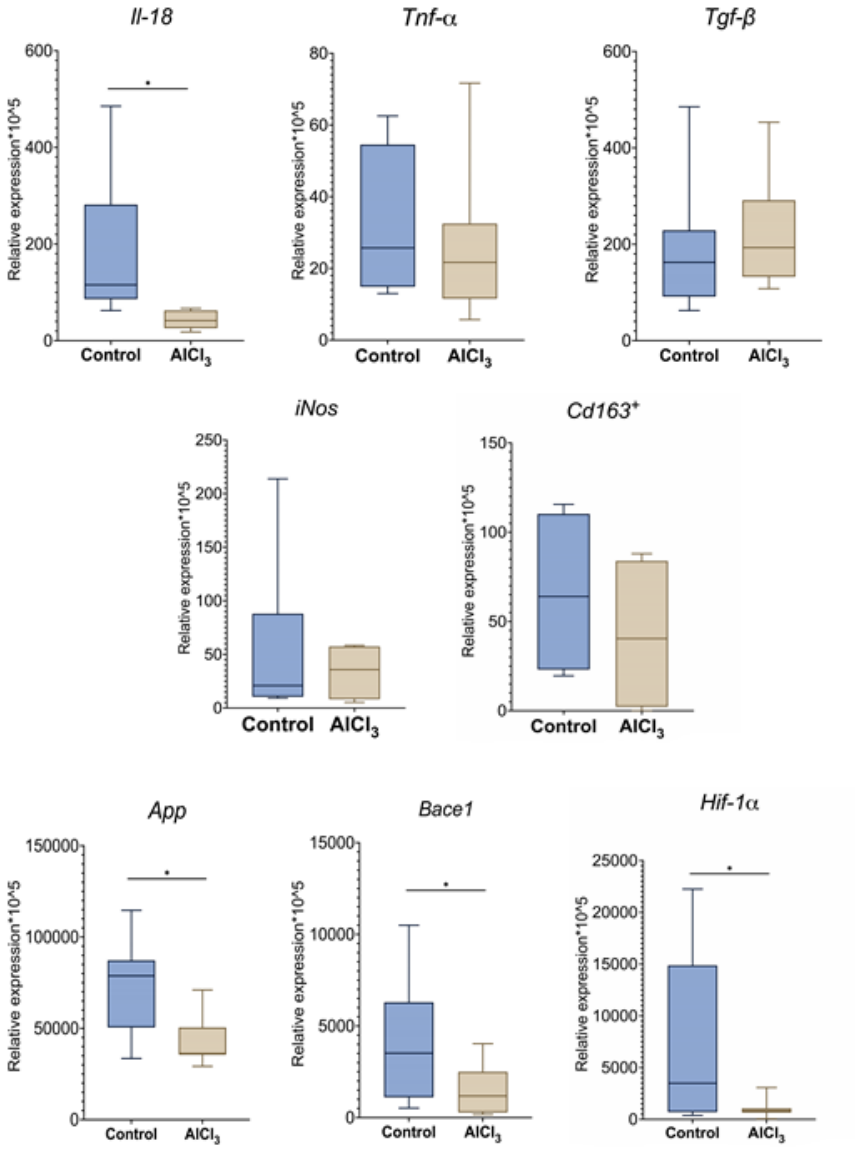

Figure 3. mRNA expression levels of pro-inflammatory cytokines Il-18 and Tnf-α and anti-inflammatory cytokine Tgf-β, microglia activation markers iNos (M1) and Cd163+ (M2), App, Bace1, and Hif-1a in the prefrontal cortex in rats of control and experimental groups.

The data displayed as: line – median, box – 25-75 quartiles, whiskers – non-outlier range;

* - $p<0.05$. The Mann-Whitney test comparisons.

3.4. Flow cytometry immune phenotypic analysis

The immune phenotypic analysis of lymphocyte subpopulations and monocyte was performed to estimate the impact of AlCl3 on the relative numbers of various immune cells in peripheral blood. Flow cytometry data demonstrated statistically significant differences in the percentage of general CD3+ lymphocyte population as well as CD45R+ B-cells, but not CD43+ monocyte between the observed groups. As for lymphocyte subpopulations, both CD3+CD4+ T-helpers and CD3+CD8+ T-cytotoxic cells decreased in AlCl3-treated rats comparing with control ones, whereas CD4+/CD8+ ratio displayed that the proportion of CD4+ T lymphocyte increased in experimental group rats (Fig. 4).

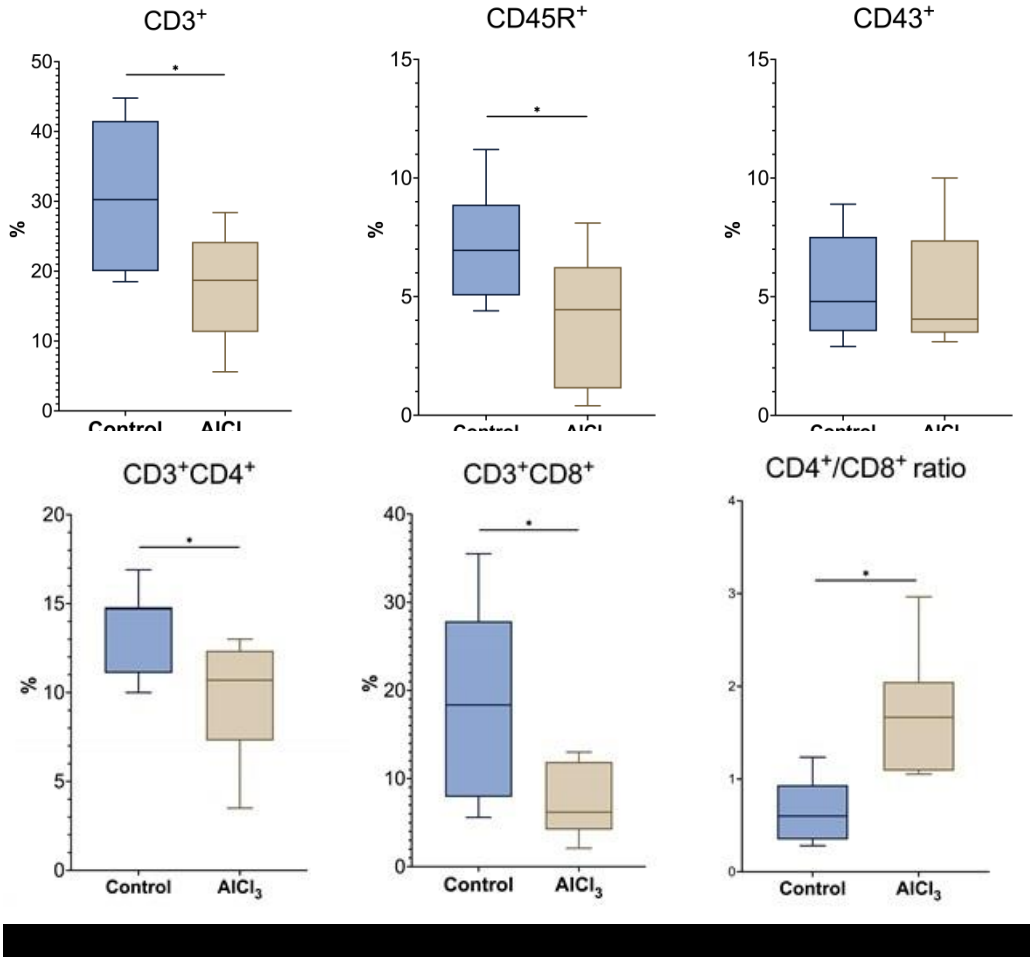

Figure 4. The percentage of general CD3+ T-lymphocyte population, CD45R+ B-cells, and CD43+ monocyte, CD3+CD4+ T-helpers, CD3+CD8+ T-cytotoxic cells, and CD4+/CD8+ ratio in peripheral blood in rats of control and experimental groups.

The data displayed as: line – median, box – 25-75 quartiles, whiskers – non-outlier range;

* - $p<0.05$. The Mann-Whitney test comparisons.

4. Discussion

The main hallmark of aging is cellular senescence manifesting in the increasing number of SASP-expressed cells. According to our data [15], aged Wistar rats of control group displayed it the same way as it appeared in humans [5]. It makes aged rats a more reliable subject to perform neurodegeneration modelling due to the presence of pro-inflammatory background of inflammaging, which is absent in adult rodents, including transgenic ones. AlCl3-based models of AD are described widely in literature, including 100 mg/kg dosage giving orally [10], [12], [13], [14], and all these researches were conducted on adult rats and mice. In our previous study, we determined several pivotal morphofunctional distinctions in microglia and immune cells of peripheral blood between groups of adult and old Wistar rats without any external exposure [15]. Now the purpose was to determine and evaluate the response of old rodents on AlCl3.

We detected a notable increasing of the relative number of hyperchromic neurons in CA3 zone and the dentate gyrus of the hippocampus in aged AlCl3-treated rats relative to control ones. We counted mostly morphologically altered neurons of more intense dying, as well as lesser size and polygonal shape, shrunken, and wrinkled. Apparently, neurons with such morphological alterations have ceased to function due to their extinction of interaction with other ones [16], [17]. The reason of more pronounced neuronal damage observed in CA3 zone and the dentate gyrus in comparison with CA1 zone could be probably explained by their different susceptibility to hypoxia. CA1 neurons are presumably more vulnerable to hypoxia and oxygen-glucose deprivation than CA3 and DG [18] probably due to their higher activity [19]. CA1 zone's prime function is the maintaining of short-term memories, whereas CA3 is mostly involved in establishing of spatial and

contextual memory [18]. The data concerning the tolerance to hypoxia changing with aging are controversial, although it might increase in advanced age as a result of adaptation processes [20]. However, in case of this particular study, AlCl3 more likely had a direct toxic impact on neurons throughout mitochondrial damage rather than aggravating hypoxic condition.

Unlike aged rats of control group, microglia cells displayed signs of dystrophy in old AlCl3-treated rats instead of activation and/or hypertrophy features. Similar findings were described by Shahidehpour et al. in elder humans, precisely patients with neurodegenerative diseases [21]. Highly likely, it is evidence of their maladaptation due to AlCl3 harmful impact and self-maintaining resources critical shortage in the same way as it occurred in neurons. Such cells are no longer capable of producing enough amounts of export proteins, which are vital for proper functioning, such as immune surveillance and synapse clearance.

The data from experiments conducted on adult AlCl3-treated rats demonstrated upregulation of pro-inflammatory mediator Tnf-a [22], [23] It was also detected in healthy aged rats in comparison with healthy adult ones, whereas the expression level of anti-inflammatory cytokine Tgf-β did the opposite [15]. Meanwhile, we observed no differences in the expression levels of Tnf-α and Tgf-β, as well as in ones of M1 microglia activation marker iNos and M2 microglia activation marker Cd163+ between experimental and control groups. It could probably be explained by dystrophic state of microglia cells, which are both reached the upregulation limits and unable to adapt to malevolent environmental conditions any longer. At the same time, the pronounced downregulation of Il-18 might be caused by neuronal hibernation and death, since they are another source of this mediator [24], [25].

Our data confirms that App and Bace1 expression levels and, therefore, these proteins' subsequent biosynthesis decreased greatly in AlCl3-treated rats relative to control group. It probably displays the advanced stage of neurodegenerative detrimental processes, when neurons are no longer capable of producing APP to form new synapses or maintain deteriorating ones. Therefore, BACE1, which is an enzyme involved in its metabolism, is no longer needed either.

Currently, the data concerning the variability of Hif-1a during the ontogenesis and its impact on age-related genes expression are scarce and controversial. It probably depends on individual hypoxia tolerance and could be both up- or downregulated with aging [20]. However, significant downregulation of Hif-1a in AlCl3-treated rats compared with control ones is likely caused by dystrophy and death of neuron and glial cells as a result of maladaptation to AlCl3 toxic effect.

We observed a statistically significant decline of general CD3+T-lymphocyte population including CD3+CD4+ T-helpers and CD3+CD8+ T-cytotoxic cells in AlCl3-treated rats comparing with control ones. Previously, no difference in there percentage was determined in Wistar rats due to aging alone [15], whereas Zhuang et al. observed its decrease under AlCl3 exposure [26]. However, previous reports [8],[26], [27] observed a decline of CD4+/CD8+ ratio as well, while our data displayed that the proportion of CD4+ T-helpers were higher in AlCl3-treated rats relative to control group. Such discrepance propably might have occured because our experiment was performed on aged rats, whilst previous ones were conducted on adult rodents. Hence, differences in T-lymphocyte population's reactions could vary greatly with aging, but future investigations are warranted.

Unlike relative number of CD3+T-lymphocyte, the decrease of CD45R+ B-cells and CD43+ monocyte percentage was detected in aged humans and rats relative to adult ones [15], [28], [29]. The cause of CD45R+ B-lymphocyte percentage was abated is probably the same as in case of general CD3+T-lymphocyte population, and it is the direct toxic effect of AlCl3. As for CD43+ monocyte, they probably might as express higher resistance to AlCl3 impact; at the same time, they could also decrease both their percentage in peripheral blood and the rate of tissue migration due to inauspicious conditions caused by AlCl3.

5. Conclusions

In regard with all reported data, AlCl3-treated aged rats demonstrated systemic maladaptation to external exposure of AlCl3. With its capability of oxidative stress enhancing, AlCl3 leads to progressive shortage of cell resources and subsequent decline of their functions, already compromised by cellular senescence itself. Unlike adult rodents, aged ones have the background of inflammaging, as elderly people do. Besides, most elderly people have some non-inflectional chronic diseases including age-related ones, such as atherosclerosis, obesity, type 2 diabetes mellitus, etc., whereas rodents do not have them. The exposure of AlCl3 could potentially be a replacement of integral cellular and molecular processes accompanying these diseases as an enhancer of inflammaging and hypoxia. These conditions make this model of neurodegeneration a reliable one to explore the initial mechanisms of such detrimental process, as well as prove aged rats more suitable subjects to perform future researches in this field.

Author Contributions: Conceptualization A.S. and A.K.; methodology, A.K.; software, A.S., E.M. and I.T.; validation, A.S., E.M. and A.K.; formal analysis, A.S. and A.K.; investigation, A.S., E.M., I.T. and A.K.; resources, A.K.; data curation, A.S., E.M. and A.K.; writing—original draft preparation, A.S. and A.K.; writing—review

and editing, A.S., E.M., I.T. and A.K.; visualization, A.S. and I.T.; supervision, A.K.; project administration, A.K. All authors have read and agreed to the published version of the manuscript.

Funding: Number of state registration of research, development, and technological work for civil purposes—122030200530-6.

Institutional Review Board Statement: The study was conducted according to the guidelines of the Declaration of Helsinki and approved by Avtsyn Research Institute of Human Morphology of "Petrovsky National Research Centre of Surgery" (Protocol 36 (12) March 28, 2022).

Informed Consent Statement: Not applicable.

Conflicts of Interest: The authors declare no conflict of interest.

References

1. WHO. "Dementia". https://www.who.int/news-room/fact-sheets/detail/dementia, 2023.
2. Streit WJ, Braak H, Del Tredici K, Leyh J, Lier J, Khoshbouei H, Eisenlöffel C, Müller W, Bechmann I.. Microglial activation occurs late during preclinical Alzheimer's disease. Glia. 2018;66(12):2550-2562.
3. Streit WJ, Khoshbouei H, Bechmann I. The Role of Microglia in Sporadic Alzheimer's Disease. Journal of Alzheimer's Disease. 2021;79(3):961-968.
4. van Dyck CH, Swanson CJ, Aisen P, Bateman RJ, Chen C, Gee M, Kanekiyo M, Li D, Reyderman L, Cohen S, Froelich L, Katayama S, Sabbagh M, Vellas B, Watson D, Dhadda S, Irizarry M, Kramer LD, Iwatsubo T. Lecanemab in Early Alzheimer's Disease. The New England Journal of Medicine. 2023;388(1):9-21.
5. Franceschi C, Campisi J. Chronic inflammation (inflammaging) and its potential contribution to age-associated diseasesThe Journals of Gerontology Series A. Biological Sciences and Medical Sciences.2014;69(1):4-9.
6. Dafsari FS, Jessen F. Depression-an underrecognized target for prevention of dementia in Alzheimer's disease. Translational Psychiatry.2020;10(1):160
7. Alzheimer's Association. Alzheimer's Disease Facts and Figures. Alzheimer's & Dementia Journal. 2018;14(3):367-429.
8. Hesamian MS, Eskandari N. Potential Role of Trace Elements (Al, Cu, Zn, and Se) in Multiple Sclerosis Physiopathology. Neuroimmunomodulation. 2020;27(4):163-177.
9. Willhite CC, Karyakina NA, Yokel RA, Yenugadhati N, Wisniewski TM, Arnold IM, Momoli F, Krewski D. Systematic Review of Potential Health Risks Posed by Pharmaceutical, Occupational and Consumer Exposures to Metallic and Nanoscale Aluminum, Aluminum Oxides, Aluminum Hydroxide and Its Soluble Salts. Critical Reviews in Toxicology. 2014:44(4) 1-80.
10. Firdaus Z, Kumar D, Singh SK, Singh TD. Centella asiatica Alleviates AlCl3-induced Cognitive Impairment, Oxidative Stress, and Neurodegeneration by Modulating Cholinergic Activity and Oxidative Burden in Rat Brain. Biological Trace Element Research. 2022;200(12):5115-5126.
11. Paxinos G, Watson C. The Rat Brain in Stereotaxic Coordinates. JBBS Elsevier Science.2013;11(9).
12. Liu YQ, Xin TR, Liang JJ, Wang WM, Zhang YY. Memory Performance, Brain Excitatory Amino Acid and Acetylcholinesterase Activity of Chronically Aluminum Exposed Mice in Response to Soy Isoflavones Treatment. Phytotherapy Research. 2010;24(10):1451-1456.
13. Thirunavukkarasu SV, Venkataraman S, Raja S, Upadhyay L. Neuroprotective effect of Manasamitra vatakam against aluminium induced cognitive impairment and oxidative damage in the cortex and hippocampus of rat brain. Drug and Chemical Toxicology.2012;35(1):104-115.
14. Jangra A, Kasbe P, Pandey SN, Dwivedi S, Gurjar SS, Kwatra M, Mishra M, Venu AK, Sulakhiya K, Gogoi R, Sarma N, Bezbaruah BK, Lahkar M. Hesperidin and Silibinin Ameliorate Aluminum-Induced Neurotoxicity: Modulation of Antioxidants and Inflammatory Cytokines Level in Mice Hippocampus. Biological Trace Element Research. 2015;168(2):462-471.
15. Sentyabreva AV, Miroshnichenko EA, Melnikova EA, Tsvetkov IS, Kosyreva AM. Morphofunctional changes of microglia in adult and old Wistar rats. Medical Immunology (Russia). 2023;25(3):527-532.
16. Zimatkin, SM, Bon' EI. Dark Neurons of the Brain. Neuroscience and Behavioral Physiology. 2018;48(8):908-912.
17. Korzhevskii DE. Neurodegeneration and Assessment of the Response of Nerve Cells to Damage In Molecular neuromorphology. (monograph). Special Lit. 2015.
18. Lana D, Ugolini F, Giovannini MG. An Overview on the Differential Interplay Among Neurons-Astrocytes-Microglia in CA1 and CA3 Hippocampus in Hypoxia/Ischemia. Frontiers in Cellular Neuroscience. 2020; 14:585833.
19. Mizuseki K, Royer S, Diba K, Buzsáki G. Activity Dynamics and Behavioral Correlates of Ca3 and Ca1 Hippocampal Pyramidal Neurons. Hippocampus. 2012:22(8):1659-1680.
20. Dzhalilova DS, Makarova OV. The Role of Hypoxia-Inducible Factor in the Mechanisms of Aging. Biochemistry (Mosc). 2022;87(9):995-1014.
21. Shahidehpour RK, Higdon RE, Crawford NG, Neltner JH, Ighodaro ET, Patel E, Price D, Nelson PT, Bachstetter AD. Dystrophic microglia are associated with neurodegenerative disease and not healthy aging in the human brain. Neurobiology of Aging. 2021; 99:19-27.
22. Jangra A, Kasbe P, Pandey SN, Dwivedi S, Gurjar SS, Kwatra M, Mishra M, Venu AK, Sulakhiya K, Gogoi R, Sarma N, Bezbaruah BK, Lahkar M. Hesperidin and Silibinin Ameliorate Aluminum-Induced Neurotoxicity: Modulation of Antioxidants and Inflammatory Cytokines Level in Mice Hippocampus. Biological Trace Element Research. 2015;168(2):462-471.
23. Nafea M, Elharoun M, Abd-Alhaseeb MM, Helmy MW. Leflunomide abrogates neuroinflammatory changes in a rat model of Alzheimer's disease: the role of TNF-α/NF-κB/IL-1β axis inhibition. Naunyn-Schmiedeberg's Archives of Pharmacology. 2023;396(3):485-498.
24. Ojala JO, Sutinen EM. The Role of Interleukin-18, Oxidative Stress and Metabolic Syndrome in Alzheimer's Disease. Journal of Clinical Medicine. 2017;6(5):55.
25. Lecca D, Jung YJ, Scerba MT, et al. Role of chronic neuroinflammation in neuroplasticity and cognitive function: A hypothesis. Alzheimer's & Dementia Journal. 2022;18(11):2327-2340.
26. Zhuang C, She Y, Zhang H, Song M, Han Y, Li Y, Zhu Y. Cytoprotective effect of deferiprone against aluminum chloride-induced oxidative stress and apoptosis in lymphocytes. Toxicology Letters. 2018; 285:132-138.
27. Zhuang C, She Y, Zhang H, Song M, Han Y, Li Y, Zhu Y. Suppressive effects of aluminum trichloride on the T lymphocyte immune function of rats. Food and Chemical Toxicology. 2012;50(3-4):532-535.

28. Dowery R, Benhamou D, Benchetrit E, Harel O, Nevelsky A, Zisman-Rozen S, Braun-Moscovici Y, Balbir-Gurman A, Avivi I, Shechter A, Berdnik D, Wyss-Coray T, Melamed D. Peripheral B cells repress B-cell regeneration in aging through a TNF-α/IGFBP-1/IGF-1 immune-endocrine axis. Blood. 2021;138(19):1817-1829.
29. Snodgrass RG, Jiang X, Stephensen CB. Monocyte subsets display age-dependent alterations at fasting and undergo non-age-dependent changes following consumption of a meal. Immunity & Ageing. 2022;19(1):41.

Article

Immediate and long-term results of Lichtenstein hernia repair

Mariia Navid [1,*], Andrej Protasov [1], Ilgar Guseinov [1], Ilya Kurikhin [1]

[1] RUDN University, Moscow, Russia;
* Correspondence: navid_mn@pfur.ru.
navid_mn@pfur.ru, https://orcid.org/0000-0003-1790-1158 (M.N);
andrei.protasov@bk.ru, https://orcid.org/0000-0001-5439-9262 (A.P);
i.i.guseynov@gmail.com, https://orcid.org/0000-0002-1290-3640 (I.G);
ilja.kurihin@gmail.com, https://orcid.org/0000-0001-9359-2620 (I.K.).

Abstract: More than 20 million inguinal hernioplasties are performed annually worldwide by various methods [1]. The Lichtenstein operation recommended by the European Society of Herniologists as the "gold standard" in open inguinal hernia treatment, despite its leading position in the world, has a number of disadvantages. According to the studies of some surgeons, the introduction of implants has a correlation with the development of local wound complications and chronic pain syndrome in the postoperative period. And the percentage of recurrences after Lichtenstein hernioplasty ranges from 0.8 to 8% [2]. Some authors have noted an increased frequency of pain syndrome when using the ligature method of fixation of mesh implants. Their frequency ranges from 7 to 12% [3,4]. However, the issue of fixation is still controversial [5,6,7].
Aim of the study: to compare the results of Lichtenstein inguinal hernioplasty using self-fixing implants and implants requiring ligature fixation.

Keywords: inguinal hernioplasty, Progrip, fixation-free hernioplasty, Lichtenstein procedure, self-fixing implant.

Citation: Navid M, Protasov A, Guseinov I, Kurikhin I. Immediate and long-term results of Lichtenstein hernia repair. Journal of Clinical Physiology and Pathology (JISCPP) 2023; 2 (4): 14-16.

https://doi.org/10.59315/JISCPP.2023-2-4.14-16

Academic Editor: Igor Kastyro

Received: 10.10.23
Revised: 03.11.23
Accepted: 14.12.23
Published: 29.12.23

Publisher's Note: International Society for Clinical Physiology and Pathology (ISCPP) stays neutral with regard to jurisdictional claims in published maps and institutional affiliations.

1. Materials and Methods

The immediate results of 626 inguinal hernioplasty according to Lichtenstein were analyzed (510 - in the group with the ligature method of polypropylene implant fixation, 116 - with the self-fixing Parietene Progrip). The mean age of patients in the groups was 56.4±0.95 years. The proportion of patients with bilateral localization of inguinal hernias was 40.4% in the first group and 42.2% in the second group. All hernias were primary in nature. To assess the nature and size of the hernia, we used the classification recommended by the European Hernia Society (EHS) for inguinal hernias. L-type hernias were detected in 307 patients (60,2%) in the first group and in 51 (44,0%) in the second; M-type hernias accounted for 203 patients (39,8%) and 65 patients (56,0%) respectively (fig.1).

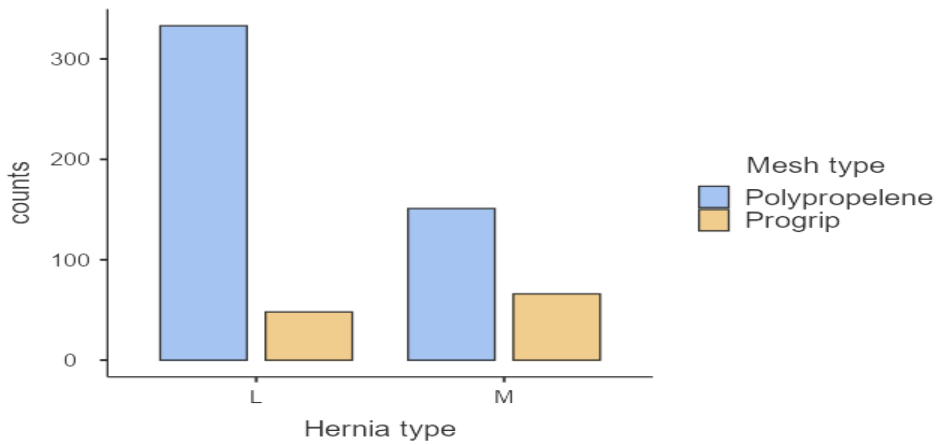

Figure 1. Distribution of patients by type of hernia (EHS).

We evaluated the time of surgical intervention, intraoperative complications in groups, early postoperative complications, presence of pain syndrome, foreign body sensation, and timing of analgesic administration as an indirect sign of the duration of postoperative pain. In 64 out of 100 patients, the long-term results were analyzed by assessing the quality of life according to the EuraHS Qol questionnaire.

2. Results

We observed a significant decrease in the mean operation time in the group with the use of Progrip self-fixing mesh, the latter amounting to 45.0 minutes. While fixation of polypropylene mesh lengthened the operation time by an average of 20.9 minutes. (45.0±1.49 sd=16.0 vs. 65.9±0.653 sd=14.7; p<0.01). We were able to indirectly estimate the duration of pain syndrome in the postoperative period in the groups based on the duration of analgesic intake (fig.2).

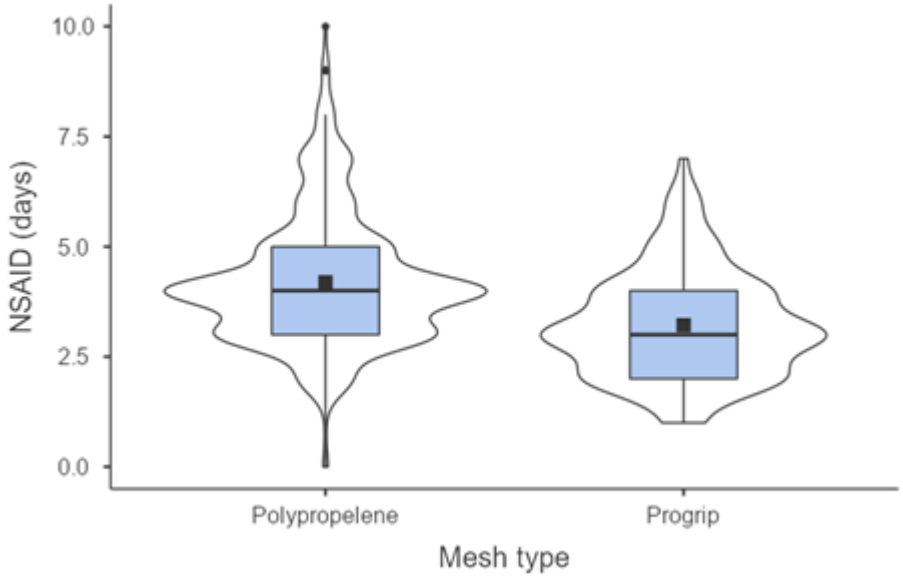

Figure 2. The duration of non-steroidal anti-inflammatory drugs in groups.

In the first group the average duration of non-steroidal anti-inflammatory drugs was 4.19 days, in the second group - 3.22 days (4.19±0.065 vs 3.22±0.113 U=17679 p<0.0001 (Mann-Whitney test)) – Table 1

Table 1. Average rates of NSAID use in comparison groups.

	Group	N	Mean	Median	SD	SE
NSAID (days)	Polypro-pelene	510	4.19	4.00	1.46	0.0647
	Progrip	116	3.22	3.00	1.21	0.113

In the early postoperative period, we observed 171 (27.3%) local complications. The wound complications in both groups were dominated by soft tissue hematomas and seromas: 85 (13.6%) and 36 (5.8%), respectively. Overall, after evaluating inflammatory wound complications in both groups, we also obtained no significant differences ($\chi 2$=1.01, df=1, p=0.314). Analyzing the long-term results of treatment, we also found no statistically significant differences in the comparison groups for all quality of life indicators of the EHS questionnaire (p=0.543).

However, after hernioplasty using polypropylene implant with ligature fixation in the long-term follow-up period (up to a year) there was a tendency to increase the quality of life due to the decrease in the severity of pain syndrome and increase in the activity of patients. Recurrence of the disease was noted in 6 patients (1.2%) in the group with polypropylene implant fixation. No recurrences were found among the examined patients after fixation-free hernioplasty. There was no statistically significant difference in the comparison groups by this indicator.

3. Conclusions

The observed results in the Parietene Progrip group had no statistically significant differences with the group where suture fixation of polypropylene implant was used in the context of the incidence of wound complications, disease recurrence and quality of life in long-term follow-up (P>0,05). However, the use of self-fixing implants has notable advantages associated with a reduction in operative time ($p<0.01$), pain severity ($p<0.01$), and the timing of analgesic administration in the early postoperative period (4.19±0.065 vs 3.22±0.113 U=17679 $p<0.0001$).

Application of artificial intelligence:

The article is written without the use of artificial intelligence technologies.

Acknowledgments.

Support for this study was provided by the university of RUDN.

Conflicts of Interest: The authors declare no conflict of interest.

References

1. Zezarahova MD. CHOOSING A RATIONAL WAY TO TREAT INGUINAL HERNIAS IN PATIENTS WITH RISK FACTORS. Kuban State Medical Institute. 2007;21 (in Russian).
2. Prudnikova EA, Alibegov RA. Inguinal hernias: modern plastic surgery methods. Bulletin of the Smolensk Medical Academy.2010;4:104-108.
3. Vizgalov SA, Smotrin SM. Inguinal hernias: modern aspects of etiopathogenesis and treatment. Journal of Grodno State Medical University. 2010; 4:17-22.
4. Starling, JR. Mesh Inguinodynia After Inguinal Herniorrhaphy. Abdominal Wall Hernias. 2001; 734–736.
5. Mazin JB. Post-Operative Inguinodynia from Hernia Surgery. Practical pain management. 2010; 10(3).
6. Bullen NL, Hajibandeh S, Hajibandeh S, Smart NJ, Antoniou SA. Suture fixation versus self-gripping mesh for open inguinal hernia repair: a systematic review with meta-analysis and trial sequential analysis. Surgical Endoscopy. 2021;35(6):2480-2492.
7. Honeypalsinh H. M. Comparison of progrip mesh v/s conventional mesh in lichtenstein's inguinal hernia repair. International Journal of Biomedical Research 2016; 7(10):738-742.

Lecture

The use of eTEP hernioplasty in the treatment of ventral hernias

Ilya Kurikhin[1,*], Dmitrii Titarov[1]

[1] RUDN University, Moscow, Russia;
* Correspondence: kurikhin_iv@pfur.ru
kurikhin_iv@pfur.ru, https://orcid.org/0000-0001-9359-2620 (I. K.);
titarov_dl@pfur.ru, https://orcid.org/0000-0002-3608-9209 (D. T.)

Abstract: This article is devoted to one of the methods of treatment of ventral hernias, namely eTEP hernioplasty (Enhanced-view Totally Extraperitoneal Technique). The purpose of the work is a comprehensive review of the surgical technology, comparison of technologies proposed by various authors and highlighting the features of the endoscopic anatomy of the anterior abdominal wall and of the surgical techniques. After that we collected data on the long-term results from these authors, and based on them concluded that all the presented techniques were acceptable and safety. However, to date, in our opinion, insufficient attention has been paid to two aspects of this operation, namely fixation of the prosthesis and drainage of the retromuscular space. It is also worth noting that the issue of specific endoscopic anatomy of the anterior abdominal wall in the aspect of surgical treatment of ventral hernias is discussed by a small number of authors, while the same anatomical landmarks may have different names. In this work, we have combined all the best practices and suggestions from the authors of publications on this topic. This work was presented at 1st Congress of International Society for Clinical Physiology and Pathology (ISCPP 2023).

Keywords: ventral hernia, surgery, extended totally extraperitoneal, hernioplasty, laparoscopy, long-term outcomes

Citation: Kurikhin I., Titarov D. The use of eTEP hernioplasty in the treatment of ventral hernias. Journal of Clinical Physiology and Pathology (JISCPP) 2023; 2 (4): 17-21.

https://doi.org/10.59315/JISCPP.2023-2-4.17-21

Academic Editor: Igor Kastyro

Received: 09.10.23
Revised: 16.11.23
Accepted: 20.12.23
Published: 29.12.23

1. Introduction

Surgery of the anterolateral abdominal wall hernias has undergone revolutionary changes from plastic surgery with local tissue to minimally invasive laparoscopic and extraperitoneal treatment methods using mesh implants.

We consider eTEP hernioplasty (Enhanced-view Totally Extraperitoneal Technique) to be one of the promising methods for treating ventral hernia. The eTEP hernioplasty method was proposed less than 15 years ago and during this time has already been introduced in medical institutions in many countries around the world. The essence of the operation is dissection of the retromuscular space and augmentation of the anterior abdominal wall by suturing the hernia defect and installing a mesh implant retromuscularly.

2. Patients and Methods

We aimed to conduct an analysis that could help improve the results of eTEP hernioplasty in the treatment of ventral hernias by identifying the most effective surgical techniques for performing the operation.

The first work with a detailed description of eTEP-hernioplasty technique of a ventral hernia was written by I. Belyansky, who published impressive results of performing eTEP-hernioplasty of a ventral hernia according to Rives-Stoppa with posterior separation according to Y. Novitsky in 2016 on the example of three patients with complex ventral hernias with numerous large fascial defects and deformations of the abdominal wall, which necessitated access through the abdominal cavity. In 2018, he was also the first to publish a paper describing the technique for performing the eTEP Rives-Stoppa procedure with direct access to the retromuscular space.

3. Results

The author's publications highlight several technical points that must be observed for the best result [3, 4]:

1. To facilitate dissection in the retrorectal space laterally towards the linea semilunaris, the free edge of the posterior layer of the rectus sheath is retracted medially using atraumatic clamps.

2. During dissection of the retromuscular space, it is necessary to visualize the deep inferior epigastric artery, which runs along the posterior caudal aspect of the rectus abdominis muscle.

3. The neurovascular bundles that pass between the internal oblique and transverse muscles, and then perforate the rectus abdominis muscle (usually 5-6 pieces on each side), are an anatomical landmark, because are located at the lateral edge of the rectus muscle, and therefore are the lateral border of dissection. They must be preserved to prevent disfunction and atrophy of the rectus abdominis muscle. During insufflation, previously horizontally oriented vessels are pulled upward, which is why this landmark was called the "lamp post sign" in the study by Ramana [16].

4. When suturing the anterior layer of the rectus abdominis sheath - if there is a large so-called "dead" space in the subcutaneous tissue - after reduction of the hernial sac, incisions are made in the dermis to create skin folds, and this prevents postoperative deformation and the formation of seroma.

The authors describing their experience in treating a ventral hernia using this technology are unanimous in the issue of the patient's position on the operating table, as well as in the adoption of anatomical landmarks for installing ports and lateral boundaries of dissection, with the exception of Kumar [6], who presented a modification of the operation in 2021 using 3 ports instead of 4, but subsequently the technology for performing the operation remains without fundamental changes relative to the one proposed by Belyansky.

Ramana [16] in his work described the above-mentioned "lamppost sign" and a number of other important anatomical landmarks:

1. "Volcano sign" - after performing a crossover during treatment of the hernial sac, the latter, due to insufflation into the retromuscular space, takes on the appearance described in the work as "edges of a volcano"; we propose the translation "slopes of a volcano". During preperitoneal dissection between the posterior layers of the rectus abdominis muscle sheaths, the hernial contents are compared to magma, and the overall picture looks like a volcanic eruption.

2. "Mercedes-Benz sign" - a diagram of the relationship between the vas deferens, lower epigastric and gonadal vessels in the preperitoneal tissue of the groin area; the same as the "inverted Y" in the work of Furtado [5] in relation to the surgical treatment of inguinal hernias;

3. "Frenulum sign" - this is how the connection of the upper edges of the posterior layer of the rectus sheath with the xiphoid process is described; these "frenulum" must be crossed to completely unite the two retromuscular spaces when the hernia is localized M1 and M2 in order to avoid recurrence of the hernia in this area.

Table 1. Summary data on the results of eTEP hernioplasty by various authors.

Author	Number of patients	Observation period, month	Average area of hernia defect, cm2	S of mesh, cm2	Length of operation, minutes	Length of stay, days	Complications
Andreuccetti J, 2021	19	24	21	380	171	3,9	1 seroma 1 early adhesive intestinal obstruction
Baig SJ, 2019	21	2	45,33	25x20 eTEP RS 30x30 eTAR	176	-	1 seroma 1 divergence of the anterior sheath 1 hernia recurrence 1 chronic pain syndrome
Belyansky I, 2018	37	1	-	-	198	1	2 seromas 1 adhesive intestinal obstruction (1 month)
Burdakov VA, 2019	150	12	-	502,8	109,2	4,6	1 aneurysm of MCA upture 2 retromuscular haematoma 3 seromas with symptoms 4 chronic pain syndromes
Köhler G, 2019	31	8	34,5 (3.6–64)	420 (144–600)	128 (81–221)	3	1 conversion (peritoneal injury) 1 surgical site infection 1 eventration with strangulation of the small intestine

Kopteev NR, 2022	58	24	51,0±63,5	468±212	156±63,6	4,03	in the preperitoneal tissue (reoperation, 5 days after operation) 4 seromas 1 retromuscular haematoma
Lu R, 2019 (lap-eRS)	120	6	5,5	526.3±294.7	120,4	1	4 seromas (3 subcutaneous, 1 retromuscular), 1 incompetence of the suture of the posterior sheath of the rectus abdominis muscle (IPOM, 10 day after operation) 1 intestinal obstruction (resection of bowel, 26 day after operation)
Lu R, 2019 (robo-eRS)	86	6	7,1	507.5 ± 178.6	174,7	1	2 hernia recurrence 4 retromuscular seromas 3 haematoma 1 hernia recurrence
Mitura K, 2023	11	7	38.5 (16.5–96.0)	486 (280–590)	204 (158–295)	3.4	2 seromas 1 haematoma 1 early adhesive intestinal obstruction
Morrell A, 2020	74	8	5,6 см (width!)	456.5 (150–630)	174.4 (66–301)	1,5	10 seromas 4 haemaoma 1 surgical site infection 4 seromas with symptoms
Orlov BB, 2022	202	1	-	-	180	5	1 hernia recurrence 1 retromuscular haemotamponade 1 subcutaneous haematoma 1 small bowel perforation
Penchev D, 2019	27	1	71.4±47.1	428.4±220.6	186±62	2,9	none
Prakhar G, 2020	171	6	51.35	397.56±208.83	176.75±62.42	2.18	7 paralytic ileus 5 surgical site infection 3 hernia recurrence
Radu VG, 2020	60	15	99.5 (6-375)	28x17	140-290	-	4 conversion 1 seroma 2 chronic pain syndrome
Rajkiran K, 2019	24	6	to 7 см (width!)	15x15 or 30x30	169,8	2,16	none
Salido Fernandez S, 2020	40	10	100	400±199	126±36	1	1 early adhesive intestinal obstruction 1 small bowel perforation 1 hernia recurrence 2 incompetence of the suture of the posterior sheath of the rectus abdominis muscle
Sanna A, 2019	18	1	43.31	267.47±84.94	125.64±27.21	2.7	1 subcutaneous haematoma 2 seromas with symptoms

4. Discussion

Most authors [1, 8, 11, 12, 15, 17] agree that initial insufflation is carried out to a pressure of 12 mmHg, with the exception of Belyansky [3, 4] and Morrell [10], who recommend 15 mmHg.

Also, most authors note the convenience of reducing pressure in the cavity when tightening the suture at the stage of suturing the anterior leaf of the rectus sheath, although specific values may differ: Radu [13, 14] recommends reducing it to 5-6 mm Hg, while Morrell [10] advises stopping at 8-10 mmHg.

Opinions differ most regarding the issue of fixation of the mesh prosthesis. We, like a number of specialists - Lu [7], Mitura [8], Penchev [11] - prefer not to use any fixing devices. However, a number of authors use both the placement of the mesh without fixation and with its fixation. Axial sutures can be used, as in Kumar [6], or suturing the implant at the corners, as recommended by Prakhar [12]; the use of tackers at specific points is also mentioned - for example, by Rajkiran [15]; and fixation of the mesh with fibrin glue by Baig [2]. In the work of Sanna [17], a lightweight large-pored polypropylene mesh was secured with 8 ml of fibrin glue and additionally in the area of the pubic bone with tackers. Andreuccetti et al. [1] used in different cases both fixation with glue or staples, and placement of mesh without fixation.

Most authors drain the intervention area situationally, leaving this issue to the discretion of the operating surgeon. Possible criteria for the advisability of leaving drainage are described - for example, Prakhar [12] recommends draining the intervention area if a relatively large space has been separated or diffuse bleeding is noted. Mitura [9], Mitevski [8] and Lu [7], on the contrary, in all cases left suction drains, the drain was removed after 1-2 days. However, some authors systematically refuse to install drains - for example, Baig [2], Kumar [6] adhere to this tactic. In all cases, an abdominal bandage is fastened on the operating table, and this is considered sufficient to prevent the formation of seroma and hematoma..

5. Conclusions

Evaluating the information obtained from the analyzed sources, we came to the following conclusions:

1. eTEP hernioplasty is being performed for ventral hernias more and more often and has results comparable in effectiveness and safety to other popular methods of minimally invasive hernioplasty.

2. The issue of specific endoscopic anatomy of the anterior abdominal wall in the aspect of surgical treatment of ventral hernias is discussed by a small number of authors, while the same anatomical landmarks may have different names.

3. There is no clear opinion on the issue of fixation of the prosthesis and drainage of the retromuscular space; more statistical data is required to form a consensus.

Application of artificial intelligence:

The article is written without the use of artificial intelligence technologies.

Author Contributions: Conceptualization, formal analysis, investigation, writing—original draft preparation, I.K..; writing—review and editing, supervision, project administration, D.T.

All authors have read and agreed to the published version of the manuscript.

Informed Consent Statement: Informed consent was obtained from all subjects involved in the study.

Conflicts of Interest: The authors declare no conflict of interest.

References

1. Andreuccetti J, Sartori A, Lauro E, Crepaz L, Sanna S, Pignata G, Bracale U, Di Leo A. Extended totally extraperitoneal Rives-Stoppa (eTEP-RS) technique for ventral hernia: initial experience of The Wall Hernia Group and a surgical technique update. Updates in Surgery. 2021;73(5):1955-1961
2. Baig SJ, Priya P. Extended totally extraperitoneal repair (eTEP) for ventral hernias: Short-term results from a single centre. Journal of Minimal Access Surgery. 2019;15(3):198-203.
3. Belyansky I, Reza Zahiri H, Sanford Z, Weltz AS, Park A. Early operative outcomes of endoscopic (eTEP access) robotic-assisted retromuscular abdominal wall hernia repair. Hernia. 2018;22(5):837-847.
4. Belyansky I, Zahiri HR, Park A. Laparoscopic Transversus Abdominis Release, a Novel Minimally Invasive Approach to Complex Abdominal Wall Reconstruction. Surgical Innovation. 2016;23(2):134-41.
5. Furtado M, Claus CMP, Cavazzola LT, Malcher F, Bakonyi-Neto A, Saad-Hossne R. SYSTEMIZATION OF LAPAROSCOPIC INGUINAL HERNIA REPAIR (TAPP) BASED ON A NEW ANATOMICAL CONCEPT: INVERTED Y AND FIVE TRIANGLES. Arquivos Brasileiros de Cirurgia Digestiva : ABCD.2019;32(1):1426.

6. Kumar A, Taggarsi M, Subhash RC. A Novel Minimally Invasive Retro Rectus Repair of Ventral Hernia: Comparing Kumar-Subhash's modified eTEP technique with Laparoscopic Intraperitoneal Onlay Mesh Hernioplasty. The Physician. 2021; 7(1), 1-11.
7. Lu R, Addo A, Ewart Z, Broda A, Parlacoski S, Zahiri HR, Belyansky I. Comparative review of outcomes: laparoscopic and robotic enhanced-view totally extraperitoneal (eTEP) access retrorectus repairs. Surgical Endoscopy. 2020 ;34(8):3597-3605.
8. Mitevski A, Markov P. eTep-retromuscular Repair for Ventral Hernia; a Technique Closest to Ideal. Lietuvos chirurgija.2020; 29;19(3-4):151-5
9. Mitura K, Rzewuska A, Skolimowska-Rzewuska M, Romańczuk M, Kisielewski K, Wyrzykowska D. Laparoscopic enhanced-view totally extraperitoneal Rives-Stoppa repair (eTEP-RS) for ventral and incisional hernias - early operative outcomes and technical remarks on a novel retromuscular approach. Videosurgery and other Miniinvasive Techniques. 2020;15(4):533-545.
10. Morrell ALG, Morrell AC, Cavazzola LT, Pereira GSS, Mendes JM, Abdalla RZ, Garcia RB, Costa TN, Morrell-Junior AC, Malcher F. Robotic assisted eTEP ventral hernia repair: Brazilian early experience. Hernia. 2021;25(3):765-774.
11. Penchev D, Kotashev G, Mutafchiyski V. Endoscopic enhanced-view totally extraperitoneal retromuscular approach for ventral hernia repair. Surgical Endoscopy. 2019;33(11):3749-3756.
12. Prakhar G, Parthasarathi R, Cumar B, Subbaiah R, Nalankilli VP, Praveen Raj P, Palanivelu C. Extended View: Totally Extra Peritoneal (e-TEP) Approach for Ventral and Incisional Hernia-Early results from a single center. Surgical Endoscopy. 2021;35(5):2005-2013.
13. Radu VG, Lica M. The endoscopic retromuscular repair of ventral hernia: the eTEP technique and early results. Hernia. 2019;23(5):945-955.
14. Radu VG. Retromuscular Approach in Ventral Hernia Repair - Endoscopic Rives-Stoppa Procedure. Chirurgia (Bucur). 2019;114(1):109-114.
15. Rajkiran K Deshpande, Sumit Talwar. A novel laparoscopic approach: (e-TEP) technique in ventral abdominal hernia-our experience. International Journal of Surgery. 2019;3(4):22-25.
16. Ramana B, Arora E, Belyansky I. Signs and landmarks in eTEP Rives-Stoppa repair of ventral hernias. Hernia. 2021;25(2):545-550.
17. Sanna A, Felicioni L, Cecconi C, Cola R. Retromuscular Mesh Repair Using Extended Totally Extraperitoneal Repair Minimal Access: Early Outcomes of an Evolving Technique-A Single Institution ExperienceJournal of Laparoendoscopic & Advanced Surgical Techniques and Videoscopy. 2020;30(3):246-250.

Article

Functional and hormone changes in ice hockey players using Cytoflavin

Victoria Zaborova [1,2,*], Vladislav Kurshev [1], Kira Kryuchkova [1]

[1] Institute of Clinical Medicine, Sechenov First Moscow State Medical University, Moscow, Russia;
[2] Laboratory of Sports Adaptology, Moscow Institute of Physics and Technology (National Research University), Dolgoprudny, Russia;
* Correspondence: zaborova_v_a@staff.sechenov.ru;

Abstract: The purpose of the study was to assess the effect of 35-day Cytoflavin consumption on hormonal status, blood lactate level and functional parameters in elite ice hockey players. Material and methods: the study included 60 male professional hockey players (aged 19 to 36 years) divided into two groups of 30 subjects. Group I underwent a course of metabolic therapy with the use of succinic acid (Cytoflavin) for 35 days. Group II whose pharmacological support included only "basic" sports nutrition did not include succinic acid preparations or other metabolic agents. All patients underwent blood pressure and heart rate measurements, laboratory tests, pulse oximetry, ergospirometry. Trends in lactate levels in the blood and hormonal status in athletes were assessed. Moreover, such parameters as testing time, maximum heart rate, maximum oxygen consumption (VO2max), aerobic and anaerobic threshold pulse, time to reach the aerobic and anaerobic threshold were analyzed. Results: athletes who received a course of metabolic therapy on the 35th day of the preparatory period showed a significant increase in the indicators of maximum oxygen consumption (VO2max), the time of the test and the time of the anaerobic threshold ($p<0.05$), which, against the background of a statistically significant decrease in lactate levels ($p=0.014$) indicates an improvement in aerobic performance and the possibility of faster recovery of athletes after physical exertion compared with athletes who did not receive metabolic therapy with succinic acid. Conclusion: The results obtained allow us to recommend the use of step therapy with succinic acid as a metabolic therapy for professional hockey players in the preparatory period.

Keywords: ice hockey players; Cytoflavin; hormonal status; lactate level; functional parameters; aerobic fitness; overtraining.

Citation: Zaborova V., Kurshev V., Kryuchkova K. Functional and hormone changes in ice players using Cytoflavin. Journal of Clinical Physiology and Pathology (JISCPP) 2023; 2 (4): 22-28.

https://doi.org/10.59315/JISCPP.2023-2-4.22-28

Academic Editor: Igor Kastyro

Received: 13.10.23
Revised: 01.11.23
Accepted: 07.12.23
Published: 29.12.23

1. Introduction

Ice hockey is a physiologically complex sport that requires aerobic and anaerobic energy metabolism. The aerobic level of hockey players increases as they grow up, physically and physiologically mature [1], [2]. At the same time, performance in sports requiring the development of aerobic endurance largely depends on the capabilities of the system for the delivery and removal of energy metabolism products, as well as the oxidative potential of working muscles and the availability of energy substrates [3], [4].

The sport of the highest achievements with its physical and psycho-emotional loads requires a new level of adaptation from the human body, the achievement of which without additional intervention becomes extremely difficult [5]. Overtraining is the accumulation of training and/or non-training stress, leading to a long-term decrease in performance in the presence or absence of corresponding physiological and psychological signs and symptoms of poor adaptation, due to which recovery of performance can take several weeks or months [6]. A highly qualified athlete constantly balances between the optimal level of training and overtraining. Overtraining can be experienced in the course of the athlete's sports career; up to 20% of highly qualified athletes in the general selection, made without taking into account specialization, and up to 70% of elite athletes in sports associated with the predominant development of endurance [7].

The most important problem to this day remains the provision of the body with energy substances and the complete removal of metabolites. In the context of such problems, there is a physiologically justified need for the use of non-marketing ergogenic means of correcting metabolic disorders, which are designed to activate and shorten the time of the body's adaptive reactions to progressively increasing workouts [8].

The main pharmacological means necessary for highly qualified hockey players in the annual training cycle, taking into account the functional state of the limiting systems, are biologically active additives of complex restorative action, neurotropic agents, adaptogens, means of protection and restoration of the ligamentous-articular apparatus [9]. Recently, succinic acid preparations have been increasingly used in sports, which increase adaptation to stress and have a stimulating effect on the processes of cellular respiration and energy formation [4], [10]. Therefore, the aim of our study was to assess the effect of 35-day Cytoflavin consumption on hormonal status, blood lactate level and functional parameters in elite ice hockey players.

2. Materials and Methods

The study was approved by the Ethics Committees of the Federal Scientific Center of Physical Culture and Sports (protocol number 14 dated 25 November 2019). All subjects included in this study provided written informed consent. The study involved 60 professional male hockey players aged 19 to 36 years, whose average age was 24.1±3.8 years. All athletes, depending on the application of the pharmacological support scheme, were divided into two groups of 30 people, comparable in age, anthropometric, clinical and instrumental indicators. Of these, 25 athletes are Masters of sports of international class (MSIC), 26 athletes are masters of sports (MS) and 9 athletes are candidates for Masters of sports (CMS).

Group I consisted of 30 people who, against the background of "basic" sports nutrition, underwent a course of metabolic therapy with the use of succinic acid (Cytoflavin) according to the following scheme: 2 tablets 2 times a day with an interval between doses of 8-10 hours 30 minutes before meals, without chewing, washed down with sweet tea, for 35 days. The course of taking the drug was 35 days.

Group II consisted of 30 people whose pharmacological support included only "basic" sports nutrition and did not include succinic acid preparations or other metabolic agents.

All patients underwent blood pressure and heart rate measurements, laboratory tests, pulse oximetry, ergospirometry.

Laboratory tests included a biochemical blood test to determine the level of lactic acid (lactate), as well as an assessment of hormonal status to determine the level of testosterone, cortisol and thyroid-stimulating hormone (TSH). The calculation of the "anabolism index" (AI) was carried out according to the formula: AI (in %) = Testosterone / Cortisolx100.

Pulse oximetry was performed using the PulseOx 7500 apparatus (SPO Medical, Israel), the parameters of oxygenated hemoglobin (peripheral oxygen saturation) SpO2 and heart rate were evaluated. Ergospyrography-treadmill testing with gas analysis was carried out using: the Quark PFT modular system (Italy), the Treadmill MTM-1500 med treadmill from SCHILLER (Germany), the NihonKohden electrocardiograph (Japan) of the CARDIOFAXGEM series. Such parameters as testing time, maximum heart rate, maximum oxygen consumption (VO2max), aerobic and anaerobic threshold pulse, time to reach the aerobic and anaerobic threshold were analyzed.

All parameters were evaluated before the study (baseline values), on the 14th and 35th day of the study (training).

The research materials were subjected to statistical processing using parametric and nonparametric analysis methods in accordance with the results of checking the compared aggregates for the normality of the distribution. Statistical analysis was carried out using the IBM SPSS Statistics program.23. Arithmetic averages (M) and mean square deviations (SD) were calculated. The differences in the indicators were considered statistically significant at a significance level of $p<0.05$. Comparison of the indicators measured in the nominal scale was carried out using the Pearson criterion $\chi 2$.

3. Results

The study of hormonal status parameters in dynamics showed the absence of statistically significant changes in cortisol parameters in both groups throughout the study period ($p>0.05$), however, it is necessary to note the multidirectional dynamics of cortisol levels in the groups (Table 1, Fig. 1, 2).

Table 1. Trends in hormonal status parameters of athletes by groups

Parameter	Time point	Group I	Group II
Cortisol (mcg/l)	Pre-study	254,32±34,34	237,8±29,13
	Day 14	258,44±28,76	243,04±28,46
	Day 35	245,56±34,71	245,72±25,08
Testosterone (nmol/L)	Pre-study	17,84±4,76	17,06±4,61
	Day 14	18,62±4,83″	16,64±4,26′

	Day 35	18,52±4,81″	16,68±4,01
AI (%)	Pre-study	7,01±2,17	7,27±2,14
	Day 14	6,58±2,13	6,94±1,95
	Day 35	7,81±2,79	7,62±2,18

′p ‹ 0.01, ″p ‹ 0.001 – statistical significance of differences compared to the baseline.

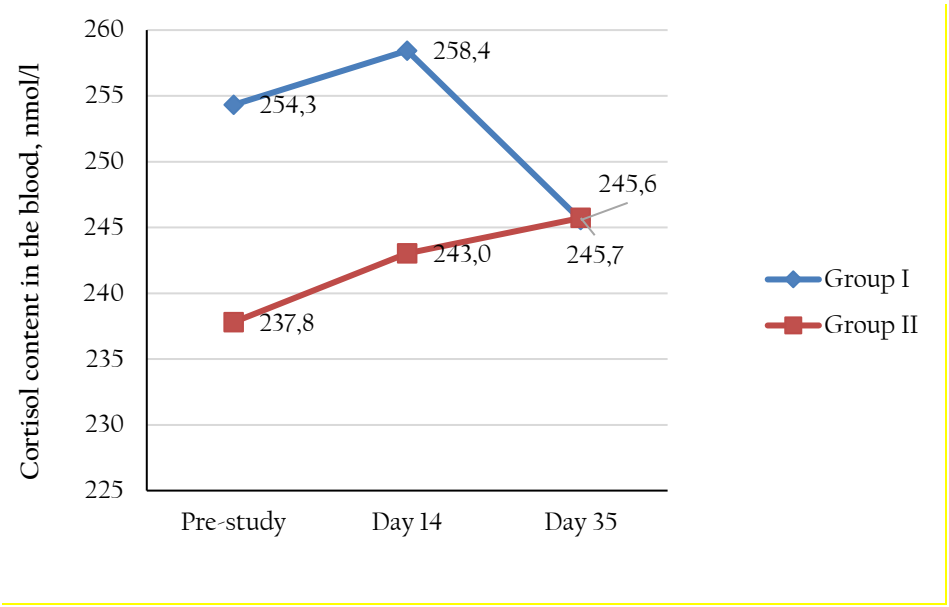

Figure 1. Trends in cortisol levels in the blood of athletes by groups

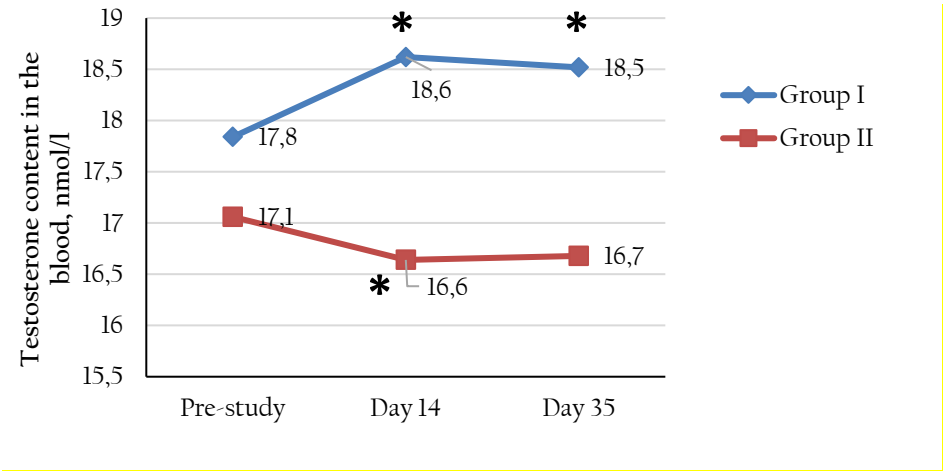

Figure 2. Trends in testosterone levels in the blood of athletes by groups (* p‹0.05 – statistical significance of differences within each group compared to the baseline)

Thus, in the group I, there was a decrease in cortisol levels by an average of 3.7% from 254.32±34.34 to 245.56±34.71 mcg/l (p›0.05), while in the group II there was an increase in cortisol levels by an average of 3.3% from 237.8±29.13 to 245.72±25.08 mcg/l (p›0.05). Analyzing the dynamics of testosterone levels, it should be noted its statistically significant increase in group I throughout the study from 17.84±4.76 to 18.52±4.81 nmol/L (p‹0.001), while in group II there was a statistically significant decrease in this parameter from 17.06±4.61 to 16.64±4.26 nmol/L (p=0.016) on the 14th day, and stabilization by the 35th day of the study at the level of 16.68 ±4.01 nmol/L.

A study of the trends of the anabolism index, which characterizes the degree of overtraining of athletes, showed its increase in the group I by an average of 14.2%, in the comparison group – by 4.8%.

The examination of the trends in lactate content in the blood of athletes of the main group on the 35th day of the study showed a statistically significant decrease in it both before training

(p=0.14) and after training (p=0.14) compared with baseline indicators. The data obtained indicate that the use of Cytoflavin helps to prevent the accumulation of excess lactic acid in the muscles, which is considered as the main cause of fatigue (Table 2, Fig. 3).

Table 2. Trends in lactate levels in the blood of athletes by groups

Time point	Training stage	Group I	Group II
Before the study	Before training	2,02±0,32	1,9±0,29
	After training	4,58±0,49	4,47±0,4
Day 35	Before training	1,86±0,24	1,94±0,23
	After training	4,48±0,43	4,64±0,51
Significance level, p	Before training	0,014	0,566
	After training	0,014	0,222

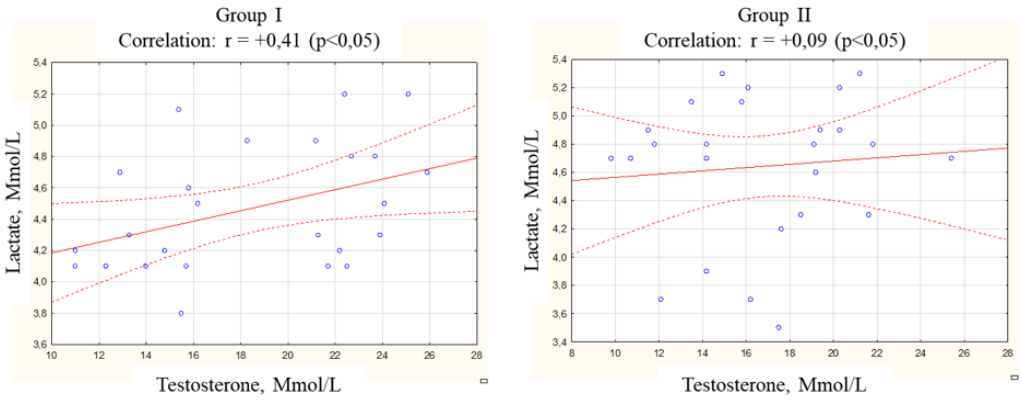

Figure 3. The correlation between lactate and testosterone levels on the 35th day of observation

The study of functional diagnostic parameters during metabolic correction revealed the absence of statistically significant differences in blood pressure from baseline and between groups (p>0.05) (Table 3, Fig. 4).

Table 3. Trends in blood pressure and pulse oximetry indicators in athletes by groups

Parameter	Time point	Group I	Group II
Systolic blood pressure, mmHg	Before the study	123,96±4,8	121,52±5,87
	Day 35	122,8±3,25	121,2±4,4
Diastolic blood pressure, mmHg	Before the study	76,6±5,02	76,04±3,81
	Day 35	76,0±4,08	77,4±3,57
Heart rate	Before the study	62,6±4,97	61,08±5,11
	Day 35	62,4±3,59	62,0±4,22′
SpO_2, %	Before the study	98,32±0,9	98,28±0,89
	Day 35	98,92±0,64″	98,40±0,71*

*p ‹ 0.05 – significance of differences compared to group I, 'p ‹ 0.05, "p ‹ 0.001 – statistical significance of differences compared to the baseline.

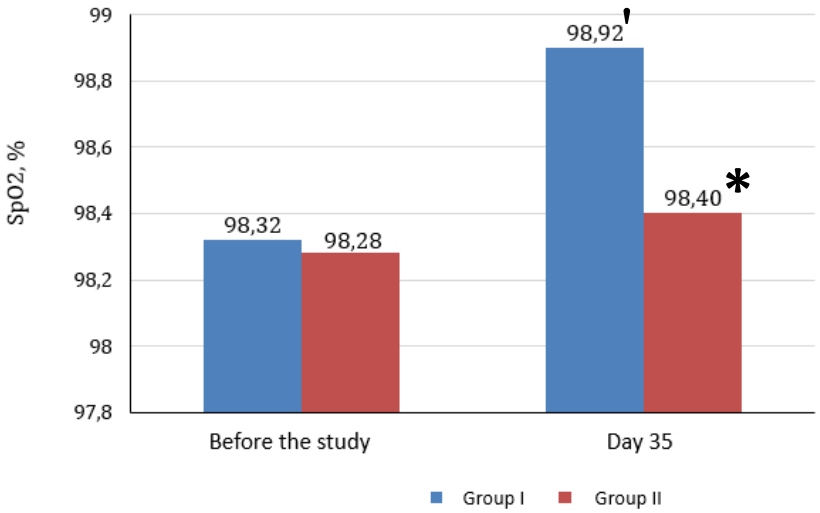

Figure 4. Trends in blood oxygen saturation (SpO2) (*p ‹ 0.05 – significance of differences compared to group I, 'p=0.001 – statistical significance of differences compared to the baseline)

Analysis of pulse oximetry results revealed statistically significant dynamics of blood oxygen saturation in the main group from 98.32±0.9 to 98.92±0.64 (p=0.001), as well as significant differences in SpO2 on the 35th day of the study between the groups. (p=0,009). In the group II, changes in the SpO2 index were not statistically significant throughout the study (p=0.503).

The assessment of heart rate indicators revealed a statistically significant increase in heart rate compared to baseline values (p=0.045) in the group II on the 35th day of the study.

Evaluation of ergospirometry parameters revealed a statistically significant increase in all studied parameters in both groups (p‹0.01). However, on the 35th day of the study, statistically significant differences were noted between the groups in terms of maximum oxygen consumption, test time and anaerobic threshold time. In the main group, these parameters were statistically significantly higher than similar parameters in the comparison group (p‹0.05) (Table 4, Fig. 5).

Table 4. Trends in ergospirography parameters in athletes depending on the intake of Cytoflavin

Parameter	Time point	Group I	Group II
Maximum heart rate, beats/min	Before the study	178,88±10,85	176,96±6,78
	Day 35	188,00±11,31	180,32±21,16
Significance level, p		‹0,001	‹0,001
Test time, min	Before the study	12,53±1,40	11,98±0,9
	Day 35	14,15±1,30	13,27±1,04*
Significance level, p		‹0,001	‹0,001
VO2 Max (ml/kg/min)	Before the study	46,99±3,17	47,21±2,84
	Day 35	52,25±4,20	49,06±2,76*
Significance level, p		‹0,001	‹0,001
Heart rate of the anaerobic threshold, beats/min	Before the study	170,3±10,93	167,84±7,52
	Day 35	174,6±10,92	172,84±8,95
Significance level, p		‹0,001	‹0,001
Anaerobic threshold time, min	Before the study	10,36±1,31	10,24±1,04
	Day 35	11,97±1,28	11,32±0,93*

Significance level, p		‹0,001	‹0,001
Heart rate of the aerobic threshold, beats/min	Before the study	106,12±11,80	100,84±8,45
	Day 35	115,76±10,08	112,48±6,65
Significance level, p		‹0,001	‹0,001
Aerobic threshold time, min	Before the study	2,97± 0,9	2,71±0,63
	Day 35	3,60±0,85	3,35±0,70
Significance level, p		‹0,001	‹0,001

*p ‹ 0.05 – significance of differences compared to group I

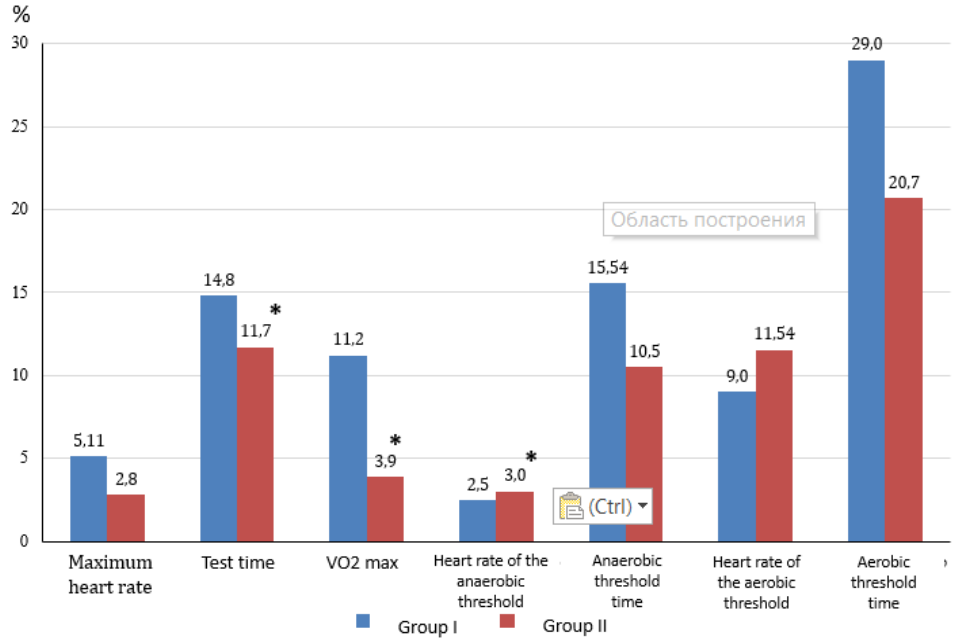

Figure. 5. Increase in ergospirography parameters on the 35th day of the study (*p ‹ 0.05 – significance of differences compared to group I)

The average increase in the index of maximum oxygen consumption in the group I was 11.2%, while in the group II the increase in the parameter was only 3.9% (p=0.003); the parameter of the test time increased in the group I by 12.9%, in the group II – by 10.8% (p<0.05) (median increase this parameter was 14.8%, in the group II – by 11.6%); the increase in the average time to reach the anaerobic threshold in the group I was 15.5%, in the group II – 10.5% (p=0.045).

4. Discussion

Earlier it was shown that cytoflavin promotes physical fitness of athletes by improving energy supply, psycho-emotional state and competitive form. It is recommended to use cytoflavin for the preparation of athletes in the pre-competition period [11]. It is known that the use of step therapy with succinic acid as a metabolic therapy allows to stabilize hemoglobin indicators, significantly reduce the degree of damage to the cells of the muscular system and heart muscle, increase the anabolism index by 14.2% due to a statistically significant increase in testosterone levels and a decrease in cortisol levels.

Analyzing the obtained parameters, it should be noted that a decrease in testosterone levels as an indicator of the intensity of anabolism processes and an increase in cortisol levels as a parameter of the intensity of catabolism processes in the body in group II may indicate that an athlete is in a state of chronic stress, fatigue, in other words, overtraining. At the same time, the revealed dynamics of testosterone and cortisol parameters in the main group may indicate an improvement in the recovery processes in the body after exertion and a better formation of exercise tolerance when bringing metabolic therapy with the use of Cytoflavin.

The revealed change in the level of blood oxygen saturation during metabolic correction with the use of Cytoflavin may be associated with both an improvement in microcirculation and changes in the erythrocytes themselves or in their ability to bind oxygen.

The results obtained during ergospirography in the main group indicate an improvement in aerobic performance, which is not only the basis for demonstrating high achievements in various sports, but also a means of the best and fastest recovery of athletes after physical exertion.

In turn, an increase in the time to reach the anaerobic threshold against the background of a decrease in lactate indicators suggests a more successful elimination of oxygen debt, which is the key to the processes of recovery and fitness of the athlete.

5. Conclusion

The use of step-by-step therapy with succinic acid as metabolic therapy in hockey players in the preparatory period makes it possible to increase blood oxygen saturation, increase the anabolism index, which indicates the formation of exercise tolerance, improvement of recovery processes after exertion and the absence of signs of overtraining.

At the same time, a significant increase in the index of maximum oxygen consumption, an increase in the time of the test and the time to reach the anaerobic threshold, as well as an increase in the time to reach the anaerobic threshold against the background of a decrease in lactate parameters during metabolic correction with the use of succinic acid preparation allows to improve the parameters of aerobic performance and increase the level of exercise tolerance compared to with athletes who have not had metabolic therapy.

The results obtained allow us to recommend the use of step therapy with succinic acid as a metabolic therapy for professional hockey players in the preparatory period.

Application of artificial intelligence:

The article is written without the use of artificial intelligence technologies.

Author Contributions: Conceptualization, V.Z.; methodology, V.K..; software, V.K; validation, V.Z.; formal analysis, V.Z.; investigation, K.K.; resources, K.K.; data curation, K.K..; writing—original draft preparation, V.K.; writing—review and editing, K.K.; visualization, V.Z..; supervision, V.Z.; project administration, V.K.. All authors have read and agreed to the published version of the manuscript."

Funding: This study was not supported by any external sources of funding.

Institutional Review Board Statement: The study was conducted according to the guidelines of the Declaration of Helsinki and approved by the Institutional Ethics Committee of the Federal state budgetary institution Federal Scientific Center of Physical Culture and Sports (protocol number 14 dated 25 November 2019).

Informed Consent Statement: Informed consent was obtained from all subjects involved in the study.

Conflicts of Interest: The authors declare no conflict of interest.

References

1. Leiter JR, Cordingley DM, Macdonald PB. Aerobic Development of Elite Youth Ice Hockey Players. The Journal of Strength and Conditioning Research. 2015;29(11):3223-3228.
2. Ransdell LB, Murray TM, Gao Y. Off-ice fitness of elite female ice hockey players by team success, age, and player position. The Journal of Strength and Conditioning Research 2013;27(4):875-884.
3. Montgomery DL. Physiology of ice hockey. Sports Med. 1988;5(2):99-126.
4. Zaborova V, Kurshev V, Kryuchkova K, Anokhina V, Malakhovskiy V, Morozova V, Sysoeva V, Zimatore G, Bonavolontà V, Guidetti L, Dronina Yu, Kravtsova E, Shestakov D, Gurevich K, Heinrich K. Metabolic and Body Composition Changes in Ice Hockey Players Using an Ergogenic Drug (Cytoflavin). Biology (Basel). 2023;12(2):214.
5. Zemková E, Kováčiková Z. Sport-specific training induced adaptations in postural control and their relationship with athletic performance. Frontiers in Human Neuroscience. 2023;16.
6. Morgan WP, Brown DR, Raglin JS, O'Connor PJ, Ellickson KA. Psychological monitoring of overtraining and staleness. British Journal of Sports Medicine. 1987;21(3):107.
7. Lehmann M, Foster C, Gastmann U, Keizer H, Steinacker JM. Definition, Types, Symptoms, Findings, Underlying Mechanisms, and Frequency of Overtraining and Overtraining Syndrome. Overload, Perform Incompetence, Regen Sport. 1999:1-6.
8. Rodriguez NR, DiMarco NM, Langley S. Position of the American Dietetic Association, Dietitians of Canada, and the American College of Sports Medicine: Nutrition and athletic performance. Journal of the American Dietetic Association. 2009;109(3):509-527.
9. Lambrianides Y, Epro G, Smith K, Mileva KN, James D, Karamanidis K. Impact of Different Mechanical and Metabolic Stimuli on the Temporal Dynamics of Muscle Strength Adaptation. The Journal of Strength and Conditioning Research. 2022;36(11):3246-3255.
10. Okovityi SV, Rad'ko SV.. [The application of succine in sports]. Vopr Kurortol Fizioter Lech Fiz Kult. 2015;92(6):59-65.
11. Kosinets VA, Stolbitskiĭ VV, Shturich IP. The use of cytoflavin in sports nutrition. Clinical Medicine. 90(7):56-58.

Article

Predictors of the formation of pathological conditions of landing participants in the Arctic latitudes considering the trans-latitudinal flight along ultradian rhythms

Anastasia Bashkireva[1,*], Sergey Chibisov[2], Tatyana Bashkireva[3]

[1] Department of Medical Biological and Psychological Foundations of Physical Education, Ryazan State University named after S.A. Yesenin, Ryazan, Russia;
[2] Department of General Pathology and Pathological Physiology named after V.A. Frolov Institute of Medicine, RUDN University, Moscow, Russia;
[3] Department of General and Pedagogical Psychology, Academy of Law and Administration of the Federal Penitentiary Service of Russia, Ryazan, Russia
* Correspondence: bashkireva32@gmail.com;

Abstract The article looks at what causes landing participants in the Arctic to develop health problems during trans-latitudinal flights that last 28 hours, focusing on ultradian rhythms. Landing performed from a height of 10 km to the territory of the Russian islands in the Arctic Ocean. Holter monitoring used in the studies. Predictors were determined by normalized indicators of heart rate variability. The identified violations are typical for classes 06, 07, 11 of ICD-11 (International Classification of Diseases).

Keywords: ultradian rhythms, predictors, pathological conditions, trans-latitudinal flight, heart rate variability, desaturation, dyschronism.

Citation: Bashkireva A., Chibisov S., Bashkireva T. Predictors of the formation of pathological conditions of landing participants in the Arctic latitudes considering the trans-latitudinal flight along ultradian rhythms. Journal of Clinical Physiology and Pathology (JISCPP) 2023; 2 (4): 29-31.

https://doi.org/10.59315/JISCPP.2023-2-4.29-31

Academic Editor: Igor Kastyro

Received: 24.10.23
Revised: 27.11.23
Accepted: 12.12.23
Published: 29.12.23

1. Introduction

Over the past ten years, scientists studying chronobiology have focused on biological rhythms such as ultradian. Ultradian rhythms during periods of active work of the human body in various conditions of its activity have not been studied enough. This applies not only to labor activity but also to educational, sports and others.

The term "ultradian rhythms" is aperiodic [1]. To describe the biological phenomena of life more accurately [2], some call them "episodic ultradian events" while in physiology, they referred to as "basic rest-activity cycle" (BRAC) [3]. Studying ultradian rhythms can show how the body works during busy times, like work. Such studies can provide the key to understanding the formation of pathological conditions and disease [4].

2. Patients and Methods

HOLTERLIVE hardware complex was used to analyze heart rate variability in ISCIM6.0. Spectral analysis indicators were of the greatest interest: HF, LF, VLF, ULF (m/s2 and % ratios), their amplitudes (A), stress index (SI). The drawings of the phase portraits make using the ISCIM6.0 software. Phase portraits show the body's state, including normal, before illness, and when the body can't adapt to illness. To study ultradian rhythms in the active physical phase of a person, it is most expedient to use the method of heart rate variability. The method has over 40 indicators that are sensitive to spatio-temporal physical and cognitive loads, including extreme conditions.

The psychological state of Arctic landing participants evaluated with the SAM method (well-being, activity, and mood). This technique is valid and widely used in biomedical research.

Eight men participated in the study. They were aged 28 to 50 and had experience in landing on limited sites in extreme conditions due to their parachute training (from 300 to 15 thousand jumps).

The uniqueness of the study lies because the Arctic landing conducted for the first time in the world from a height of 10 km to the islands of the Arctic Ocean. The flight crossed one time zone, but the temperature shifted from mild to Arctic.

The measurements were performed: from the moment of installing Holter monitoring devices when boarding the plane, landing on the islands and returning to the original base. The air temperature of the airfield at the time of departure was +17o, the air temperature at the time of leaving

the aircraft was -60o, and landing - 5o. Recording of ultradian rhythms of heart rate variability conducted for 20 hours.

3. Results

3.1. Heart rate variability.

The data received indicate that, regardless of age, there is an overstrain of functional systems. What is typical of the disruption of adaptive reactions and corresponds to the formation of a pathological condition. It was revealed that the range of these differences in terms of AHF amplitude was 93%, and SI -89%. Between the amplitudes of ALF and AVLF dense areas of scattering observed, VLF did not exceed 280 ms2/Hz (Fig.).

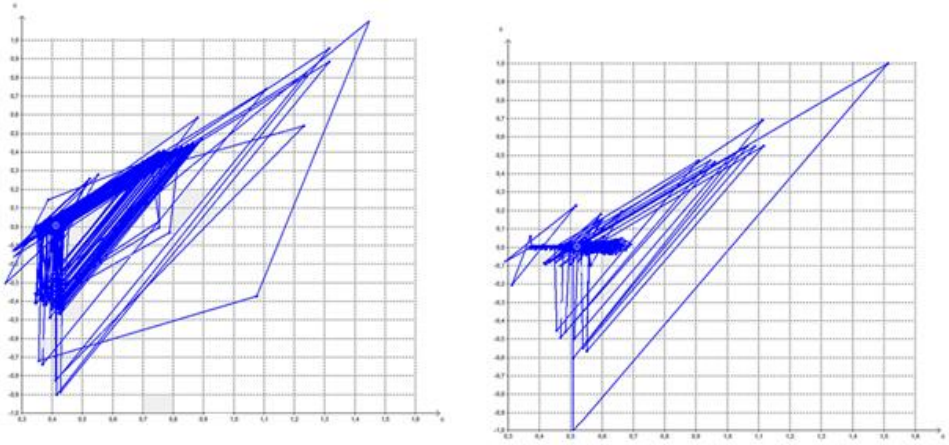

Figure. Phase portrait and HRV values in specialists aged 33 and 50 after landing in arctic conditions

The data received indicates that the activity of the vagus nerve increases with age in extreme situations. Which indicates parasympathicotonia, which characterized by a decrease in the response of the sympathetic department during stress; there is a need for urgent adaptation of the body. Accordingly, the activity of the autonomous circuit increases. Synchronization of heart rate control processes occurs.

There were a high level of individual differences in the group. Comparison of the maximum and minimum values in terms of AHF was 79%, SI - 86%, ALF - 75%. According to the AVLF, all participants had dense areas of scattering, and the VLF exceeded 400 ms2 /Hz.

It was also found that the higher the VLF, the lower the RMSSD ($r = \neg 0.929$; $P < 0.001$) and SDNN ($r = \neg 0.898$; $P < 0.001$). The body's autonomous circuit is regulating the heart rhythm, which leads to an increase in the sympathetic branch and a desire for self-regulation.

Health risks like vasodilatation and cardiogenic collapse can occur if people over 50 try to overcome the challenges of the Arctic such as time zones, high altitude, low temperatures, and other factors.

Normative indicators of heart rate variability such as SDNN, HF%, LF%, VLF%, and TP m/s2 were used to identify the pathophysiological state of Arctic landing participants during their trans-latitudinal flight along ultradian rhythms.

Mathematical modeling using SDNN suggests that the trans-latitudinal Arctic flight participants could have microcirculatory disorders in their brain tissue. The examined patients have a chronotropic reaction, obvious violations of the innervation of the conduction system of the heart.

The obtained data of correlation analysis characterizes dysfunction of heart rate regulation and decrease in resistance associated with desaturation. This can be seen as internal dyschronism. [5]. Internal dyschronism occurs between the biological rhythms of the body. Human factors like lack of sleep, disrupted routines, and mental health issues can cause various disorders. In the absence of obvious nosological changes, it can serve as a sign of premorbid conditions [5, 6]. The body reacts to Arctic conditions during the trans-latitudinal flight.

4. Discussion

During a flight in the Arctic with technical support for critical infrastructure, participants experience external dyschronism and individual adaptation to unfavorable factors based on heart rhythm control. External dyschronism occurs between external environmental rhythmic factors and the body's own rhythms. Flights across time zones or latitudes cause these changes. The results obtained indicate a stable formation of pathological conditions.

It has been established that under conditions of high-altitude hyperoxia-hypoxia up to 10,000 m, accompanied by desaturation followed by the use of oxygen apparatus for breathing: the resistance decreases, the activity of the parasympathetic link increases, which is typical for a violation of the function of regulating the regulation of the heart rhythm. This considered as an internal dyschronism and a sign premorbid state of the body. There is also a cross-adaptation to a complex of adverse factors.

According to the GSAM method, during the training camp, all the subjects noted good health and mood. At the same time, 87% felt tension, drowsiness, a desire to rest, lack of attention and efficiency, which negatively affected the cognitive reactions of the landing participants.

5. Conclusions

Thus, the analysis of the results of the study showed that the predictors of the formation of pathological conditions according to ultradian rhythms of heart rate variability in landing participants on the Arctic islands, considering trans-latitudinal flight, were both psychological indicators and cardiovascular indicators of heart rate variability: HR, MxDMn, RMSSD, SDNN; SI spectrum power: HF, LF, VLF, ULF TP; ULF / HF are reflected in classes 06, 07, 11 of ICD 11. The method of heart rate variability in the study of ultradian rhythms is the most practical and scientifically based method for determining the predictors of the formation of pathological conditions of the human body under the influence factors of stress of various natures.

To ensure the safety of landing in arctic conditions and prevent the occurrence of the human factor, it is necessary to consider the health of specialists and their adaptive capabilities. Based on the results of the study, it is recommended that it is advisable to approach the selection of specialists to perform complex tasks in extreme conditions of professional activity. Particular attention should be paid to the formation of group synchronization. It should be emphasized the importance of the organization of nutrition, sleep and rest for the successful completion of tasks, in conditions that are especially dangerous for human life. When professionals train for extreme situations, a doctor or psychophysiologist should supervise them. This helps with rehabilitation, monitors their health and mental state, and regulates work and rest.

Application of artificial intelligence:

The article is written without the use of artificial intelligence technologies.

Author contributions: Conceptualization, A.B., S.Ch. and T.B.; methodology, A.B., S.Ch. and T.B.; software, A.B., T.B.; validation, A.B., T.B.; formal analysis, S.Ch.; investigation, A.B., T.B.; resources, A.B., T.B.; data curation, A.B., S.Ch. and T.B.; letter - preparation of the original draft, A.B., S.Ch. and T.B.; writing-reviewing and editing, A.B., S.Ch. and T.B.; visualization, A.B.; supervision, T.B.; project administration, A.B., T.B. All authors have read and agreed with the published version of the manuscript.

Conflicts of Interest: The authors declare no conflict of interest.

References

1. Daan S, Aschoff J. Short-term rhythms in activity. In: Aschoff J., editor. Biological Rhythms. Plenum Press.1981; 491–498.
2. Blessing W, Ootsuka Y. Timing of activities of daily life is jaggy: How episodic ultradian changes in body and brain temperature are integrated into this process. Temperature 2016; 3: 371–383.
3. Nelson W, Liang Tong Y, Lee J, Halberg F. Methods for cosinor-rhythmometry. Chronobiologia. 1979, 6: 305–323.
4. Grace H Goh, Shane K Maloney, Peter J Mark, Dominique Blache Episodic Ultradian Events-Ultradian Rhythms. Biology (Basel) 2019 8(1): 15
5. Katenis GS, Chibisov SM, Agarval RK. The actual terms of modern chronobiology The journal of scientific articles "Health & education millennium". 2015, 17(1).
6. Brodsky V. Circahoralian (Ultradian) metabolic rhythms. Biochemistry. 2014, 79: 483–495.

Article

Theory of macular diseases in terms of glymphatic fluid circulation

Juldyz Beisekeeva [1,*], Alexander Samoylenko [2], Sergei Kochergin [3]

[1] Department introduction to the clinic, South Kazakhstan Medical Academy, Shymkent, The Republic of Kazakhstan;
[2] Samoylenko Eye Clinic, Moscow, Russian Federation;
[3] Department of Ophthalmology, Russian Medical Academy of continuous Postdiploma education of Health Ministry, Moscow, Russian Federation;
* Correspondence: julbs2015@gmail.com;
julbs2015@gmail.com, https://orcid.org/0000-0002-2453-7035 (J.B.);
ophthalm@yandex.ru , https://orcid.org/0000-0002-5796-6012 (A.S.);
prokochergin@rambler.ru, https://orcid.org/0000-0002-8913-822x (S.K.)

Abstract: This article is an analysis of theoretical aspects of etiopathogenesis of the macular zone of the eye in terms of glymphatic circulation of tissue fluid. To date, a lot of data has been accumulated on functional and structural changes of the macular zone in normal and in various pathologies. The genesis of macular oedema along with subretinal and choroidal neovascularisation could be highlighted and understood from a different point of view if assuming the presence of the glymphatic para- and perivascular fluid flow within the retina, channels in the vitreous body and the choroid. Clinical features of the various eye diseases including hereditary, highlight the paravascular glymphatic outflow routes. The totality of data on various eye diseases, as well as the revealed clinical features of their course based on the latest scientific data and glymphatic flow in the nervous tissue allowed us to make assumptions about the presence of new physiological patterns of fluid flow in the posterior segment of the eye and formulate a new concept of pathogenesis of macular diseases.

Keywords: cystoid macular oedema, macular hole, Irvine-Gass syndrome, glympha, intra-ocular fluid, transient macular oedema, age-related macular degeneration.

Citation: Beisekeeva J., Samoylenko A., Kochergin S. Theory of macular diseases in terms of glymphatic fluid circulation. Journal of Clinical Physiology and Pathology (JISCPP) 2023; 2 (4): 32-41.

https://doi.org/10.59315/JISCPP.2023-2-4.32-41

Academic Editor: Igor Kastyro

Received: 02.10.23
Revised: 23.11.23
Accepted: 18.12.23
Published: 29.12.23

1. Introduction

The etiopathogenesis of Irwin-Gass syndrome or pseudophakic cystic macular oedema (CMO) is not completely clear. It is generally believed that seepage from parafoveolar capillaries, which is recorded on fundus angiography (FA), leads to the formation of intraretinal cysts mainly in the outer nuclear layer. But macular oedema, observed in such hereditary diseases as X-linked retinoschisis, retinitis pigmentosa and Goldman-Favre syndrome, as a rule, manifests itself without seepage according to FA data [1]. The same absence of dye leakage from the parafoveolar capillaries is observed in maculopathy on the background of hypotension [2] and in drug-induced oedema from the action of nicotinic acid [3], drugs of the taxane group [4] and cefuroxime [5]. However, it should be noted that in hereditary degenerative diseases, the pattern of percolation in FA in the macular zone is similar to that observed in aphakia and posterior uveitis [6]. Despite a big step forward in the treatment of wet age-related macular degeneration due to anti-VEGF drugs, there are still unresolved issues concerning the etiopathogenesis of age-related macular degeneration (AMD), relapses of neovascularization and the so-called accumulation of intraretinal fluid [7,8]. There is also no single concept of etiopathogenesis of macular ruptures to date. Glymphatic pathways of fluid circulation in the posterior segment of the eye can answer many questions related to these conditions. Aim of this study is to highlight the macular disorders in terms of glymphatic fluid flow and to generate new theoretical concept of macular diseases.

2. Methods:

literature review and analysis.

3. Results

3.1. Glymphatic circulation pathways in the eye

Lymphatic outflow is provided mainly by the conjunctival collectors [9] with the participation of the so-called uveolymphatic pathway [10,11]. At the end of the 20th century, a consensus was reached according to which the vitreous body, the interstitium between the glial cells of the optic nerve, the soft meninges between the septa of the optic nerve, the perivascular spaces and the subarachnoid space of the optic nerve, all together constitute a single pre–lymphatic space [12]. Perivascular channels in the adventitia of cerebral vessels (Virchow-Robin spaces) were described in 1859. In 2012, Iliff and colleagues "rediscovered" these spaces in the form of a single network of interconnected paravascular spaces of arteries and veins that circulate interstitial fluid with the excretion of metabolic products along the processes of astrocytes [13]. So, a new point of view on the exchange of interstitial fluid in the brain arose due to the so-called glymphatic system, which provides fluid exchange between paravascular spaces, nervous tissue and subarachnoid space with the participation of circadian rhythm and pulse wave [13-15]. It has been experimentally shown that the glymphatic outflow pathways of the eye include the vitreous body, the paravascular spaces of the retinal vessels and the suprachoroidal space [16]. Wang and co-authors (2020) proved that in mice with experimental glaucoma, fluid from the vitreal cavity enters directly into the interaxonal space of the optic nerve and moves centripetally, whereas in healthy mice, fluid is absorbed into the paravenous spaces of the retina, from where it flows along the axons of ganglion and amacrine cells along the gradient of hydrostatic pressure and is absorbed into the venous capillaries of the optic nerve membranes [16]. It is important to note that the interaxonal current in the optic nerve in rodents practically stopped when atropine and pilocarpine were instilled and was more pronounced in the light than in the dark [16]. Clinical ophthalmologists have suggested that interstitial glymphatic current in the thickness of the retina is involved in the pathogenesis of microcystic maculopathy at the level of the inner nuclear layer with the participation of Muller cells [17], as well as in the pathogenesis of paravascular posterior uveitis [18,19].

Clinical manifestations of diabetic maculopathy and retinopathy involving the vitreous body also confirm the great importance of glymphatic intraocular fluid circulation in their pathogenesis. We assumed that the fluid normally enters the premacular bag from the anterior segment of the eye through the central channel and is absorbed along the pressure gradient into the thickness of the retina in the fovea along with tissue fluid secreted by the macular choriocapillary lobule [20]. Further, this fluid flows in the thickness of the glymphatic spaces of the inner layers of the retina, where only the superficial and intermediate vascular networks are surrounded by perivascular astrocytes. The deep vascular plexus is surrounded only by the processes of Muller cells, therefore, excess tissue fluid from the outer layers of the retina is normally excreted through the retinal pigment epithelium (RPE), and with its excess into the vitreous body and into the glymphatic spaces of the inner layers of the retina and into the venous collection of the optic nerve sheaths, as was shown by experiment on rodents [16]. Venules predominate in the capillary network of the optic nerve disc, and there are also many astrocytes in this zone, which suggests the function of glymphatic outflow of tissue fluid in the optic cup area.

3.2. Pseudophakic CMO

The frequency of pseudophakic CMO is from 1 to 10%, which is similar to the frequency of transient macular oedema in the early stages after cataract surgery due to the toxic effect of cefuroxime 3.5% [21]. It is assumed that the etiology of the first one is associated with inflammatory factors and an imbalance between the rate of capillary filtration and the rate of fluid outflow from the retina through the perivascular interstitium. The second one is associated with dysfunction of the RPE proton pump and retention of the outflow of tissue fluid between the outer layers of the retina and choriocapillaries (Fig.1).

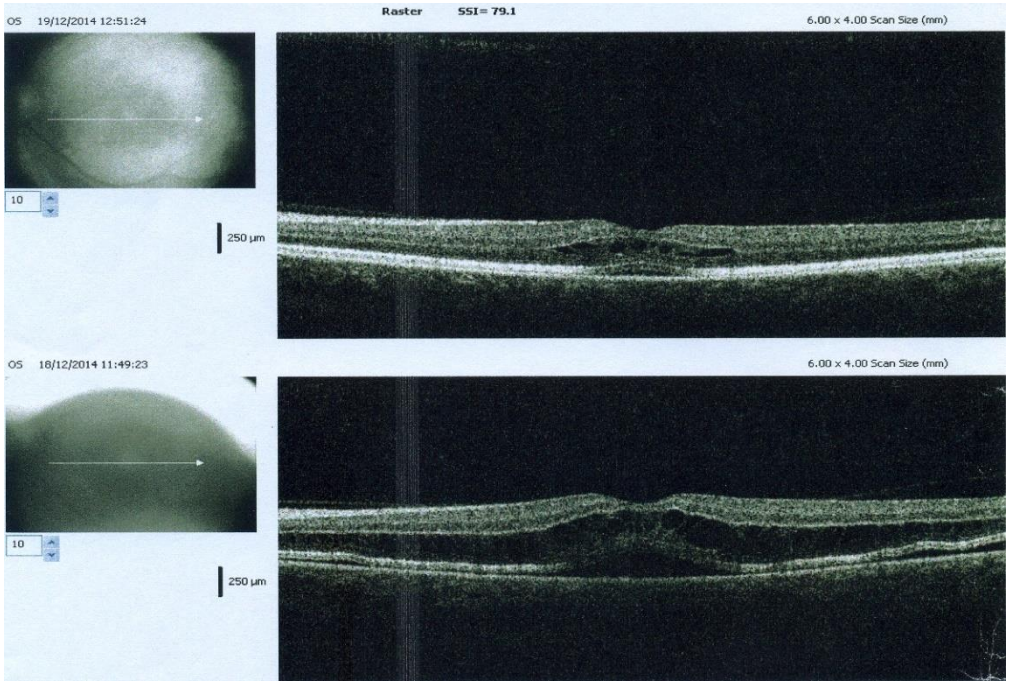

Figure 1. OCT picture of acute transient oedema after cataract surgery.

It is likely that pseudophakic CMO and serous retinal detachment (SRD) have common etiopathogenetic pathways of disorder of the water transport function of RPE [22-24]. A defect in the RPE was found between the optic disc and the macula in the FA in a patient with transient macular oedema from cefuroxime, while the authors noted the similarity of the OCT picture of the condition they described with Vogt-Koyanagi-Harada syndrome [5]. It is interesting to note that neovascularization in Vogt-Koyanagi-Harada syndrome is most often located in this zone – juxtapapillary between the optic disc margin and macula, where the perforant artery penetrates into the thickness of the retina.

In pseudophakic CMO, anatomical and functional recovery is possible in 80% of cases, but in chronic CMO, in addition to cavities in the outer retina, histologically observed: perivascular infiltration by inflammatory cells, Muller cell oedema, mitochondrial oedema in the pre-laminar axons of ganglion cells, astrocyte degeneration and occlusion of surface capillaries of the retina [25,26]. The hydrostatic pressure gradient over the fovea is 3 times higher than over the optic nerve disc [20], which provides a flow of tissue fluid along papillomacular bundle into the lymphatic spaces of the optic nerve in addition to the difference in osmotic pressure of this fluid between the fovea region and the periphery of the retina. This may explain the pathogenesis of pseudophakic CMO and the observed histological changes. The largest and thickest choriocapillary lobule is located under the macula, the RPE cells are the widest and tallest here, and the elastic sieve-like layer of the Bruch membrane is the thinnest here [27].

In pseudophakic CMO, glymphatic flow in the macula probably fails because of weakened fluid flow through the central channel into the premacular sac and increased fluid secretion from the choriocapillaries or because of retention of its outflow towards the choroid. As a result, fluid accumulates in the outer retina. It does not have time to be transported by Muller cells into the vitreous body due to the presence of an ionic gradient limit and accumulates around retinal vessels for outflow through perivascular glymphatic spaces. The opening of the endothelium of retinal capillaries is probably compensatory and adaptive in order to improve the outflow of accumulated tissue fluid in the outer retina. With normalization of the functioning of the proton pump, the described imbalance of flow of tissue fluid from the choriocapillaries is restored. This is confirmed by the positive effect of carboanhydrase inhibitors in the course of cystic CMO. Muller cells, forming a framework in the foveolar zone, contain receptors for carboanhydrase inhibitors on their membrane, regulate the composition of extracellular fluid due to voltage-dependent ion channels, and also due to the presence of glutamate and GABA receptors, regulate depolarization of neurons and intracellular calcium levels [28].

Thus, we assume that it is the activation of the perivasal lymphatic outflow of fluid that causes the appearance of a cystic pattern and the leakage of the dye during FA. Only in this case there is an outflow of tissue fluid into the perivascular space and further into the paracellular spaces of the optic nerve. That is why diffuse macular oedema in uveitis is a poor prognostic sign, because there is no activation of the outflow of interstitial fluid. It which accumulates excessively

in the thickness of the retina due to RPE dysfunction. The absence of normal tissue metabolism leads to the death of retinal neurons, followed by a decrease in central vision.

The lens contains melanopsin [29], a protein that is also expressed in the macular retina on specialized melanopsin-containing ganglion cells involved in the regulation of circadian rhythm through the suprachiasmatic nucleus and epiphysis. Also, in the thickness of the retina in the outer nuclear and ganglion layers, MT1 melatonin receptors are expressed [30]. The absence of which leads in mice to an increase in intraocular pressure by 5 mm Hg at night and to the death of up to 30% of ganglion cells with age [31]. The protein dystrophin, also expressed in the macular zone and in the thickness of the lens, also affects the intraocular pressure. The absence of this gene in mice leads to a decrease in intraocular tone and is also associated with Alzheimer's disease. It is known that the transmembrane protein BEST 1 belongs to the family of calcium-activated anion channels regulating transepithelial transport of chlorides, is associated with the β-subunit of Ca2+ channels and is located on the basolateral membrane of the RPE [32].

Thus, there is a circulation of tissue and intra-ocular fluid (IOF) in the thickness of the retina, the optic nerve and the central channel of the vitreous body. At the same time, at night, there is an outflow of tissue fluid in the thickness of the retina from the macular zone towards the optic nerve along a pressure gradient, probably mainly in the thickness of the ganglion nerve fibre layer. This glymphatic outflow, which occurs only at night, depends on pressure gradients, head position, pulse pressure and the coordinated functioning of aquaporin-4 and G-protein receptors in the glial spaces of the retina. In the brain, for example, perivascular glymphatic spaces expand at night in order to increase the inflow of cerebrospinal fluid, followed by outflow together with tissue glymphatic fluid [33]. It has been established in rodents that aquaporin-4 on Muller cells and astrocytes is highly expressed, mainly along the border between the inner limiting membrane (ILM) and vitreous body. In the process, networks in the inner and outer plexiform layers opposite the capillary networks and is less expressed on fibrous astrocytes of the optic nerve and its soft sheaths [34].

The relationship between cataract surgery and macular pathology has been noticed for a long time. It was found that in the early stages (maximum values after 1 month) after uncomplicated cataract surgery, there is a thickening of the ganglion cell complex-the inner plexiform layer [35]. CMO in patients with ophthalmohypertension in the background of prostaglandin intake can occur on the artiphakic eye even 9 months after cataract surgery [36] and even 24 months later [37], as well as against the background of drug withdrawal in refractory operated glaucoma [38]. I.e., in some circumstances, there is a direct relationship between the values of IOP and the thickness of the retina in the macular area. We also observed appearance of CMO in several clinical cases when using prostaglandin analogues in patients with artiphakia, which resorbed when they were cancelled with an increase in IOP. Given the presence of prostaglandin receptors in the retina [39], these observations are quite understandable.

3.3. Hydrodynamic theory of the development of macular diseases

- Age-related macular degeneration manifests itself with a decrease in the flow rate of lymphatic tissue fluid in the thickness of the retina and from under the RPE in this area. A decrease in the flow of glymphatic fluid occurs with age with a decrease in heat production in the retinal pigment epithelium, which leads to a decrease in convection and circulation of tissue fluid in the foveolar zone, accumulation of metabolic products and deposition of retinal and subretinal druzens.
- Idiopathic degenerative/age-related macular holes from a hydrodynamic point of view can be explained by a violation of the flow of tissue fluid through the thickness of the retina at the point of entry into the fovea both from the premacular bag and from under the RPE. In this case, a hole in the fovea occurs with an increase in the flow rate of the interstitial fluid in the thickness of the retina in the radial direction against the background of an increase in the contractile activity of the processes of Muller cells. Macular hole is detected, as a rule, in the morning after sleeping in a horizontal position, in particular, and on the first day after phacoemulsification, which confirms the hypothesis of a radial-longitudinal glymphatic flow of tissue fluid in the inner layers of the retina in the macula. The fact that in case of macular hole, as a rule, there are no concomitant macular druzens indirectly confirms the first two points.
- Epiretinal fibrosis occurs with a decrease in the rate of outflow of IOF diffused from front to back towards the RPE and choriocapillaries along the posterior hyaloid membrane into the thickness of the inner layers of the retina. Stagnation of tissue fluid, coupled with an increase in the concentration of proinflammatory factors and protein fractions that have passed through the external hematophthalmic and/or hematopoietic barriers, leads to the deposition of inflammatory products on the surface of the posterior hyaloid and/or internal boundary membranes. Thus, idiopathic epiretinal fibrosis occurs as an "attempt" to suspend the amount of diffused fluid from the vitreous body into the thickness of the retina and RPE, as well as in the opposite direction during inflammatory and infectious processes of the posterior segment.

4. Discussion

4.1 AMD

Deposition of pigment granules from RPE in the thickness of the neuroepithelium occurs in maculopathy against the background of tamoxifen [40], as well as in the late stages of age-related macular degeneration. It is known that retinal vessels radially diverge on average of 8.9 ± 0.23 around the foveola, and arterioles are usually located above the venules [41]. There are more diverting venules in the parafoveolar zone than arterioles. I.e., there are about 8 channels located radially around the foveola, and one vertical from the central channel of the vitreous. Moreover, the latter plays one of the leading roles in the pathogenesis of macular diseases, since posterior vitreous detachment (PVD) is reliably a factor of protection against both pseudophakic cystic macular oedema [42] and AMD [43]. It has also been found that in diabetes mellitus, partial PVD contributes to increased proliferation, and full PVD causes a stop of the proliferative process [44].

In patients with AMD, when stimulated by a light wavelength of 488 nm, increased emission is observed with autofluorescence at the level of the Bruch membrane and subretinal deposits, in contrast to the control group without AMD [45]. This indicates an altered chemical composition of the intercellular fluid in this zone, probably due to a primary change in the outflow rate of the interstitial fluid, followed by the activation of inflammatory factors on such metabolic products as beta-amyloid, etc.

The macula has a high density of green and red cones that express carbohydrase, but in the foveola there are only blue cones that do not express carbohydrase receptors [46] and a special type of Muller astrocytic cells on the roof of the foveolar fossa. These data may indicate that through the foveola, there is normally an outflow of tissue and intraocular fluid towards the RPE and into the thickness of the retina at night and an influx during the day from the choriocapillaries to cool the RPE and remove metabolic products.

Carboanhydrase inhibitors in some patients with primary glaucoma cause choroidal effusion, which may indicate a significant outflow of intra-ocular fluid through the retina into the suprachoroidal space in these patients, especially given the presence of carboanhydrase receptors in the RPE and glia [47]. It is known that the perichoroidal space, behind on the nasal side of the eyeball, ends 2-3 mm from the exit point of the optic nerve. On the temporal side – at the central fossa of the retina, and in front – at the attachment point of the ciliary body to the scleral spur. The lymphatic vessels of the conjunctiva are maximally developed from below-inside the eyeball and have nasal-ventral and temporal-dorsal polarization [8]. The number of vorticose veins collecting blood from the choroid clearly does not allow taking the entire volume of tissue fluid, and part of the tissue fluid goes through the suprachoroidea and sclera into the lymphatic collectors of the face and neck [9]. But the central region of the retina has an additional, autonomous glymphatic outflow of tissue fluid along the glial spaces of the retina itself into the thickness of the optic nerve and its para-sheaths space.

The shape of the drusen with the convex side up indicates that the delay of tissue current and fluid stasis occurs precisely in the direction from under the RPE towards the vitreous body. The etiopathogenesis of AMD is unknown for certain changes in the structure of choriocapillaries, etc., although much is clear about the pathogenesis of this disease, including activation of the complement system and cytokines. We assume that the triggering moment of AMD is not just physiological photo-oxidative stress in the central zone of the retina, namely, a decrease in the rate of hydrodynamic flows in the macula and the occurrence of fluid stasis. A decrease in the metabolic rate in this zone and the accumulation of detritus: intralaminar basal deposits, soft and dry drusens also occur. Figure 2 shows the accumulation of fluid in the perithyroidal pocket, which is located between the Bruch membrane and hyperreflective deposits in the thickness of the detached retinal pigment epithelium which correlates with the activity of the neovascular membrane in AMD [8]. The process of neovascularization in AMD itself may be the primary adaptive factor for eliminating excess interstitial fluid accumulating in this zone through newly formed "fenestrated" vessels. It has been proven that endothelial vascular growth factor (VEGF) is the main element for the pathogenesis of wet AMD, and it also reduces the hydraulic bandwidth throughout RPE [48].

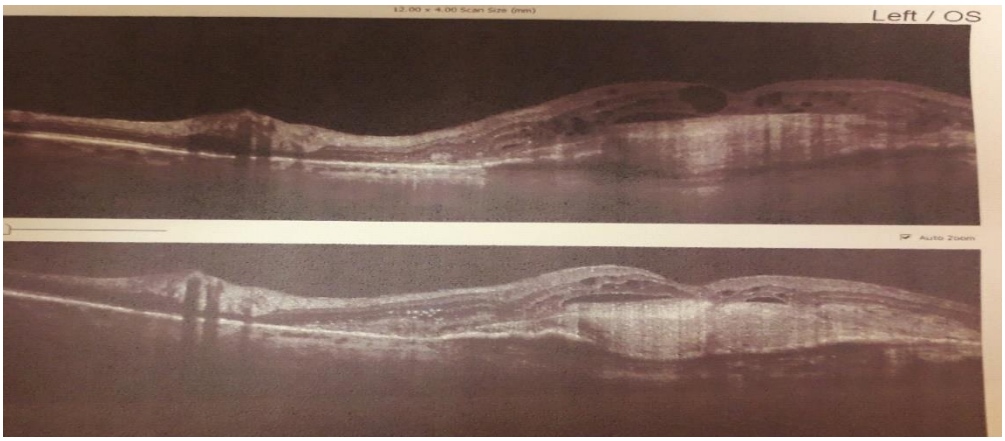

Figure 2. OCT picture of a patient with a wet form of AMD after 3 injections of anti-VEGF therapy with the presence of a prechoriodal pocket and accumulation of fluid around the scar

Thus, we assume that a decrease in the hydrodynamic parameters of the rate of transition of IOF into the interstitial fluid of the inner layers of the retina, as well as a decrease in the rate of tissue fluid exchange between the choriocapillary lobule and the outer layers of the retina are the main glymphatic components of the etiopathogenesis of age-related degenerative diseases of the macular zone. The hydrostatic pressure gradient between the vitreous, sensorineural and pigment epithelium, calculated in the area of the foveolar fossa, is about Δ 5 mm Hg. [20], which is confirmed by experimental data [49], therefore, even a slight decrease in the rate of inflow of IOF through the central channel into the macular sac and/or a decrease in the rate of fluid outflow through the RPE towards the choroid can lead to stasis of the interstitial fluid in this zone. The main reason for the decrease in the rate, is probably age-related in the production of IOF by ciliary processes and altered regulation of the transport of tissue fluid in the macula. A change in osmotic gradients between the external hematophthalmic barrier and the interphotoreceptor space, leading to fluid stasis under RPE and "intoxication" by products of the exchange of choriocapillaries, RPE cells and photoreceptors, also occurs. It is important to note that damage to ganglion cells in AMD occurs much more significantly in the exudative form of AMD than in the non-exudative form.

4.2 Macular hole

To date, there are several theories of the development of macular hole. The theory of Gass (1973), based on the disorder of functions of Muller cells located Z-shaped in the thickness of the macular zone, is complemented by the traction theory. Alpatov (2005) proved that cystic retinal oedema with subsequent trophic disorder forms the basis of structural and functional disorders around the hole, and epiretinal membranes can also form at the last stage of hole formation, after the development of complete PVD [50].

The initial or first stage (1a) of idiopathic age-related macular hole presupposes the elevation of the neuroepithelium under the foveola. i.e., the influx of fluid from under the RPE secreted by the choriocapillary lobule exceeds its absorption rate into the thickness of the retina. Further excess inflow of tissue fluid can lead to the formation of intraretinal cysts when local compensation pathways are activated by Muller cells and ILM astrocytes, but eventually leads to a divergence of the retina in the radial direction. It is known that macular hole most often primarily manifest in the morning. During the night, fluid accumulates in the thickness of the retina, which could not be "pumped" along the perivasal outflow pathways, as well as due to a violation of the physiological process of vertical outflow of tissue fluid towards the choroid due to a violation of the transport function of the RPE. Therefore, an excess of tissue fluid is formed, aiming to "go down the sides" into the thickness of the retina, while the entry point is the foveola. Hydrodynamic flows of interstitial fluid rushing along the gradient of hydrostatic pressure towards the optic disc along the axons of the ganglion cells of the papillo-macular bundle and below in the plexiform layers are normally carried out due to the processes of Muller cells and glial astrocytes, as well as convection. But when certain conditions are combined: degenerative glial changes and/or functional disorders (failure of regulation by the dopamine-melatonin system in the retina, decreased blood flow in the macular choroidal lobule, etc.), these outflow pathways are disrupted, and a macular hole occurs.

OCT images of the macular zone of the operated macular hole show that fluid accumulation in the early postoperative period (up to 1 month) occurs in the same "spaces" as in CMO: in the cystic cavities in the outer plexiform and nuclear layers (Fig. 3 and 4) and directly under the foveola (Fig.3).

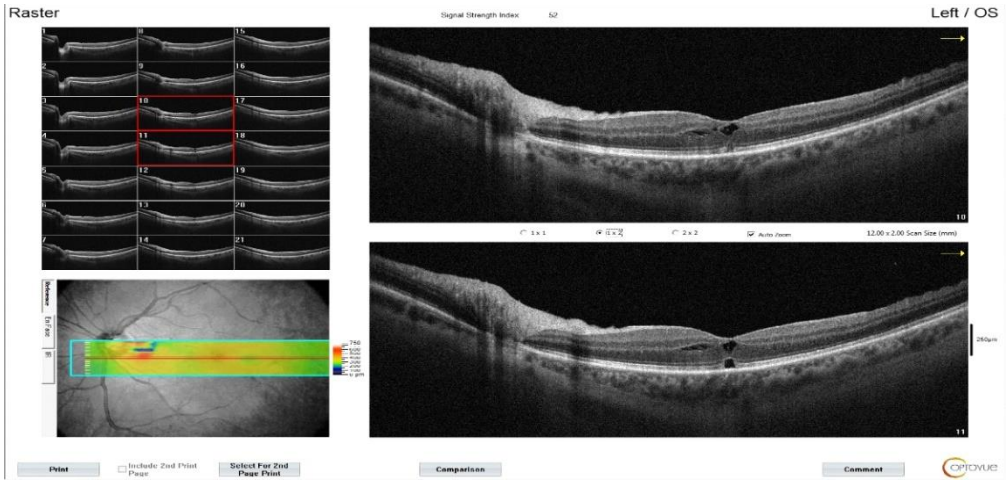

Figure 3. OCT picture of the macular interface in the early postoperative period of macular hole surgery.

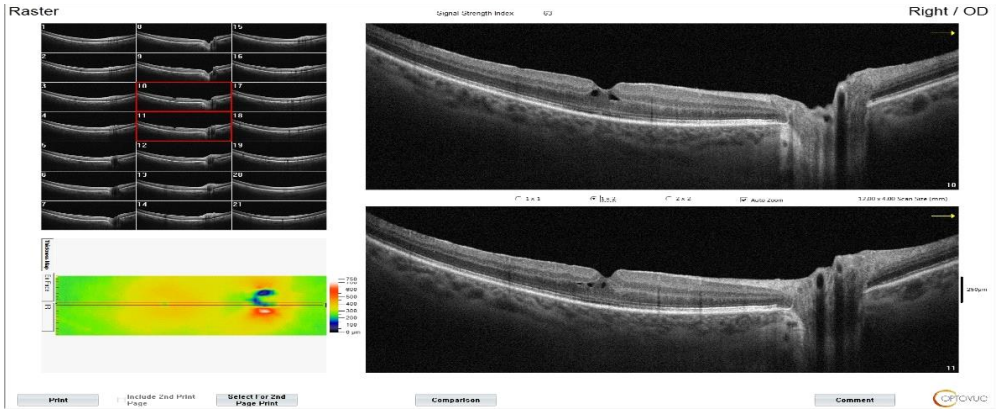

Fig. 4. OCT picture of operated macular hole with cavities in the outer layers of the retina in the early postoperative period

Thus, convection in the foveolar zone, which increases during the day under the influence of light and chemical reactions, leads to the formation of cysts with violations in the glymphatic outflow at night against the background of a malfunction in the functioning of the RPE. The dopamine-melatonin system of macular RPE and neuroepithelium performs a regulatory role and depends on circadian rhythms on the day-night principle. At night, the outflow of tissue fluid goes through the glymphatic paravasal spaces of the retina and optic nerve (central vascular bundle and venules of meningeal membranes). During the day, under the influence of light, the glymphatic fluid flows along the axons of ganglion cells and mainly through retinal veins, as well as through the capillary network of the choroid, ciliary body and optic nerve into venous and lymphatic collectors. The production of a residence permit occurs in the ciliary processes and choriocapillary lobules mainly at night and in the morning in order to activate the circulation of tissue fluid with which it is mixed.

In the macular zone there is a "crossroads" regulated by the dopamine-melatonin system through the suprachiasmal nucleus, which, thanks to the RPE, Muller cells, glial astrocytes and paravasal spaces, provides a bidirectional fluid flow in the thickness of the retina in two planes: longitudinally radial to the optic disc and transversely through the thickness of the retina. A schematic representation of the circulation of tissue fluid in the central zone is shown in Fig. 5.

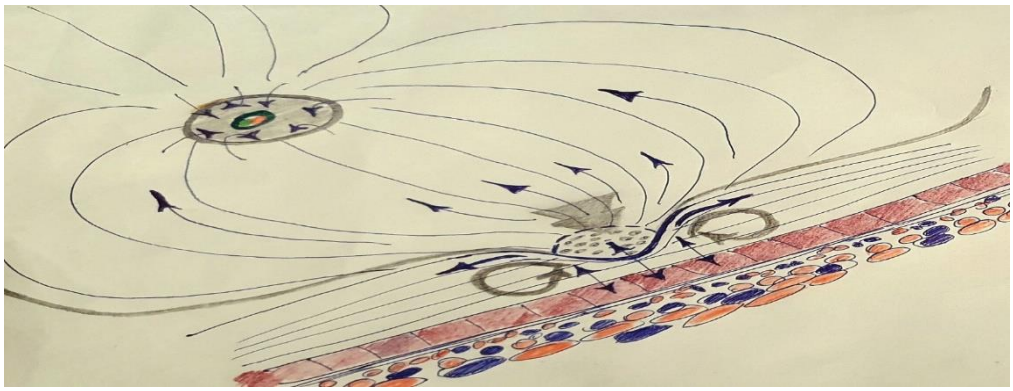

Fig. 5 Schematic representation of tissue fluid circulation in the central area of the retina. The blue arrows represent the interaxonal fluid flow (along the surface capillary network). The gray thick arrow above the foveola is the IOF flow from the central channel through and into the thickness of the retina. Gray arrows around the foveola in the thickness of the retina – the direction of fluid flow under the action of convection.

5. Conclusions

In the posterior segment of the eye, in addition to a slight fluid flow from front to back towards the RPE, there are two ways of tissue fluid flow: the first is radial, which is caused by fluid flow along the axons of ganglion cells along the paravasal pathways of the superficial capillary network into the thickness of the axons of the optic nerve. The second is longitudinal in the outer layers of the retina, draining into the paravascular glymphatic spaces of the optic nerve and to a lesser extent under the RPE in the choriocapillaries. The first one functions mainly at night in a horizontal position under the influence of gravity and hydrodynamic gradients of the bags and channels of the vitreous body and the pressure of the cerebrospinal fluid, and the second direction of the tissue fluid flow occurs during the day and is due to the electrochemical potential of the visual act, i.e. heating of the retina in the macular zone and the difference in temperatures in different parts of the retina, i.e. convection.

Application of artificial intelligence:

The article is written without the use of artificial intelligence technologies.

Acknowledgments: None.

Author Contributions Author Contributions: Conceptualization, J.B., A.S. and S.K.; methodology, J.B..; investigation, J.B. and A.S.; writing—original draft preparation, J.B..; writing—review and editing, J.B, A.S. and S.K..; visualization, J.B and A.S..; supervision, S.K.; All authors have read and agreed to the published version of the manuscript.

Funding: No funding

Institutional Review Board Statement: Obtained.

Informed Consent Statement: Informed consent was obtained from all subjects involved in the study.

Conflicts of Interest: The authors declare no conflict of interest.

References

1. Ouyang Y, Keane PA, Sadda SR, Walsh AC. Detection of cystoid macular edema with three-dimensional optical coherence tomography versus fluorescein angiography. Investigative Ophthalmology & Visual Science. 2010;51(10):5231-5218.
2. Erichev VP, Petrov SYu, Orekhova NA, El'murzaeva LKh. Hypotony maculopathy after glaucoma surgery:pathogenic mechanisms, diagnostic tools, and treatment modalities. Russian Journal of Clinical Ophthalmology. 2020;20(1):26-31 (in Russ)
3. Gass JD. Nicotinic acid maculopathy. American Journal of Ophthalmology.1973;76(4):500-510
4. Bourla DH, Sarraf D, Schwartz SD. Peripheral retinopathy and maculopathy in high-dose tamoxifen therapy. American Journal of Ophthalmology. 2007;144(1):126-128.
5. Chlasta-Twardzik E, Nowinska A, Wylegata E. Acute macular edema and serous detachment on the first day after phacoemulsification surgery: A case report. American Journal of Ophthalmology Case Reports. 2020; 20:100905
6. Spalton DJ, Bird A.C, Clearly PE. Retinitis pigmentosa and retinal oedema. British Journal of Ophthalmology, 1978, 62, 174-182.
7. Budzinskaya MV, Plyukhova AA. New qualitative Methods for Assessing the "Fluid" in the retina in age-related macular degeneration. Ophthalmology in Russia. 2021;18(2):222-227. (in Russ).
8. Cozzi M, Monteduro D, Parrulli S, Ristoldo F, Corvi F, Zicarelli F, Staurenghi G, Invernizzi A. Prechoroidal cleft thickness correlates with disease activity in neovascular age-related macular degeneration. Graefe's Archive for Clinical and Experimental Ophthalmology. 2022;260(3):781-789.
9. Subileau M, Vittet D. Lymphatics in eye fluid homeostasis: minor contributors or significant actors? Biology. 2021;10,582.

10. Chernkykh VV, Bgatova NP. Lymphatic structures of the eye and uveolymphatic (metabolic) pathway of intraocular fluid outflow. Part 1. Russian journal of glaucoma. 2018;17(1):3-13 (In Russ)
11. Yücel YH, Johnston MG, Ly T, Patel M, Drake B, Gümüş E, Fraenkl SA, Moore S, Tobbia D, Armstrong D, Horvath E, Gupta N. Identification of lymphatics in the ciliary body of the human eye: a novel "uveolymphatic" outflow pathway. Experimental Eye Research. 2009; 89(5):810-819.
12. Petrov SYu. Lymphatic system of the eye. Russian journal of glaucoma. 2011;3:58-62 (In Russ).
13. Iliff JJ, Wang M, Liao Y, Plogg BA, Peng W, Gundersen GA, Benveniste H, Vates GE, Deane R, Goldman SA, Nagelhus EA, Nedergaard M. A paravascular pathway facilitates CSF flow through the brain parenchyma and the clearance of interstitial solutes, including amyloid ß. Science Translational Medicine.2012; 4 (147):147-151.
14. Iliff JJ, Wang M, Zeppenfeld DM, Venkataraman A, Plog BA, Liao Y, Deane R, Nedergaard M. Cerebral arterial pulsation drives paravascular CSF-interstitial fluid exchange in the murine brain. The Journal of Neuroscience, 2013;13(46):18190-18199.
15. Mestre H, Mori Y, Nedergaard M. The brain glymphatic system: current controversies. Trends in Neurosciences. 2020; 43 (7):458-466.
16. Wang X, Lou N, Eberhardt A,Yang Y, Kusk P, Xu Q, Förstera B, Peng S, Shi M, Lardon-de-Guevara A, Delle C, Sirgurdsson B, Xavier ALR, Ertürk A, Libby RT, Chen L, Thrane AS, Nedergaard M. An ocular glymphatic clearance system removes ß-amyloid from the rodent eye. Science Translational Medicine. 2020; 12
17. Petzold A. Retinal glymphatic system: an explanation for transient retinal layer volume changes? Brain, 2016;139 (11);2816-2819.
18. Denniston AK, Keane PA. Paravascular pathways in the eye: is there an "Ocular Glymphatic System"? Investigative Ophthalmology & Visual Science. 2015;56(6):3955-3956.
19. Errera M-H, Coisy S, Fardeau C. Retinal vasculitis imaging by adaptive optics. Ophthalmology. 2014; 121:1311-1312.
20. Beisekeeva J, Kulumbetova J, Beisekeev S, Kochergin SA. Hydrostatic pressure gradients and a new membrane-glymphatic theory of primary glaucoma. Investigative Ophthalmology & Visual Science. 2022;7(1): 14-25.
21. Beisekeeva J, Bezrukov AV, Kochergin SA. Acute transient macular edema after uneventful cataract surgery. Ophthalmology in Russia. 2021;18(3):442-450 (in Russ).
22. Boulanger G, Weber M. Irvine Gass syndrome and central serous chorioretinopathy, pure coincidence or non fortuitous association? Report of three cases. French Journal of Ophthalmology. 2009; 32(8):566-571
23. Astroz P, Balaratnasingam C, Yannuzzi LA. Cystoid macular edema and cystoid macular degeneration as a result of multiple pathogenic factors in the setting of central serous chorioretinopathy. Retinal Cases and Brief Reports.2017; 1:197-201.
24. Iida T, Yannuzzi LA, Spaide RF et al. Cystoid macular degeneration in chronic central serous chorioretinopathy. Retina. 2003 ;23(1):1-7;137-145.
25. Michels RG, Green WR, Maumenee AE. Cystoid macular edema following cataract extraction (The Irvine-Gass Syndrome): a case studied clinically and histopathologically. Ophthalmic Surgery.1971; 2:217-221.
26. McDonnell PJ, de la Cruz ZC, Green WR. Vitreous incarceration complicating cataract surgery: a light and electron microscopic study. Ophthalmology. 1986;93:247-253.
27. Beisekeeva ZhS, Kulumbetova DE, Kochergin SA. Lymphatic circulation of the eye: anatomical-histo-physiological aspects. Modern science: actual problems of theory and practice. Natural and Technical Sciences, 2022; 3:7-12. (in Russ).
28. Newman E, Reichenbach A. The Muller cell: a functional element of the retina. Trends in Neurosciences, 1996, 19(8):307-312.
29. Alkozi HA, Wang X, Perez de Lara MJ, Pintor J. Presence of melanopsin in human crystalline lens epithelial cells and its role in melatonin synthesis. Experimental Eye Research. 2017;154:168-176
30. Sengupta A, Baba K, Mazzoni F et al. Localization of melatonin receptor 1 in mouse retina and its role in the circadian regulation of the electroretinogram and dopamine levels. Public Library of Science. 2011; 6(9):1-7.
31. Tosini G, Alcantara-Conteras S, Sengupta A, Baba K. Removal of melatonin receptor type 1 increases intraocular pressure and retinal ganglion cells death in the mouse. Investigative Ophthalmology & Visual Science. 2010; 51: 1628.
32. Milenkovic VM, Krejcova S, Strauß. Interaction of Bestrophin-1 and Ca 2+ Channel ß-subunits: identification of new binding domains on the Bestrophin-1 C-terminus. Public Library of Science One.2011; 6(4):19364.
33. Mogensen FL-H, Delle C, Nedergaard M. The Glymphatic system (en)during inflammation. International Journal of Molecular Sciences. 2021; 22:7491.
34. Nagelhus EA, Veruki ML, Torp R, Haug FM, Laake JH, Nielsen S, Agre P, Ottersen OP. Aquaporin-4 water channel protein in the rat retina and optic nerve: polarized expression in Muller cells and fibrous astrocytes. The Journal of Neuroscience. 1998; 18 (7): 2506-2519.
35. Sari ES, Ermis SS, Yazici A, Koytak A, Sahin G, Kilic A. The effect of intracameral anesthesia on macular thickness and ganglion cell-inner plexiform layer thickness after uneventful phacoemulsification surgery: prospective and randomized controlled trial. Graefe's Archive for Clinical and Experimental Ophthalmology. 2014;252(3):433-9.
36. Makri OE, Tsapardoni FN, Plotas P, Ifantis N, Xanthopoulou PT, Georgakopoulos CD. Cystoid macular edema associated with preservative-free latanaprost after uncomplicated cataract surgery: a case report and review of the literature. BMC Research Notes.2017;10 (1):127
37. Weisz JM, Bressler NM, Bressler SB, Schachat AP. Ketorolac treatment of pseudophakic cystoid macular edema identified more than 24 months after cataract extraction. Ophthalmology. 1999;106(9):1656-9.
38. Nikolaenko VP, Terekhova IV, Panova TYu, Antonova AV. Treatment of refractory glaucoma combined with cystic macular edema. Ophthalmological statements. 2017;10 (2):36-39. (in Russ).
39. Schlötzer-Schrehardt U, Zenkel M, Nüsing RM. Expression and localization of FP and EP prostanoid receptor subtypes in human ocular tissues. Investigative Ophthalmology & Visual Science. 2002;43(5):1475-87.
40. Hui-Bon-Hoa AA, Defoort-Dhellemmes S, Tran THC. Atrophic tamoxifen maculopathy French Journal of Ophthalmology. 2011;34(1):35.1-5. French.
41. Yu PK, Balaratnasingam C, Cringle SJ, McAllister IL, Provis J, Yu DY. Microstructure and network organization of the microvasculature in the human macula. Investigative Ophthalmology & Visual Science. December 2010;51(12):6735-43..
42. Gulkilik G, Kocabora S, Taskali M, Engin G. Cystoid macular edema after phacoemulsification: risk factors and effect on visual acuity. Canadian Journal of Ophthalmology. 2006;41(6):699-703.
43. Bakaliou A, Georgakopoulos C, Tsilimbaris M, Farmakakis N. Posterior Vitreous Detachment and Its Role in the Evolution of Dry to Wet Age Related Macular Degeneration. Clinical Ophthalmology. 2023;17:879-885.
44. Akhmanitskaya LI. Violation of vitreous homeostasis in children with retinopathy of prematurity (experimental clinical study). Dissertation for the degree of Candidate of Medical Sciences.2016;28. (in Russ).
45. Marmorstein AD, Sakaguchi H, Hollyfield JG. Spectral profiling of autofluorescence associated with lipofuscin, Bruch's membrane, and sub-RPE deposits in normal and AMD eyes. Investigative Ophthalmology & Visual Science. 2002; 43(7):2435-41.

46. Nork TM. Acquired color vision loss and a possible mechanism of ganglion cell death in glaucoma. Transactions of the American Ophthalmological Society. 2000; 98:331-363.
47. Nagelhus EA, Mathiisen TM, Bateman AC, Haug FM, Ottersen OP, Grubb JH, Waheed A, Sly WS. Carbonic anhydrase XIV is enriched in specific membrane domains of retinal pigment epithelium, Muller cells, and astrocytes. Proceedings of the National Academy of Sciences of the United States of America. 2005;102(22):8030-5.
48. Dahrouj M, Alsarraf O, McMillin JC, Liu Y, Crosson CE, Ablonczy Z. Vascular endothelial growth factor modulates the function of the retinal pigment epithelium in vivo. Investigative Ophthalmology & Visual Science. 2014;55(4):2269-75.
49. Smith DW, LeeC-J, Gardiner BS. No flow through the vitreous humor: How strong is the evidence? Progress in Retinal and Eye Research. 2020:100845.
50. Alpatov S.A. Patterns and mechanisms of development of idiopathic macular ruptures, development of pathogenetic principles of treatment. Abstract for the degree of Doctor of Medical Sciences. 2005:5 (in Russ).

Article

Anhedonia, Decrease in Exploratory Activity, and Changes in the Level of Anxiety in Rats Under Chronic Ultrasound Exposure

Anna Gorlova [1], Dmitry Pavlov[2], Anatoly Inozemtsev [1,*]

[1] Department of Higher Nervous Activity Lomonosov Moscow State University, Moscow, Russia;
[2] Research Institute of General Pathology and Pathophysiology, Moscow, Russia
* Correspondence: a_inozemtsev@mail.ru; Tel.: +74959395001;
a_inozemtsev@mail.ru, https://orcid.org/0000-0002-5059-3241 (A.I.).

Abstract: In this work we investigated the effect of chronic ultrasonic exposure to variable frequencies in the range of 20-45 kHz for 1, 2 and 3 weeks on anxiety, exploratory activity and anhedonia in rats. The animals recorded the development of anhedonia and a decrease in exploratory activity in the Open Field, Elevated Cross Maze and Dark Light Chamber tests, indicating the formation of a depressive-like state in them. These behavioural changes were manifested simultaneously after 2 weeks of ultrasound exposure. At the same time, the rats did not show a decrease in horizontal activity, as well as the ratio of time spent in open and closed areas of the arena.

Keywords: rats, ultrasound, depression-like state, anxiety, exploratory activity, anhedonia.

Citation: Gorlova A., Pavlov D., Inozemtsev A. Anhedonia, Decrease in Exploratory Activity, and Changes in the Level of Anxiety in Rats Under Chronic Ultrasound Exposure. Journal of Clinical Physiology and Pathology (JISCPP) 2023; 2 (4): 42-48.

https://doi.org/10.59315/JISCPP.2023-2-4.42-48

Academic Editor: Igor Kastyro

Received: 11.10.23
Revised: 02.11.23
Accepted: 07.12.23
Published: 29.12.23

Publisher's Note: International Society for Clinical Physiology and Pathology (ISCPP) stays neutral with regard to jurisdictional claims in published maps and institutional affiliations.

1. Introduction

More than 350 million people worldwide are currently diagnosed with a depressive disorder [Pehrson, Sanchez, 2015], so it is an urgent problem to study the development of a depressive-like state in experimental animals. Most of the existing models are based on direct physical effects on the experimental animal [Grigoryan, Gulyaeva, 2015; Duman, 2010], but the so-called emotional stress is closer to the causes of human depression development. One way to build such a model could be to use an unpredictable alternation of positive and negative stimuli, as was done in the experiments of I.P. Pavlov's associates when creating functional disorders of higher nervous activity.

On the basis of such alternation a new ultrasonic model of depressive-like state of animals was developed and tested [Morozova et al., 2016; Gorlova et al., 2017]. Ultrasound frequencies of 20-45 kHz, which fall within the range of normal rodent vocalization, are used as a stressor, with frequencies of 20-25 kHz being classified as so-called "negative", as they are emitted by animals during pain stimulation or defeat in a fight, and frequencies of the 25-45 kHz range being classified as "positive", as they are emitted by rats during food reinforcement or coitus [Brudzynski, 2007; Litvin et al., 2007]. In the model used, frequencies in the range of 20-45 kHz are randomly presented and produce a clash of opposing emotional and motivational stimuli. Thus, the stressor factor of this model can be considered one of the closest to the causes of stress-induced depressive disorder in humans, and the model of chronic ultrasonic exposure itself can be considered as a model of chronic information uncertainty [Ushakova et al., 2019; Morozova et al., 2007].

An increased level of anxiety often serves as a hallmark of rodent behavior with induced depression-like state [Zhang et al., 2017]. Typically, depression-like states and anxiety disorders are studied together by experimenters, as increased anxiety and depressive disorders can occur simultaneously [Estrela et al., 2015]. However, these conditions are not necessarily related to each other and have different etiologies (Knyazev et al., 2016). For example, some patients are found to have depression associated with anhedonia, an inability to experience pleasure, but not associated with increased anxiety. This raises the question of the relationship between anhedonia and anxiety in experimental animals in different models of depression-like states.

An interesting issue remains the analysis of stress-induced changes in research activity in animals, which is an important indicator of natural interest in novelty [Stepanichev et al., 2014]. In the available studies devoted to simulating the depressive-like state in rodents, exploratory activity has not been considered before in a whole battery of tests, although its close relationship, for example, with passive behaviour in stressful situations has been noted [Mällo et al., 2007].

The objectives of this work were to comprehensively study anhedonia, changes in anxiety levels and exploratory activity in rats during the development of a depressive-like state in an ultrasound stress model.

2. Patients and Methods

Experiments were performed on male Sprague-Dawley rats from the Central Laboratory Animal Breeding Facility of the Russian Academy of Sciences (Andreevka). At the beginning of the experiment, the animals were 2.5 months old. The animals were kept in individual polycarbonate cages of 30 × 20 × 15 cm at a constant temperature of 23°C, controlled direct light, 12:12 h, and free access to water and food. Rat housing and all experimental procedures were performed in accordance with international animal handling regulations (European Community Directive 2010/63 of 22 September 2010). Three experimental groups and four control groups were used. The experimental groups were subjected to continuous exposure to ultrasonic waves in the range 20-45 kHz for 1, 2 or 3 weeks; the control groups were not stressed. Three control groups were used to study the contribution of individual housing; the animals were kept in separate cages for 1, 2 or 3 weeks under conditions identical to those of the experimental groups except for ultrasound exposure. In the fourth control group, rats were kept 5 animals each in 55 × 35 × 20 cm cages. Each group consisted of 10 individuals. The animals were not exposed to any other potentially stressful conditions. All rats involved in the experiment were intact and had not previously participated in other experiments.

Ultrasonic exposure in the 20-45 kHz range was performed using an ultrasonic generator (Wietech, Belgium); the sound pressure level at the experiment distance of 1.5 m to the animal cage was 80 dB.

One day after the end of the ultrasound exposure, behavioural testing was carried out. Animal behavior in all tests was recorded by digital video camera and analyzed using computer program RealTimer (Open Science, Russia). The intervals between the tests for all groups were one day. The following behavioral tests were used:

- Sucrose solution preference test. For 24 h, rats were simultaneously given access to choose between two identical drinkers, one containing 1% sucrose solution and the other containing plain water. The location of the drinkers was changed after 12 h to eliminate the effect of site preference. Sucrose solution preference was calculated using the following formula: Preference = (weight of sucrose solution/total weight of fluid consumed) × 100%. Consumption of water and sucrose solution was estimated by weighing the drinkers before and after the experiment.

- Open field test. The rat was placed in a 45 × 45 × 40 cm grey plastic chamber, divided into peripheral and central sectors. The total time the rat spent in the central and peripheral sectors and the number of perfect racks, as well as the number of crossed sectors, were recorded for 5 min.

- Elevated cross maze test. The rat was placed in a setup consisting of two closed (29 cm high walls) and two open (0.5 cm high sides) arms measuring 52 × 14 cm, with a central platform measuring 14 × 14 cm, placed 100 cm above the floor. The test animal was placed in the centre of the unit and the time spent in closed and open arms, the number of perfect stances, peeks from closed arms into the open arms of the maze and peeks from the open arms were recorded for 5 min.

- Dark Light Chamber Test. The rat was placed in a unit consisting of two compartments measuring 30 × 30 × 32 cm. One compartment was darkened, the other was brightly illuminated. For 5 min, the total time the animal spent in the bright compartment, the number of stoops made in the bright compartment, and the number of peeks from the dark compartment were recorded.

- Statistics. Data on measured behaviors were expressed as Mean±SEM. Statistical analyses were performed using two-factor ANOVA for significance of single and ultrasonic factors, followed by post hoc analysis with Fisher's LSD test. Differences were considered statistically significant at $p < 0.05$. A Kolmogorov-Smirnov test was performed beforehand, the results of which did not negate the normal distribution, except for the number of hangings from the open arm of the elevated cruciform labyrinth. For this case, the Kruskal-Wallis test was used, followed by a Dunn's multiple comparison test. A one-way ANOVA was used for statistical analysis of sucrose solution preference prior to the experiment. GraphPadPrism version 6.0 software was used for statistical analysis.

3. Results

There was no statistically significant difference in sucrose preference between the groups before the experiment ($F6.63 = 0.12$, $p = 0.96$, one-way ANOVA, Figure 1(a)). There was no statistically significant interaction between the single content and ultrasound factors ($F9.54 = 0.36$, $p = 0.699$, two-way ANOVA), and no statistically significant effect of the individual content factor on sucrose solution preference ($F3.54 = 2.43$, $p = 0.097$, two-way ANOVA). However, the factor of chronic ultrasound exposure was statistically significant ($F3.54 = 8.42$, $p = 0.0054$, two-way ANOVA). Reduced preference for sucrose solution relative to plain water was evident after 2

weeks of stress exposure (p = 0.0313, post hoc Fisher's LSD test) and persisted after 3 weeks of exposure (p = 0.0046, post hoc Fisher's LSD test; Fig. 1(b).

There was no statistically significant interaction between the single content and ultrasound exposure factors in the Open Field test (F9.54 = 0.31, p = 0.733, two-way ANOVA), no statistically significant effect of the individual content factor (F3. 54 = 0.07, p = 0.927, two-way ANOVA) and a statistically significant effect of the ultrasound exposure factor (F3.54 = 0.13, p = 0.725, two-way ANOVA) on the ratio of time spent by animals in the central sector to time spent in the periphery (Figure 2 (a)).

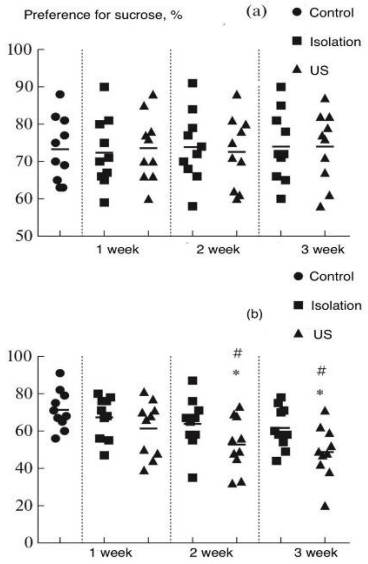

Figure 1. Effect of ultrasound on the preference of sucrose in rats. 2 and 3 weeks of ultrasound stress resulted in a decrease of the sucrose preference in comparison with the control group (* – p ‹ 0.05, Fisher's LSD test) and relevant groups in which rats were housed individually for 2 or 3 weeks (# – p ‹ 0.05, Fisher's LSD test). (a) – Sucrose preference at the beginning of the experiment. The group names correspond to the way they were subsequently distributed. (b) – Sucrose preference of the experimental groups.

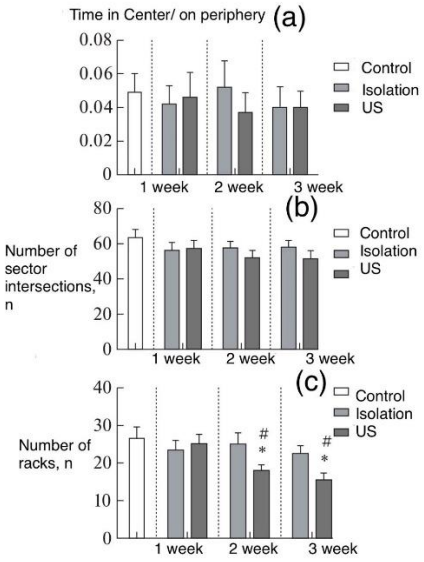

Figure 2. Effect of ultrasound on the behavior of rats in the Open Field test. (a) – Chronic ultrasound stress did not change the proportion between time spent in the central area and time spent in the periphery. (b) – Chronic ultrasound stress did not change the number of crossed sectors. (c) – 2 and 3 weeks of ultrasound stress resulted in a decrease of the number of rearings in comparison with the control group (* – p ‹ 0.05, Fisher's LSD test) and relevant groups in which rats were housed individually for 2 or 3 weeks (# – p ‹ 0.05, Fisher's LSD test).

There was also no statistically significant interaction between the single confinement and ultrasonic exposure factors (F9.54 = 0.48, p = 0.622, two-way ANOVA), no statistically significant effect of the individual confinement factor (F3.54 = 0.15, p = 0.865, two-way ANOVA) and no statistically significant effect of the ultrasonic exposure factor (F3.54 = 1.12, p = 0.295, two-way ANOVA) on the number of sectors crossed (Fig. 2 (b)). Thus, the effect of the ultrasound on the level of anxiety and horizontal activity in the Open Field test was found to be insignificant. Regarding the number of perfect racks, there was no statistically significant interaction between the single content and ultrasound factors (F9.54 = 2.33, p = 0.106, two-way ANOVA) and no statistically significant effect of the individual content factor (F3.54 = 2.05, p = 0.09, two-way ANOVA) on this parameter. However, the effect of the ultrasound exposure factor was statistically significant (F3.54 = 4.66 p = 0.035, two-way ANOVA). Namely, a decrease in the number of perfect racks was registered after 2 weeks (p = 0.0471, post hoc Fisher's LSD test) and after 3 weeks of stress exposure (p = 0.0256, post hoc Fisher's LSD test; Fig. 2(c).

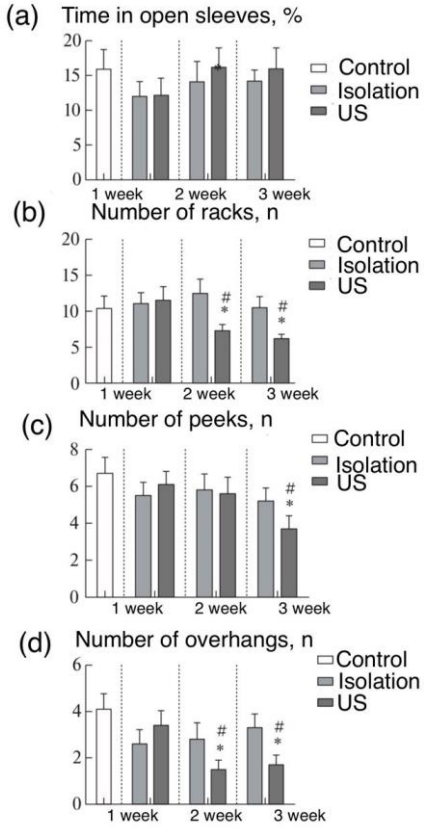

Figure 3. Effect of ultrasound on the behavior of rats in the "Elevated plus-maze" test. (a) – Chronic ultrasound stress did not change the percent of time spent by animals in the open arm of the maze. b) – 2 and 3 weeks of ultrasound stress led to a decrease in the number of rearings compared with the control group (* – p ‹ 0.05, Fisher's LSD test) and relevant groups in which rats were housed individually for 2 or 3 weeks (# – p ‹ 0.05, Fisher's LSD test). (c) – 3 weeks of ultrasound stress led to a decrease in the number of looking-outs compared with the control group (* – p ‹ 0.05, Fisher's LSD test) and relevant groups in which rats were housed individually for 3 weeks (# – p ‹ 0.05, Fisher's LSD test). (d) – 2 and 3 weeks of ultrasound stress led to a decrease in the number of hanging outs compared with the control group (* – p ‹ 0.05, Fisher's LSD test) and relevant groups in which rats were housed individually for 2 or 3 weeks (# – p ‹ 0.05, Fisher's LSD test).

In the Elevated Cross Labyrinth test, there was no statistically significant interaction between the single content and ultrasound exposure factors (F9.54 = 0.08, p = 0.922, two-way ANOVA), no statistically significant effect of the individual content factor (F3. 54 = 0.92, p = 0.404, two-way ANOVA) and a statistically significant effect of the ultrasonic exposure factor (F3.54 = 0.43, p = 0.516, two-way ANOVA) on the percentage of time rats spent in the open arm (Figure 3 (a)). When the number of racks performed by the animals was considered, there was no statistically significant interaction between the factors single confinement and ultrasonic exposure (F9.54 = 2.03, p = 0.141, two-way ANOVA), no statistically significant effect of the factor individual confinement (F3. 54 = 1.96, p = 0.152, two-way ANOVA), but there was a statistically significant effect of the ultrasound exposure factor (F3.54 = 6.2, p = 0.0159, two-way ANOVA): rats committed

fewer stoops after 2 weeks (p = 0.0455, post hoc Fisher's LSD test) and after 3 weeks exposure to ultrasound (p = 0.0394, post hoc Fisher's LSD test; Fig. 3 (b). There was also no statistically significant effect of the individual confinement factor on the number of peeks performed by the rats (F3.54 = 2.19, p = 0.145, two-way ANOVA), but there was a significant interaction of confinement and exposure to ultrasound (F9.54 = 3.41, p = 0.0402, two-way ANOVA) and a statistically significant effect of the ultrasound exposure factor (F3.54 = 5.31, p = 0.079, two-way ANOVA). Rats made fewer peeks after 3 weeks of stress exposure (p = 0.0247, post hoc Fisher's LSD test; Fig. 3 (c). There was a difference between groups in the number of hopping out of open maze arms (H = 19.82, p = 0.003, Kruskall-Wallis test). The rats made fewer hopping after 2 weeks (p = 0.0337, Dunn's test), and after 3 weeks of stress exposure (p = 0.0135, Dunn's test; Fig. 3 (d).

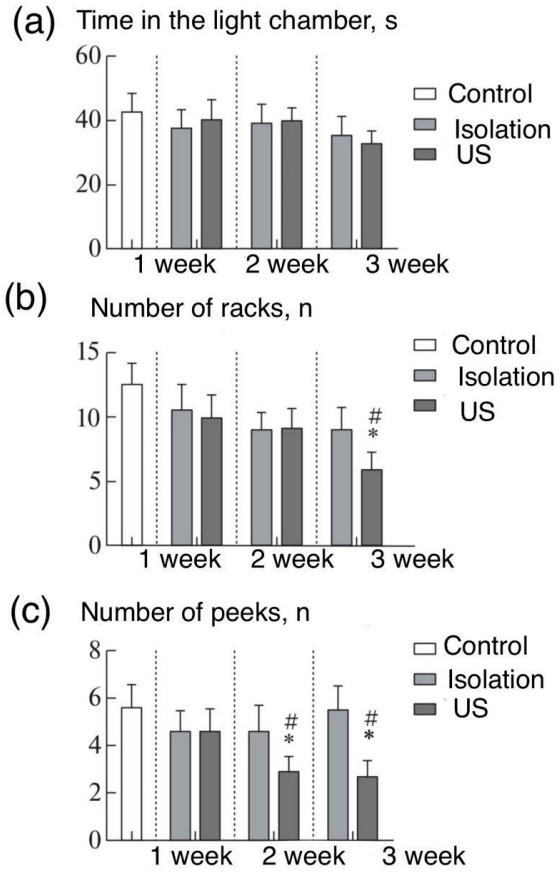

Figure 4. The influence of ultrasound on the behavior of rats in the "Dark-Light box" test. (a) – Chronic ultrasonic stress did not lead to a change in the time spent by the animals in the light box of the arena. (b) – 3 weeks of ultrasound stress led to a decrease in the number of rearings compared with the control group (* – $p < 0.05$, Fisher's LSD test) and relevant groups in which rats were housed individually for 3weeks (# – $p < 0.05$, Fisher's LSD test). (c) – 2 and 3 weeks of ultrasound stress led to a decrease in the number of looking-outs compared with the control group (* – $p < 0.05$, Fisher's LSD test) and relevant groups in which rats were housed individually for 2 or 3 weeks (# – $p < 0.05$, Fisher's LSD test).

There was no statistically significant interaction between the single content and ultrasound exposure factors (F9.54 = 0.136, p = 0.873, two-way ANOVA), a statistically significant effect of the individual content factor (F3. 54 = 0.0144, p = 0.969, two-way ANOVA) and a statistically significant effect of the ultrasound exposure factor (F3.54 = 0.617, p = 0.543, two-way ANOVA) on the time the rats spent in the light compartment (Figure 3 (a)). There was also no statistically significant interaction between the factors single housing and ultrasonic exposure (F9.54 = 1.79, p = 0.176, two-way ANOVA) and no statistically significant effect of the factor individual housing (F3.54 = 2.32, p = 0.134, two-way ANOVA) on the number of stances the animals performed. However, the effect of exposure to ultrasound was significant (F3.54 = 3.19, p = 0.049, two-way ANOVA). Rats performed fewer stoops after 3 weeks of stress exposure (p = 0.036, post hoc Fisher's LSD test; Fig. 4 (b). In addition, there was no statistically significant interaction between the single confinement and ultrasonic exposure factors (F9.54 = 1.26, p = 0.292, two-way ANOVA) and no statistically significant effect of the individual confinement factor (F3.54 = 0.46, p = 0.632, two-way ANOVA) on the number of times rats looked out of the dark compartment, but the effect of the ultrasonic

exposure factor was significant ($F_{3.54} = 4.27$, $p = 0.0436$, two-way ANOVA). The rats committed fewer racks after 2 weeks ($p = 0.047$, post hoc Fisher's LSD test) and after 3 weeks of stress exposure ($p = 0.044$, post hoc Fisher's LSD test; Fig. 4 (d).

4. Discussion

One of the classic signs of clinical depression is a decreased capacity for pleasure. Normally, rodents prefer to consume a sweetened solution, while in the presence of a depressive-like state this preference is absent, which is considered as anhedonia (Overstreet, 2013). The test for the development of anhedonia is the most common criterion for determining a depressive-like state in rodents [Moreau, 2012]. According to our data, chronic exposure to variable frequency ultrasound for 2 weeks or more can induce anhedonia in rats, which confirms the validity of this model.

It is known from the literature that most theoretical and experimental studies emphasize the close relationship between anxiety and the development of both human clinical depression [Rallis et al., 2014; Fan et al., 2015] and rodent depression-like state [Beerya, Kauferb, 2015; Huang et al., 2017; Neumann et al., 2011; Frazer, Morilak, 2005]. However, increased anxiety levels in rodents do not always manifest together with the development of depressive-like disorders, similar to what is observed in patients with clinical depression [Ju et al., 2018; Knyazev et al., 2016]. Therefore, it was of interest for us to assess the possible change in the level of anxiety accompanying the development of depression-like state in rats in a new model of chronic ultrasound exposure.

The data on the effect of chronic ultrasound exposure on anxiety levels in rats were contradictory. On the one hand, similar results were observed in all tests aimed at examination of anxiety: namely, experimental groups of rats did not spend statistically significantly less time in the central sector in the "Open Field" test, open arms in the "Elevated Cross Labyrinth" test or light chamber in the "Dark Light Chamber" test, which may be regarded as a sign of absence of increased anxiety. On the other hand, a number of findings confirm the possibility of an increased level of anxiety under the influence of ultrasound, which is expressed in a decrease in the number of peeks into open arms of the maze and peeks out of open arms in the Elevated Cruciform Maze test, and a decrease in the number of peeks into the light chamber in the Dark Light Chamber test.

It is known that assessing the level of anxiety of an experimental animal is a complex task, since in different experimental models the same animals may exhibit different behaviour [Bourin et al., 2007; Ramos, 2008], and therefore to determine the level of individual anxiety or predisposition to the effects of emotional stress it is recommended to use several tests for the same animals [Sudakov et al., 2013]. The similarity of changes in the behavior of experimental animals traced in this work suggests the absence of development of obvious signs of anxiety associated with the depressive-like state of mice induced by chronic ultrasound exposure, however, the influence of this type of stress on the anxiety level of experimental animals cannot be completely excluded.

Thus, the data obtained in our model rather support the possibility of an anxiety-independent development of a depressive-like state, already described in the literature [Overstreet, 2012]. However, the presence of this relationship manifested at the behavioural level and the mechanisms responsible for the presence or absence of increased anxiety as a comorbidity of depressive disorder need to be further explored.

Also in the present study, research activity in experimental animals was examined in detail. It was found that rats exposed to ultrasound develop a significant decrease in exploratory activity in all of the tests used. Therefore, along with assessment of other depressive-like state parameters, this index may be considered important and meaningful for consideration in this type of research. The change in exploratory activity observed under stress in experimental animals is considered to replicate the symptoms characteristic of human depression - loss of interest in novelty and any activity [Garibova et al., 2017]. In view of this, the decrease in rat activity index during chronic ultrasound exposure once again confirms the validity of the model.

5. Conclusions

The ultrasonic stress model results in the development of anhedonia and reduced research activity in experimental animals.

Application of artificial intelligence:

The article is written without the use of artificial intelligence technologies.

Conflicts of Interest: The authors declare no conflict of interest.

References

1. Garibova TL, Kraineva VA, Voronina TA. Behavioural experimental models of depression. Pharmacokinetics and pharmacodynamics. 2017; 3: 14-19.

2. Grigoryan GA, Gulyaeva NV. Modelling depression in animals: behaviour as a basis for methodology, assessment criteria and classification. Journal of Higher Nervous Activity. 2015, 6: 643-660.
3. Gorlova AV, Pavlov DA, Ushakova VM, Zubkov EA, Morozova AY, Inozemtsev AN, Chekhonin VP. Dynamics of development of depression-like state in rats stressed by chronic exposure to ultrasound of variable frequencies. Bulletin of Experimental Biology and Medicine. 2017; 3: 271-274.
4. Morozova AY, Zubkov EA, Storozheva ZI, Kekelidze ZI, Chekhonin VP. Influence of ultrasonic radiation on the formation of symptoms of depression and anxiety in rats. Bulletin of Experimental Biology and Medicine. 2012; 12: 705-708.
5. Sudakov SK, Nazarova GA, Alekseeva EV, Bashkatova VG. Determination of anxiety level in rats: discrepancy of results in tests "open field", "cross-shaped elevated maze" and Vogel's test. Bulletin of Experimental Biology and Medicine. 2013; 10: 489-493.
6. Ushakova VM, Gorlova AV, Zubkov EA, Morozova AY, Zorkina YA, Pavlov DA, Inozemtsev AN, Chekhonin VP. Experimental models of depressive state. Journal of Higher Nervous Activity. 2019; 2: 230-247.
7. Beerya AK, Kauferb D. Stress, social behavior, and resilience: Insights from rodents. Neurobiological Stress. 2015; 1: 116–127.
8. Bourin M, Petit-Demoulière B, Dhonnchadha BN, Hascöet M. Animal models of anxiety in mice. Fundamental and Clinical Pharmacology. 2007; 21: 567–574.
9. Brudzynski SM. Ultrasonic Calls of Rats as Indicator Variables of Negative or Positive States: Acetylcholinedopamine Interaction and Acoustic Coding. Behavioural Brain Research. 2007; 182: 261–73.
10. Duman CH. Models of depression. Vitamins & Hormones. 2010; 82: 1–21.
11. da Costa Estrela D, da Silva WA, Guimarães AT, de Oliveira Mendes B, da Silva Castro AL, da Silva Torres IL, Malafaia G. Predictive behaviors for anxiety and depression in female Wistar rats subjected to cafeteria diet and stress. Physiology and Behavior. 2015; 15: 252–263.
12. Fan LB, Blumenthal JA, Watkins LL, Sherwood A. Work and home stress: associations with anxiety and depression symptoms. Occupational Medicine (Oxford University Press journal). 2015; 65 (2): 110–116.
13. Huang HJ, Zhu XC, Han QQ, Wang YL, Yue N, Wang J, Yu R, Li B, Wu GC, Liu Q, Yu J. Ghrelin alleviates anxiety- and depression-like behaviors induced by chronic unpredictable mild stress in rodents. Behavioural Brain Research. 2017; 30: 333–343.
14. Ju HB, Kang EC, Jeon DW, Kim TH, Moon JJ, Kim SJ, Choi JM, Jung DU. Associations Among Plasma Stress Markers and Symptoms of Anxiety and Depression in Patients with Breast Cancer Following Surgery. The Psychiatry Investigation. 2018; 15 (2): 133–140.
15. Frazer A, Morilak DA. What should animal models of depression model? Neuroscience & Biobehavioral Reviews. 2005; 29: 515–523.
16. Knyazev GG., Savostyanov AN, Bocharov AV, Rimareva JM. Anxiety, depression, and oscillatory dynamics in a social interaction model. Brain Research. 2016; 1644: 62–69.
17. Litvin Y, Blanchard DC, Blanchard RJ. Rat 22 kHz Ultrasonic Vocalizations as Alarm Cries. Behavioural Brain Research. 2007; 182: 166–172.
18. Mällo T, Kõiv K, O'Leary A, Eller M, Harro J. Rats with persistently low or high exploratory activity: Behaviour in tests of anxiety and depression, and extracellular levels of dopamine. Behavioural Brain Research. 2007; 177 (2): 269–281.
19. Moreau J. Simulating the anhedonia symptom of depression in animals. Dialogues in Clinical Neuroscience. 2002; 4 (4): 351–360.
20. Morozova A, Zubkov E, Strekalova T, Kekelidze Z, Storozeva Z, Schroeter CA, Lesch KP, Cline BH, Chekhonin V. Ultrasound of Alternating Frequencies and Variable Emotional Impact Evokes Depressive Syndrome in Mice and Rats. Progress in Neuro-Psychopharmacology & Biological Psychiatry. 2016; 68 (7): 52–63.
21. Neumann ID, Wegener G, Homberg JR, Cohen H, Slattery DA, Zohar J, Olivier JD, Mathe AA. Animal models of depression and anxiety: What dothey tell usabout human condition? Progress in Neuro-Psychopharmacology & Biological Psychiatry. 2011; 35: 1357–1375.
22. Overstreet DH, Wegener G. The Flinders Sensitive Line Rat Model of Depression–25 Years and Still Producing. Pharmacological Reviews. 2013; 65 (1): 143–155.
23. Overstreet DH. Modeling depression in animal models. Methods in Molecular Biology. 2012; 829: 125–144.
24. Pehrson AL, Sanchez C. Altered γ-aminobutyric acid neurotransmission in major depressive disorder: a critical review of the supporting evidence and the influence of serotonergic antidepressants. Drug Design, Development and Therapy. 2015; 19: 603–624.
25. Rallis S, Skouteris H, McCabe M, Milgrom J. A prospective examination ofdepression, anxiety and stress throughout pregnancy. Women Birth. 2014; 27 (4): 36–42.
26. Ramos A. Animal models of anxiety: do I need multiple tests? Trends in Pharmacological Sciences. 2008; 29: 493–498.
27. Stepanichev S, Dygalo NN, Grigoryan G, Shishkina GT, Gulyaeva N. Rodent Models of Depression: Neurotrophic and Neuroinflammatory Biomarkers. BioMed Research International. 2014; 2014: 1–20.
28. Zhang M, Liu Y, Zhao M, Tang W, Wang X, Dong Z, Yu S. Depression and anxiety behaviour in a rat model of chronic migraine. The Journal of Headache and Pain. 2017; 18: 1–27.

Article

Dipeptide mimetics of nerve growth factor and brain-derived neurotrophic factor, GK-2 and GSB-106 and their cytoprotective properties in the model of oxidative stress

Olga Karpukhina [1, 3], Valeriya Dubova[2] , Klara Gumargalieva[3], Polina Povarnina[4], Anatoly Inozemtsev [1,*]

[1] Department of Higher Nervous Activity Lomonosov Moscow State University, Moscow, Russia;
[2] Department of Physiology RUDN University, Moscow, Russia;
[3] Semenov Institute of Chemical Physics RAS, Moscow, Russia;
[4] FSBI «Zakusov institute of Pharmacology», Moscow, Russia;
* Correspondence: a_inozemtsev@mail.ru;
karpukhina.msu@yandex.ru, https://orcid.org/0000-0002-4642-8366 (O.K.);
valeriya.dubova7525@yandex.ru, https://orcid.org/0000-0003-1318-5078 (V.D.)
povarnina@gmail.com, https://orcid.org/0000-0003-3278-8915 (P.P.);
a_inozemtsev@mail.ru, https://orcid.org/0000-0002-5059-3241 (A.I.).

Abstract: Relevance. At the V.V. Zakusov Research Institute of Pharmacology. Zakusov dimeric dipeptide mimetics of nerve growth factor (NGF) and brain derived neurotrophic factor (BDNF), GK-2 and GSB-106, respectively, were created. GK-2 and GSS-106 were found to be similar to the corresponding full-length neurotrophins in their mechanism of action and pharmacological properties, including pronounced neuroprotective activity in vitro and in vivo. The aim of this work was to obtain additional data on the cytoprotective properties of GC-2 and GSB-106 using infusoria. Methods. Oxidative stress in Paramecium caudatum was simulated by addition of heavy metal salts (cadmium chloride, lead acetate, copper sulfate, zinc sulfate) to the medium in final concentration of 10 μM. GK-2 or GSB-106 in concentrations from 10-5 to 10-8 M were added to the medium with experimental cells 45 min before the application of oxidative stress initiator. Results. GK-2 and GSB-106 dipeptides in all studied concentrations protected cells from cell death. The maximum neuroprotective effect was shown by dipeptides in concentration of 10-8 M, thus preventing the infusoria death. Conclusion. GK-2 and GSB-106 at a concentration of 10-8 M fully protect Paramecium caudatum from death under oxidative stress induced by heavy metals.

Keywords: nerve growth factor; brain-derived neurotrophic factor; dimeric dipeptide mimetics; Paramecium caudatum infusoria; cytoprotection; oxidative stress induced by heavy metal salts.

Citation: Karpukhina O., Dubova V., Gumargalieva K., Povarnina P., Inozemtsev A. Dipeptide mimetics of nerve growth factor and brain-derived neurotrophic factor, GK-2 and GSB-106 and their cytoprotective properties in the model of oxidative stress. Journal of Clinical Physiology and Pathology (JISCPP) 2023; 2 (4): 49-52.

https://doi.org/10.59315/JISCPP.2023-2-4.49-52

Academic Editor: Igor Kastyro

Received: 27.10.23
Revised: 17.11.23
Accepted: 18.12.23
Published: 29.12.23

1. Introduction

Neurodegeneration in the brain is a key link in the pathogenesis of a number of widespread diseases, such as cerebrovascular disorders, Alzheimer's and Parkinson's diseases, depression, etc. Disability due to neurodegenerative processes is a serious social and economic problem, so the search for highly effective neuroprotective agents is an urgent task for pharmacology.

Endogenous neuroprotective proteins such as brain derived neurotrophic factor (BDNF) and nerve growth factor (NGF) have a high therapeutic potential [1]. However, the clinical use of neurotrophins is limited by their instability in biological fluids, poor ability to penetrate the blood-brain barrier and pleiotropic side-effects (2, 3).

At the V.V. Zakusov Research Institute of Pharmacology. Zakusov based on the beta bends of NGF and BDNF loops 4 dimeric dipeptides, hexamethylenediamide bis(N-monosuccinyl-L-glutamyl-L-lysine (GC-2) and hexamethylenediamide bis(N-monosuccinyl-L-seryl-L-lysine) (GSB-106) were designed and synthesized respectively [Russian patent No 2410392, 2010; US Patent No. 9683014 B2, 2017; Chinese Patent No. 102365294 B, 2016]. GK-2 and GSB-106 have been shown to activate full-length protein-specific tyrosine kinase receptors, TrkA and TrkB, respectively, and possess neuroprotective activity in vitro at micro-nanomolar concentrations in various cellular models, including oxidative stress models [46]. The neuroprotective activity of GC-2 and GSB-106 was confirmed in vivo in a model of extensive ischemic stroke caused by transient middle cerebral artery occlusion in rats [7-9]. For GK-2, it has been shown to be devoid of the major side-effects typical of NGF, namely it does not cause hyperalgesia and weight loss [6].

To obtain additional data on cytoprotective properties of GK-2 and GSB-106 dipeptides, it was of interest to study them in the model of oxidative stress in infusoria [10, 11]. Oxidative stress

is known to be one of the main mechanisms of neuronal damage in various pathologies. Heavy metal salts [11-13], exotoxicants potentially dangerous for all living organisms, are widely used to model oxidative stress both in vitro and in vivo. Ions of lead, cadmium, zinc and other heavy metals can initiate the generation of excessive amounts of reactive oxygen species [13-15], the increased level of which in the cell triggers chain reactions of oxidative degradation of biomolecules.

Unicellular organisms, infusoria in particular, represent a convenient model organism for pharmacological studies, because in this case the advantages inherent to the use of cell culture are supplemented by the fact that in this case the test system is both a single cell and an integral organism. It should be noted that for infusoria, as for other unicellular organisms, there are no data in the literature on the presence of tyrosine kinase receptors similar to those in vertebrates, which could mediate the pharmacological effects of GC-2 and GSB-106 dipeptides. However, neurotrophin-like growth factors regulating survival and proliferation have been found in infusoria [16, 17], suggesting the presence of similar receptor systems.

2. Patients and Methods

The work was performed on a culture of Ramecium caudatum, one of the most commonly used test objects for laboratory studies aimed at determining the direct effect of chemical compounds. Paramecium cell culture was grown on Lozin-Lozinsky medium with the addition of nutrient medium containing Saccharomyces cerevisiae yeast. Cells taken in the log-phase of growth were incubated at 24 ± 2 °C, pH = 6.8-7.0.

The oxidative stress was modeled [10] by adding 1 ml of aqueous solution of one of metal salts (cadmium chloride, lead acetate, copper sulfate, zinc sulfate) to 1 ml of medium containing Paramecium caudatum infusoria at final concentrations of 1; 5; 10 and 15 μM. The duration of incubation of cells in medium containing heavy metal salt was 15 min, 30 min, 45 min, 1 hour, 2 hours, 6 hours. 45 min before the addition of the oxidative stress initiator, 1 ml of GC-2 or GSB-106 solution in concentrations from 10-5 to 10-8 M was added to the medium containing experimental cells. The active concentrations of HA-2 and GSB-106 were chosen based on the previous experiments [4, 5, 18].

The pH of the medium was measured at all stages of the experiment using a Kelilong PH-221 pH-meter controller. Cell number, intensity of cell division, nature and speed of infusoria movement, and changes in cell shape were recorded. The number of cells was determined under a microscope at 7×10 magnification with video recording by counting their total number in 1 ml of culture.

The results are presented as arithmetic mean ± standard error of the mean. After testing the distribution for normality, the significance of differences between the groups was assessed using Student's t-test. The differences were considered significant at $p < 0.05$.

3. Results

Under the influence of heavy metal ions the cell number was markedly decreased, the most pronounced effects were observed at the concentrations of 10-15 μM salts of heavy metals (Fig.1). A number of morphological changes occurred in the cell, including reorganization of cytoskeleton structures leading to cell death. Swelling of cytoplasm organelles was observed, which led to the rupture of the paramecium cell membrane.

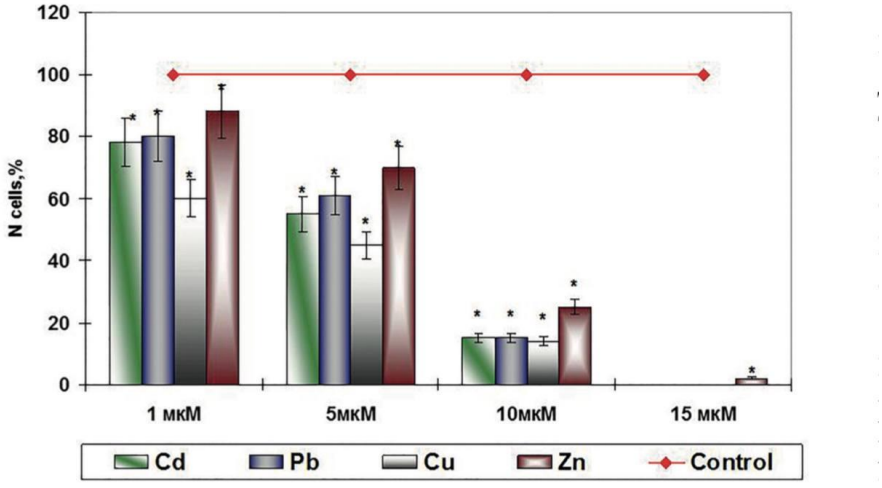

Figure 1. Effect of heavy metal salts on the survival rate of Paramecium caudatum cells after 6 h incubation Notes: Heavy metal salts (cadmium chloride, lead acetate, copper sulphate, zinc sulphate) in final concentrations of 1; 5; 10 and 15 μM were added to the medium and infusoria. The duration of incubation was 6 hours. The abscissa axis shows different concentrations of metal salts; the ordinate axis shows the number of surviving cells in % of the intact control. * - $p < 0.05$ compared to control (Student's t-test).

A decrease in the number of experimental cells as a result of destructive membrane pathology was indicative of the intensification of free-radical oxidation processes caused by heavy metal ions. After 6 h of incubation with heavy metal salts solutions (10 μM), the number of surviving cells in Ramecium caudatum culture was about 15 to 25% of the passive control (without damage) (maximum number in the medium with copper sulfate).

Dipeptides GC-2 and GSB-106 in all concentrations studied protected cells from heavy metal-induced death. The maximum neuroprotective effect of dipeptides was observed in the concentration of 10-8 M (Fig. 2). At this concentration, the compounds studied almost completely prevented cell death of infusoria even after 6 h of incubation with heavy metal salts (10 μM) (see Fig. 2).

The efficacy of GC-2 and GSB-106 in this model suggests that Paramecium caudatum has receptor systems similar to the tyrosine kinase receptors of vertebrates, which is consistent with the literature data on the presence of growth factors in infusoria that regulate survival and proliferation [16, 17].

5. Conclusions

Thus, we found that the dipeptide mimetics NGF and BDNF, respectively GC-2 and GSB-106, at a concentration of 10-8 M fully protect Paramecium caudatum cells from death under oxidative stress caused by heavy metal salts (cadmium chloride, lead acetate, copper sulfate, zinc sulfate).

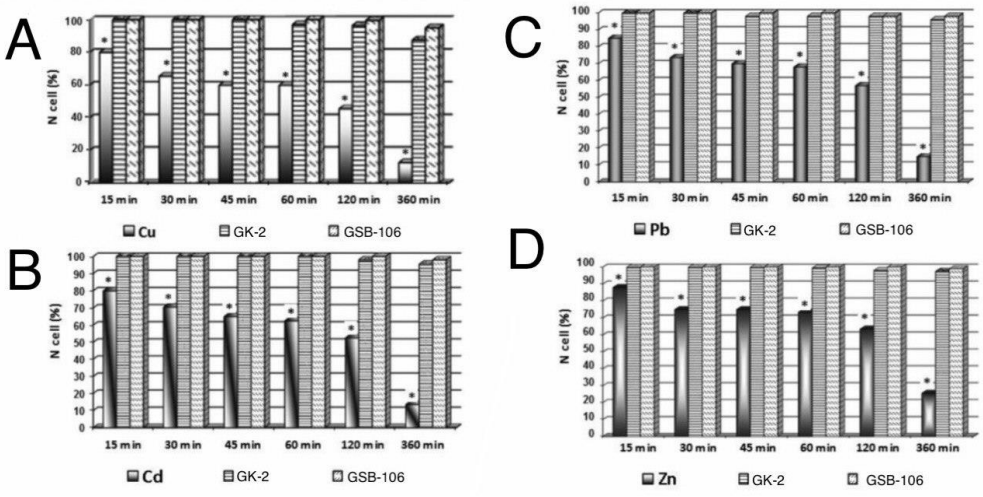

Figure 2. Effect of dimeric dipeptide mimetics NGF and BDNF, respectively GC-2 and GSB-106 at concentrations of 10-8 M on cell survival under oxidative stress induced by heavy metal salts (copper sulfate, cadmium chloride, lead acetate, zinc sulfate) (10 μM) 15, 30, 45, 60, 120 and 360 min after incubation

Notes: A, oxidative stress was induced by copper sulfate; B, oxidative stress was induced by cadmium chloride; oxidative stress was induced by lead acetate; D, oxidative stress was induced by zinc sulfate. GC-2 and GSB-106 were added to the medium 45 min before the toxin. The abscissa axis shows the time of incubation with heavy metal salts; the ordinate axis shows the number of surviving cells in % of the intact control. * - $p < 0.05$ compared to control (Student's t-test).

Application of artificial intelligence:

The article is written without the use of artificial intelligence technologies.

Conflicts of Interest: The authors declare no conflict of interest.

References

1. Allen SJ, Watson JJ, Shoemark DK, Barua NU, Patel NK. GDNF, NGF and BDNF as therapeutic options for neurodegeneration. Pharmacology & Therapeutics. 2013; 138(2):155–175.

2. Aloe L, Rocco ML, Bianchi P, Manni L. Nerve growth factor: from the early discoveries to the potential clinical use. Journal of Translational Medicine. 2012;10(1):239.
3. Dunkel P, Chai CL, Sperlágh B, Huleatt PB, Mátyus P. Clinical utility of neuroprotective agents in neurodegenerative diseases: current status of drug development for Alzheimer's, Parkinson's and Huntington's diseases, and amyotrophic lateral sclerosis. Expert Opinion on Investigational Drugs. 2012; 21(9):1267–1308.
4. Antipova TA, Gudasheva TA, Seredenin SB. In vitro study of neuroprotective properties of GK-2, a new original nerve growth factor mimetic. Bulletin of Experimental Biology and Medicine. 2011; 150 (5): 607–9. (in Russ).
5. Gudasheva TA, Tarasyuk AV, Pomogaybo SV. Design and synthesis of dipeptide mimetics of brain-derived neurotrophic factor. Bioorganic chemistry.2012; 38 (3): 280–90. (In Russ).
6. Gudasheva TA, Povarnina PY, Antipova TA, Firsova YN, Konstantinopolsky MA, Seredenin SB. Dimeric dipeptide mimetics of the nerve growth factor Loop 4 and Loop 1 activate TRKA with different patterns of intracellular signal transduction. Journal of Biomedical Science. 2015; 22(5):106.
7. Gudasheva TA, Povarnina P, Logvinov IO, Antipova TA, Seredenin SB. Mimetics of brainderived neurotrophic factor loops 1 and 4 are active in a model of ischemic stroke in rats. Drug Design, Development and Therapy. 2016; 10:3545–3553.
8. Povarnina P, Gudasheva TA, Seredenin SB. Dimeric dipeptide mimetics of NGF and BDNF are promising agents for post-stroke therapy. Journal of Biomedical Science. 2018; 11(5):100–107.
9. Seredenin SB, Povarnina PY, Gudasheva TA. An experimental evaluation of the therapeutic window of the neuroprotective activity of a low-molecular nerve growth factor mimetic GK-2. Journal of Neurology and Psychiatry named after S. S. Korsakov. 2018; 118 (7): 49. (in Russ).
10. Karpukhina OV, Gumargalieva KZ, Inozemtsev AN. The effect of antioxidant compounds on oxidative stress in unicellular aquatic organisms. In: On the borders of physics, chemistry, biology, medicine and agriculture. Research and Development. Torun: Institute for Engineering of polymer materials and Dues. 2014: 145–151.
11. Morgunov IG, Karpukhina OV, Kamzolova SV, et al. Investigation of the effect of biologically active threo-Ds-isocitric acid on oxidative stress in Paramecium caudatum. Preparative Biochemistry & Biotechnology. 2018;48(1):1–5.
12. Simmons SO, Fan CY, Yeoman K, Wakefield J, Ramabhadran R. NRF2 Oxidative Stress Induced by Heavy Metals is Cell Type Dependent. Current Chemical Genomics. 2011; 5:1–12.
13. Ercal N, Gurer-Orhan H, Aykin-Burns N. Toxic metals and oxidative stress part I: mechanisms involved in metal-induced oxidative damage. Current Topics in Medicinal Chemistry. 2001; 1 (6): 529–539.
14. Flora SJS, Mittal M, Mehta A. Heavy metal induced oxidative stress & its possible reversal by chelation therapy. Indian Journal of Medical Research. 2008; 128 (4): 501– 523.
15. Pryor WA. Oxy-radicals and related species: their formation, lifetimes, and reactions. Annual Review of Physiology. 1986; 48: 657–667.
16. Tanabe H, Nishi N, Takagi Y, Wada F, Akamatsu I, Kaji K. Purification and identification of a growth factor produced by Paramecium tetraurelia. Biochemical and Biophysical Research Communications. 1990; 170 (2): 786–792.
17. Rasmussen MI, Wheatley DN. Purification and characterisation of cell survival factor 1 (TCSF1) from Tetrahymena thermophila. Journal of Cell Communication and Signaling. 2007; 1(3-4): 185–193.
18. Gudasheva TA, Antipova TA, Seredenin SB. Novel lowmolecular-weight mimetics of the nerve growth factor. Doklady Biochemistry and Biophysics. 2010; 434: 262-5. (In Russ).

Article

Assessment of anthropometric and hemodynamic parameters in young people in the cardiovascular system adaptation ability

Semyon Myakushin[1], Valeriya Turkhnanova[1], Tatyana Vlasova[1]

[1] Institute of Medicine, National Research Ogarev Mordovia State University, Saransk, Russia;
* Correspondence: v.t.i@bk.ru;
smyakushin@mail.ru, https://orcid.org/0000-0002-2466-7681 (S.M)
turhanovalera@mail.ru, https://orcid.org/0009-0007-5465-8923 (V.T.)
v.t.i@bk.ru, https://orcid.org/ 0000-0002-2624-6450 (T.V.).

Abstract: The index of functional Changes (IFC) is a complex indicator based on the relationship between the heart rate of decrease and the associated risk of developing cardiovascular pathologies, as well as to study the state of vascular contractions, systolic and diastolic blood pressure, age, body weight and height. [2] The aim of the study is to compare the mechanisms of adaptation of the diseases of the cardiovascular system (CVS) in young men and women in the Russian Federation, to identify the main risk factors of the wall in young people depending on the functional reserves of the CVS. Materials and methods: The study includes 91 students aged 17 to 25 years. Heart rate (HR), systolic and diastolic blood pressure (SBP, DBP), height, body weight, waist and hip circumference were measured noninvasively in all participants. The ratio of waist and hip circumferences (RW/RH), body mass index (BMI) was calculated. The main tool in the study of vascular wall stiffness was photoplethysmography.
As a result of the research, an unequal distribution of IFC indicators between men and women was revealed. There were more women with a satisfactory level of adaptation, and men with the same level of IFC, therefore, less. These data indicate that men are most often at risk of developing CVS. The differences in the average values of the Kerdo index (IK). between men and women are statistically insignificant. Young people with a slight weight deficit and normal body weight have a greater potential for adaptation than people with excess body weight and obesity. According to photoplethysmography, the indicators of stiffness of vascular wall (VW) and the velocity of the pulse wave propagation through the vessels (VPWP) in young people with different adaptive reserves did not differ significantly.

Keywords: Adaptive potential, vascular wall stiffness, body mass index, anthropometry, photoplethysmography.

Citation: Myakushin S., Turkhanova V., Vlasova T. Assessment of anthropometric and hemodynamic parameters in young people in the assessment of adaptation of the cardiovascular system. Journal of Clinical Physiology and Pathology (JISCPP) 2023; 2 (4): 53-57.

https://doi.org/10.59315/JISCPP.2023-2-4.53-57

Academic Editor: Igor Kastyro

Received: 31.10.23
Revised: 30.11.23
Accepted: 15.12.23
Published: 29.12.23

1. Introduction

The cardiovascular system has adaptive capabilities, which are constantly spent on maintaining a balance between the body and the external environment [1]. The Functional Change Index (IFC) is a complex indicator that includes heart rate, blood pressure, age, body weight and height. IFC plays an important role in the body's adaptation to external factors [2]. Determining the state of the vascular wall is an urgent task for determining cardiovascular risk in patients with arterial hypertension and atherosclerosis.

Currently, diseases of the cardiovascular system (CVS) are the most common, "younger" pathology. In 2019, CVS was the main cause of 9.6 million deaths among men and 8.9 million deaths among women, which is about a third of all deaths in the world [3]. High body mass index and systolic blood pressure are risk factors for the development of CVS in middle age [4]. Early identification of risk factors and sexual characteristics of CVS adaptation is an important task of modern medicine [5].

2. Materials and Methods

The study was conducted from February to May 2023, 91 students aged 17 to 25 years took part in it, the average age of which was 19 ± 0.8 years. The sexual distribution was: (n=50) – women, (n=41) – men.

To assess the level of functioning of the cardiovascular system, the terminology of adaptation theory was used, according to which 3 groups of people are distinguished by health levels: with

satisfactory adaptation (IFC 1), with tension of adaptation mechanisms (IFC 2) and with unsatisfactory adaptation (IFC3). [6]

Heart rate (HR), systolic and diastolic blood pressure (SBP, DBP), height, body weight, waist and hip circumference were measured noninvasively in all participants. The ratio of waist and hip circumferences (RW/RH), body mass index (BMI) were calculated.

The functional change Index (IFC) was calculated using the R. Bayevsky formula:

IFC = 0.011*PR + 0.014*SBP + 0.008*DBP + 0.014*A + 0.09*BW – (0.009*H + 0.27), where IFC – the index of functional Changes; A – age, years; BW – body weight, kg; H – height, cm; SBP – systolic blood pressure, mmHg, DBP – diastolic blood pressure, mmHg; PR – pulse rate in 1 min.

Values of the adaptation index:

1.5-2.59 – satisfactory adaptation, that is, positive adaptation of the CVS to environmental conditions;

2.6-3.09 – tension of adaptation mechanisms;

3.1 and more – unsatisfactory adaptation.

Additionally, the Student coefficient was calculated (the number of degrees of freedom was calculated, and then the coefficient itself).

To assess the influence of the autonomic nervous system, the Kerdo index was used:

KI =(1-DB/HR) ×100%.

Normally, IR ranges from -10 to +10%: positive values of IR indicate a predominance of activity of the sympathetic nervous system, negative values indicate a predominance of tone of the parasympathetic nervous system.

Statistical data analysis (Statistics 13).

Photoplethysmography was the main tool in the study of vascular wall stiffness. AngioCode 301 is a mobile health tracker that allows you to assess the state of the cardiovascular system.

Vascular stiffness is an assessment of the condition of the arteries, the analysis of the parameter allows you to assess the risk of capillary damage and blood microcirculation disorders in various organs.

Stress level is a characteristic of the state of the centers regulating the cardiovascular system. Also known as the heart rate variability index.

The relative duration of systole. The ratio of the duration of systole and the total duration of the cardiac cycle (ED%) reflects the features of the working cycle of the myocardium.

The velocity of the pulse wave propagation through the vessels with a finite velocity depends on the elastic properties and geometry of the blood vessel.

3. Results and discussion

In the study conducted in groups 2 and 3, the number of men prevailed (59.1% and 76.5%), the average age of the subjects in all three groups was 20 years. The unequal distribution of IFC indicators between men and women was revealed. There were more women with a satisfactory level of adaptation - 37 people (74%), and men with the same level of IFC, therefore, less – 15 people (36.6%). The tension of adaptation mechanisms was also distributed unequally: women in this group were 18% (9 people), and men – 31.7% (13 people). 4% of women (4 people) and 31.7% of men (13 people) turned out to have an unsatisfactory level of IFC.

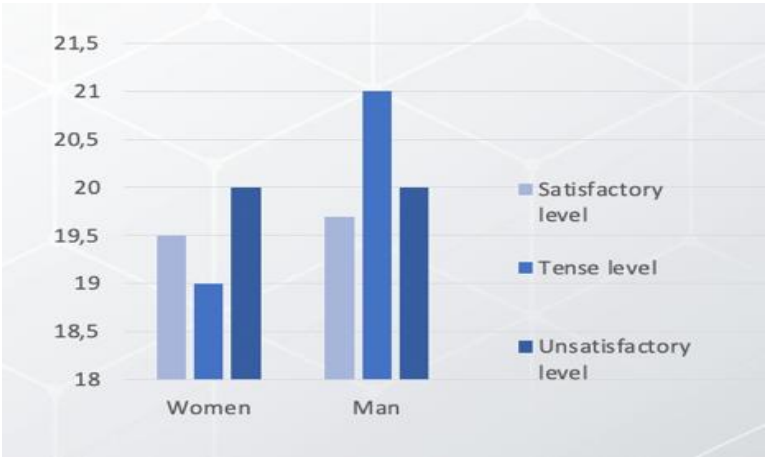

Figure 1. Average age of different sex groups with different IFC.

The calculation of the criterion χ2 revealed significant differences between the groups ($p<0.05$). These data indicate that men are most often at risk of developing CVS. Consequently, the data obtained in the study indicate a significant role of the gender factor in the ability of the CVS

to adapt to different types of stress, and a reduced level of adaptation in men relative to women was also found.

Indicators of body weight and height in men are higher than in women, which is consistent with classical anthropological concepts. At the same time, the calculation of BMI revealed a non-physiological increase in the body mass index in men. Thus, 29.3% of overweight men (12 people), and 10% of women (5 people), obese men - 9.8% (4 people), women - 6% (3 people) turned out to be overweight. These data indicate that there are more men with a higher BMI than women, which affects the level of IFC and correlates with a low ability to adapt to environmental factors.

When analyzing the body mass index (BMI) in the context of the IFC, there were significant differences between the first (20.0± 0.6) and the third group (28.3±0.6), in the second group the BMI was 22.7±0.6.

Also, assessing the waist–hip index (WHI), differences in the indicators of the first (WHI = 0.74±0.01) were found and the second group (WHI = 0.8 ±0.01), in the third group WHI was 0.83± 0.01.

When determining hemodynamic parameters, it was found that the pulse values of the second (89±1.5) and third groups (94±1.6), which were already characterized by a violation of the mechanisms of adaptation of the cardiovascular system, significantly differed from those of the group (78±1.6) with normal exercise tolerance ($p<0.05$). When analyzing blood pressure in all three groups, the following values were obtained: SBP: IFC 1 = 117 ± 11, IFC 2 = 131 ± 8, IFC 3 = 146 ± 16. DBP: IFC 1 = 74 ± 8, IFC 2 = 81 ± 5, IFC 3 = 86 ± 8 mm Hg.

When analyzing blood pressure based on the high frequency of occurrence of high normal and pathological values of DBP in the third and second groups and the reliability of differences in the average group values relative to the first group, it was found that the vascular wall in this sample of individuals is involved in the process of maladaptation.

Table 1. Hemodynamic parameters in 3 study groups. * - all indicators were statistically significant, $p<0.05$.

Indicator	Categories	Systolic blood pressure		p
		M ± SD	95% ДИ	
SBP	IFC 1	117 ± 11	114 – 120	P1,2< 0,001*
	IFC 2	131 ± 8	127 – 134	P2,3< 0,001*
	IFC 3	146 ± 16	138 – 154	P1,3< 0,001*
DBP	IFC 1	74 ± 8	72 – 76	P1,2< 0,001*
	IFC 2	81 ± 5	78 – 83	P2,3=0,036 *
	IFC 3	86 ± 8	82 – 91	P1,3< 0,001*

When calculating the Kerdo index, the predominance of the sympathetic nervous system over the parasympathetic was noted in all groups.

In the first group of SNS: total – 56% (29), increased activity 25% (13), norm 31% (16); PNS: total 44% (23), increased activity 19% (10), norm 25% (13).

In the second group: SNS: total 77% (17), increased activity 32% (7), norm 45% (10); PNS: total 23% (5), increased activity 5% (1), norm 18% (4).

In the third group: SNS: total 64% (10), increased activity 18% (3), norm 47% (8); PNS: total 36% (6), increased activity 18% (3), norm 18% (3).

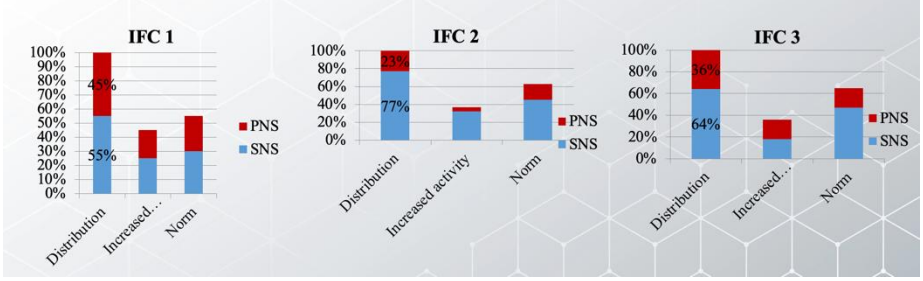

Figure 2. Calculation of the Kerdo index in three study groups. Horizontally: distribution, increased activity, norm. Vertically: in red - the parasympathetic nervous system, in blue – the sympathetic nervous system.

During the study, the following indicators were analyzed: vascular wall stiffness, systole duration, stress index and pulse wave propagation velocity.

Table 2. Analysis of the main indicators: vascular wall stiffness, duration of systole, stress index and pulse wave propagation velocity in 3 study groups. * - statistically significant indicators, p<0.05.

Indicator	Categories	Indicator		p
		Me	$Q_1 - Q_3$	
Vascular wall stiffness, %	IFC 1	-13,7	-20,3 – -7,8	0,358
	IFC 2	-16,4	-20,9 – -8,4	
	IFC 3	-16,2	-19,7 – -11,3	
Duration of systole, %	IFC 1	33	32 – 34	0,180
	IFC 2	34	32 – 34	
	IFC 3	33	32 – 35	
Stress Index, y.e.	IFC 1	94	52 – 147	0,006*
	IFC 2	117	84 – 242	
	IFC 3	197	98 – 374	
Pulse wave propagation speed, м/с	IFC 1	9,32	8,70 – 10,35	0,490
	IFC 2	9,86	9,10 – 10,49	
	IFC 3	9,97	8,95 – 10,32	

Vascular wall prestige: IFC 1 = -13.7 ±1.2 %; IFC 2 = -16.4±1.2%;IFC 3 = -16.2±1.2%; p = 0.358.

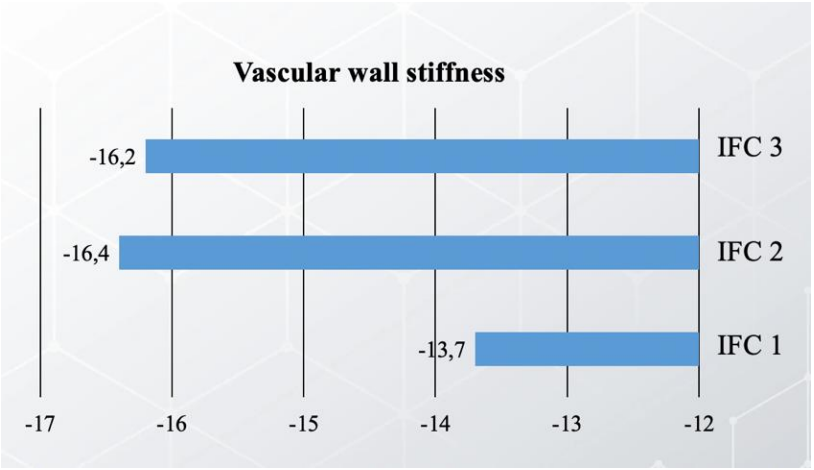

Figure 3. Stiffness of the vascular wall in the three groups being excised. The highest value is typed in IFC 2.

Stress index: CPI 1 = 94±14 c.u; CPI 2 =117±13 c.u; CPI 3 = 197±14 c.u; p = 0.006.

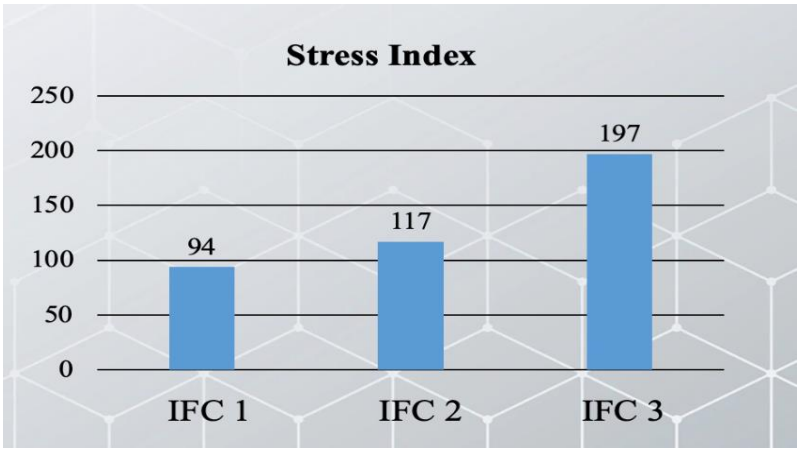

Figure 4. Stress index in the three study groups. The highest value is observed in IFC 3.

Duration of systole: IFC 1 = 33=0.3 %; And F2 = 34=0.3 %; IFC 3 = 33=0.3 %; p = 0.18.

Pulse wave propagation velocity: IFC 1 = 9.32±0.1 m/s; IFC 2 = 9.86±0.1 m/s; IFC 3 = 9.97±0.1 m/s; z = 0.49.

4. Conclusions

The state of the vascular wall in young people did not depend on the functional reserves of the CVS: according to photoplethysmography, the parameters of the stiffness of the VW and VPWP did not differ significantly in young people with different adaptive reserves. Impaired adaptation of the cardiovascular system correlates with high heart rate, high blood pressure and stress index (according to FPG). Violations of the mechanisms of adaptation of the cardiovascular system in young men are more common than in women. The adaptive response of the CVS to various influences depends on BMI. Young people with a slight weight deficit and normal body weight have a greater potential for adaptation than people with excess body weight and obesity.

Application of artificial intelligence:

The article is written without the use of artificial intelligence technologies.

Author Contributions: Conceptualization, T.V.; methodology, T.V. and S.M.; formal analysis, T.V., S.M, V.T; investigation, V.T., S.M; data curation, V.T.; writing—original draft preparation, S.M., V.T, T.V..; writing—review and editing, S.M.; visualization, V.T.; supervision, T.V.; project administration, T.V. All authors have read and agreed to the published version of the manuscript.

Informed Consent Statement: Informed consent was obtained from all subjects involved in the study.

Conflicts of Interest: The authors declare no conflict of interest.

References

1. Ponomarev DN, Suslov NS, Troshin IS. The influence of functional activity and the state of adaptive mechanisms of the cardiovascular system on the level of anxiety of students of higher medical educational institutions. International Student Scientific Bulletin.2018;5.
2. Repalova NV, Avdeeva EV. Changes in the adaptive potential of the cardiovascular system in foreign students under conditions of pre-examination stress. International Journal of Applied and Fundamental Research. 2021; 4: 12-16.
3. JACC: Cardiovascular Interventions, JACC: Cardiovascular Imaging, JACC: Heart Failure, JACC: Clinical Electrophysiology, JACC: Basic to Translational Science, JACC: Case Reports and JACC: CardioOncology
4. Sun J, Qiao Y, Zhao M, Magnussen CG, Xi B. Global, regional, and national burden of cardiovascular diseases in youths and young adults aged 15-39 years in 204 countries/territories, 1990-2019: a systematic analysis of Global Burden of Disease Study 2019. BMC Medicine. 2023;21(1):222.
5. Krayushkin AI, Perepelkin AI, Doronin AB. Interrelation of adaptive potential, hand area and chest circumference depending on body mass index in young men // International Journal of Applied and Fundamental Research. 2016;6(2):260-262

Article

Study of heart rate and corticosterone variability in the simulation of experimental rhino-surgical interventions.

Stepan Shilin[1], Yana Emets[1], Jun Hyun June[1], Irina Pinighina[1], Irina Uvartseva[1], Aleksandr Chernoyarov[1], Alexander Timoshenko[1], Alexander Markushin[1], Al Khatib Nashwan[1,2], Igor Kastyro [1,*], Igor Ganshin[1], Valentin Popadyuk [1]

[1] RUDN University;
[2] University Clinical Hospital, Damascus, Syria;
* Correspondence: ikastyro@gmail.com;
9060965527@mail.ru, https://orcid.org/0000-0003-2080-608X (S.S)
emets.yah@yandex.ru, https://orcid.org/0000-0003-3538-3737 (Y.E)
gaginmuler@gmail.com, https://orcid.org/0009-0005-0749-8387 (J.H.J)
PNG.i@inbox.ru, https://orcid.org/0000-0003-4977-4202 (I.P)
irina.uvartseva@mail.ru, https://orcid.org/0000-0002-0049-6523 (I.U)
steshartist@mail.ru, https://orcid.org/0009-0007-1167-0164 (A.C)
dr.timoshenko@gmail.com, https://orcid.org/0009-0002-2281-2889 (A.T)
markuschin17@gmail.com, https://orcid.org/0000-0003-3860-8348 (A.M)
dr.nashwan.kh@gmail.com, https://orcid.org/0009-0004-6412-6750 (A.K.N)
ikastyro@gmail.com , https://orcid.org/0000-0001-6134-3080 (I.K)
gibdoc@yandex.ru, https://orcid.org/0000-0001-5766-9416 (I.G)
lorval04@mail.ru, https://orcid.org/0000-0003-3309-4683 (V.P)

Abstract. Aims: to assess changes in the time range of heart rate variability (HRV) and plasma corticosterone concentration in rats after simulating septoplasty. Materials and methods: a septoplasty was simulated in 30 mature male Wistar rats weighing 210-290 g. An ECG was recorded with subsequent analysis of the time domain of HRV, as well as blood sampling for changes in the concentration of corticosterone in the blood plasma. Results: SDNN significantly increased in comparison with the control on days 2 and 3 ($p < 0.001$), but decreased on days 4-5 ($p < 0.001$) and 6 days ($p < 0.01$). rMSSD changed in waves with two irregular peaks on days 1 and 6. SDNN / rMSSD, in comparison with the 1st day of the postoperative period, increased on the 2nd day and continued to grow ($p < 0.05$), and on the 4th day it began to decrease ($p < 0.01$). The total power of HRV was low throughout the postoperative period ($p < 0.001$), except for the 3rd day, when it was equal to the control data. The increase in the total power indicator fell on the 3rd day after the operation ($p < 0.01$), after which its decline occurred again. The concentration of corticosterone in the blood plasma in rats was significantly higher than before ($p < 0.001$). From the 2nd to the 4th postoperative day, its plateau was determined. Conclusion: Simulation of septoplasty leads to changes in the time range of HRV, an increase in the concentration of corticosterone in the blood plasma in rats with its maximum at the time of surgery and after 24 hours, the formation of a "plateau" from the 2nd to the 4th postoperative days, which coincides with changes of HRV.

Keywords: septoplasty, heart rate variability, corticosterone, stress

Citation: Shilin S., Emets Y., June J.H., Pinighina I., Uvartseva I., Chernoyarov A., Timoshenko A., Markushin A., Nashwan A.K., Kastyro I., Ganshin I., Popadyuk V. Study of heart rate and corticosterone variability in the simulation of experimental rhino-surgical interventions. Journal of Clinical Physiology and Pathology (JISCPP) 2023; 2 (4): 58-64.

https://doi.org/10.59315/JISCPP.2023-2-4.58-64

Academic Editor: Igor Kastyro

Received: 05.10.23
Revised: 10.11.23
Accepted: 13.12.23
Published: 29.12.23

1. Introduction

The most common surgical intervention for a deviated nasal septum is still septoplasty [1, 2] and can be performed under local or general anesthesia [3]. Using biological models, we have previously shown that modeling septoplasty leads to the development of an anxiety-like state [4] as a result of swelling of the nasal mucosa, inflammatory phenomena [5], and the development of an imbalance in the autonomic nervous system (ANS) [6], which manifested by a change in the behavior of rats in an open field [4]. It was also shown that in this case, the indicators of the frequency range of heart rate variability (HRV), which characterized the shift of the ANS towards sympathicotonia, change [6]. These physiological phenomena were supported by the results of morphological studies of the hippocampus in rats. Thus, after provoking surgical inflammation on the nasal septum, the number of dark neurons and p53-positive neurons increases [7-9]. The importance of studying physiological stress reactions in biological objects is determined by the development of stress reactions and pain syndrome in patients

2. Purpose of the study

Evaluate changes in heart rate variability and corticosterone during modeling of rhinosurgical interventions in biological objects.

3. Materials and methods

3.1. Method of surgical damage:

The study involved modeling septoplasty in 30 mature male Wistar rats weighing 210-290 g. The operation was performed under general anesthesia with a solution of Zoletil 100, which was injected into the tail vein. After the animal's motor reactions died out, a zigzag scarification of the mucous membrane of the nasal septum was carried out with a metal probe - from bottom to top and from back to front (Fig. 1).

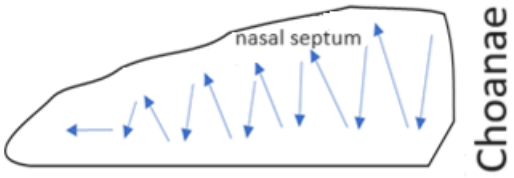

Figure 1. Scheme of modeling of septoplasty in rats - scarification of the nasal mucosa.

3.2. Electrocardiogram and heart rate variability:

Two days before the surgical intervention, all rats, under general anesthesia with a solution of Zoletil 100, were sutured with metal half-rings with capitate ends in three places - two in the back and one in the withers (Fig. 2 a, b). On the day of surgery, before the intervention itself, a control ECG recording was performed for 15 minutes on a Biopac M30-B research polygraph (California, USA). At the same time, the rats were in a free state. After the operation, the ECG was also recorded for 15 minutes daily for 6 days.

Figure 2. Scheme of applying (a) piercing (b) in rats for recording ECG on a Biopac M30-B polygraph (California, USA) (c).

From all recordings, fragments without artifacts were isolated and analyzed in the Biopack student lab 4.1 program. Recording fragments were selected 7.5 minutes (450 seconds) after the start of recording. This was due to the fact that after installing the electrodes, in the first 5-7 minutes the rat on the table got used to them and calmed down. The length of each segment was a minimum of 90 seconds for each rat. The average length of the processed ECG segments was 115±22 s.

Next, heart rate variability was analyzed according to R.M. Baevsky [11] in the Kubios HRV program (Fig. 3). Among the parameters of the HRV temporal spectrum, the following were studied: the standard deviation of R-R intervals (SDNN) between normal QRS complexes, the square root of the sum of squares of the difference in the values of successive pairs of normal R-R intervals (rMSSD), the ratio SDNN/rMSSD and total power (Total power, ms2).

Figure 3. Example of ECG data processing in Kubios HRV.

3.3. Determination of corticosterone concentration

To analyze blood plasma for the concentration of corticosterone in rats, blood was taken after recording an ECG from the tail vein before surgery, at the time of surgery, and 1-6 days after surgery. The blood obtained was immediately centrifuged [12, 13]. Blood samples were immediately centrifuged and plasma was stored at −20°C until analysis. Plasma corticosterone concentrations were quantified using ELISA. A commercial corticosterone enzyme immunoassay kit (Assay Designs Inc., Ann Arbor, Mich., USA) was used according to the manufacturer's instructions.

3.4. Statistical processing of results

Data were processed in Microsoft Exel, MATLAB, STATISTICA 12.6, JASP 0.14.0.0 software. When comparing group data before and after surgery, the Wilcoxon test was used. For each comparison, its own level of significance was determined ($p <$ from 0.001 to 0.05).

4. Results

4.1. Heart rate variability

● Standard deviation of R-R intervals. SDNN significantly increased compared to normal data on days 2 and 3 after septoplasty simulation ($p<0.001$), but decreased on days 4-5 ($p<0.001$) and 6 ($p<0.001$). 01). On days 2-3 of the postoperative period, there was a significant decrease in SDNN compared to day 1 ($p<0.01$). However, on days 4-6 there was a significant decrease ($p<0.001$) compared to the previous observation period (Table 1, Fig. 4a).

● RMSSD. The Wilcoxon test showed that the square root of the sum of the squares of the difference in the values of successive pairs of normal R-R intervals, compared with control data, one day after surgery significantly increased ($p<0.01$), but on the 2nd-5th ($p<0.001$) and on the 6th ($p<0.01$) day it was significantly below normal. The dynamics of changes in rMSSD had a wave-like character with two uneven peaks on days 1 and 6 (Table 1, Fig. 4b). Moreover, on the 4th day its minimum average value was recorded for the entire observation period after modeling septoplasty.

● SDNN/rMSSD. The nature of changes in the average values of this indicator was different from rMSSD. Thus, compared with preoperative values, it was significantly higher on days 2-5 ($p<0.001$), and significantly lower one day after the septoplasty simulation ($p<0.001$). Compared to the 1st day of the postoperative period, on the 2nd day there was an increase in the STDNN/rMSSD ratio ($p<0.001$). On the third day it also continued to increase ($p<0.05$), on the 4th day it decreased ($p<0.01$) compared to the previous day, and continued to significantly decrease only on the 6th day after surgery ($p< 0.05$) (Table 1, Fig. 4c).

● Total HRV power. An assessment of the overall power showed that modeling septoplasty led to a significant decrease in power throughout the entire postoperative period ($p<0.001$), except for the 3rd day, when no significant difference was found compared to the control. The increase in the total power indicator occurred on the 3rd day after surgery ($p<0.01$), after which it decreased again ($p<0.01$) (Table 1, Fig. 4d).

Table 1. Dynamics of changes in time domain parameters and total power of heart rate variability after modeling septoplasty in rats

HRV parameters	Control data	Postoperative period					
		1 day	2 day	3 day	4 day	5 day	6 day
SDNN (ms)	4,76±0,24	4,52±0,25	5,27±0,26	5,1±0,15	4,01±0,26	4,21±0,28	4,41±0,15
rMSSD (ms)	3,96±0,22	4,28±0,34	3,36±0,35	2,94±0,17	2,73±0,25	2,91±0,26	3,41±0,33
SDNN/ rMSSD (ms)	1,2±0,11	1,06±0,11	1,57±0,14	1,73±0,14	1,47±0,13	1,45±0,11	1,29±0,11
Total power (ms2)	27,19±2,95	19,14±2,06	18,49±3,09	24,96±3,23	15,08±3,37	16,75±2,67	18±2,27

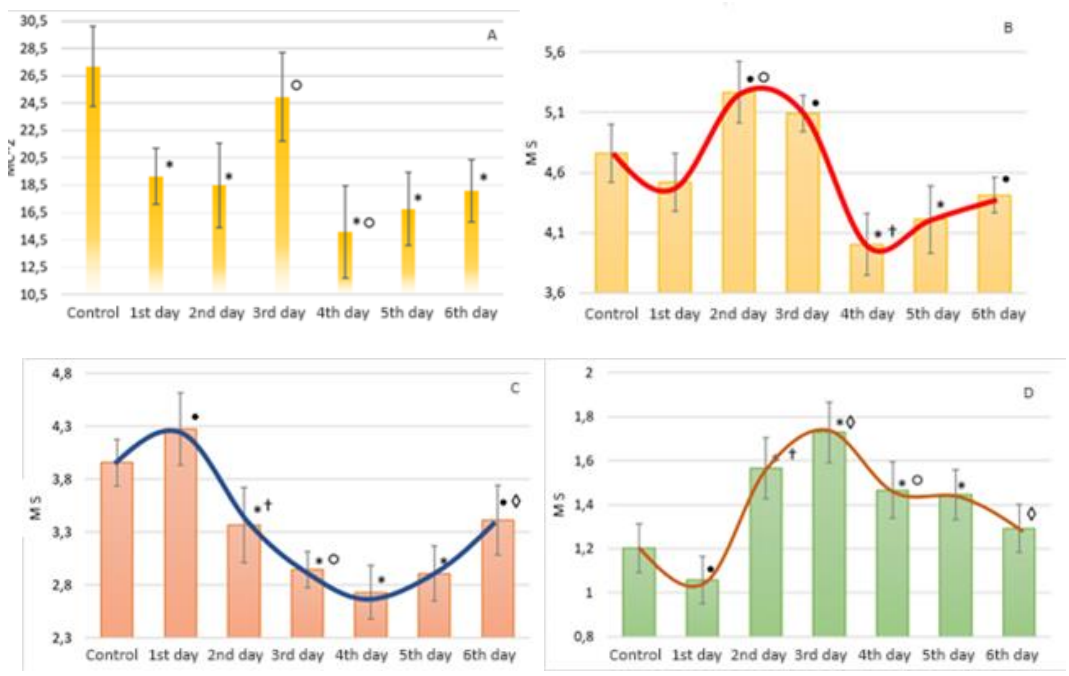

Figure 4. Changes in HRV after modeling septoplasty in the time spectrum: a-standard deviation of R-R intervals (SDNN) between normal QRS complexes; b-rMSSD (the square root of the sum of the squares of the difference in values of consecutive pairs of normal R-R intervals); c – the ratio STDNN/rMSSD; d – total power. Note: * - significant difference between preoperative data (control) and postoperative data at p<0.001; ● - significant difference between preoperative data (control) and postoperative data at p<0.01; † - significant difference between follow – up periods after surgery at p<0.001; o – significant difference between follow-up periods after surgery at p<0.01; ◊ - significant difference between follow-up periods after surgery at p<0.05.

4.2. Corticosterone

According to the Wilcoxon test, at the time of septoplasty modeling and throughout the entire postoperative period, the concentration of corticosterone in the blood plasma of rats was significantly higher than before it (p<0.001). The maximum level of the hormone of the adrenal cortex was noted at the time of the operation itself; a day later its concentration decreased significantly (p<0.001), and from the 2nd to the 4th postoperative day its plateau was determined (Fig. 3.6). But

from the 5th day, the concentration of corticosterone in the blood plasma in rats continued to decrease ($p<0.01$) (Table 2).

Table 2. Corticosterone concentration values in rats after septoplasty simulation.

	control	operation	1 day	2 day	3 day	4 day	5 day	6 day
ng/ ml	38,57±2 ,12	195,77±4, 43	159,87± 7,89	121,05±6,7 5	122,55±5, 38	118,4±5, 7	102,7±5, 3	61,7±4, 46

5. Discussion.

SDNN represents rapid changes associated with parasympathetic activity. Although SDNN is considered to be a measure of overall HRV power and is sensitive to both sympathetic and parasympathetic input, it is, however, more reflective of parasympathetic tone [14, 15]. Low overall HRV, defined by low SDNN values, reflects decreased parasympathetic and/or increased sympathetic activity [16]. Thus, it was previously shown that an increase in SDNN values corresponded to high activity of the vagus nerve [17]. It is known that SDNN corresponds to the high-frequency component of the HRV frequency domain and characterizes vagal activity [18]. After septoplasty, an increase in SDNN occurred on days 2-3, which corresponded to an increase in plasma corticosterone levels in rats. Consequently, sympathicotonia was observed during this period, since it is known that an increase in the level of glucocorticoids in the blood plasma under conditions of acute or chronic stress occurs against the background of sympathicotonia [19], but against the background of depletion of the sympathoadrenal system under conditions of desynchronosis, its level may decrease [20]. However, on days 1 and 4-6 after surgery, the power of SDNN was either equal to or lower than control data against the background of a persistent increase in the concentration of corticosterone levels in the blood of animals. It can be concluded that, indeed, both the sympathetic and parasympathetic nervous systems contribute to changes in SDNN, and SDNN in some cases cannot be interpreted unambiguously.

RMSSD characterizes the activity of the parasympathetic division of the ANS [21], and it correlates well with the high-frequency component (HF) of the frequency domain of HRV [22]. In our study, the highest rMSSD values were observed 1 day after surgery, which can be explained by a disruption of normal adaptive processes, since under normal stress conditions the tone of the sympathetic nervous system prevails, along with activation of the hypothalamic-pituitary-adrenal axis [23]. These results are consistent with a drop in the overall power of HRV in the first two days after surgery, which may also indicate a breakdown in adaptive reactions in response to damage to the nasal septum and subsequent sensory deprivation of the peripheral part of the olfactory analyzer [5].

The ratio of SDNN to rMSSD can characterize vagosympathetic balance and is quite consistent with LF/HF (the ratio of the low-frequency component to the high-frequency component of the HRV frequency spectrum or the vagosipathic index) [24]. Moreover, in the absence of differences in SDNN and rMSSD, SDNN/rMSSD may show a difference between study groups [24]. For example, if SDNN/RMSSD is an appropriate expression of LF/HF, higher SDNN/RMSSD, for example in fibromyalgia, compared with healthy controls, characterizes a shift in the balance of the ANS towards the sympathetic component, which is consistent with other studies [25, 26]. Changes in SDNN/rMSSD confirm the idea that on the first day after septoplasty modeling in rats, disadaptation reactions develop, which are manifested by an increase in the activity of the parasympathetic nervous system against the background of an increase in corticosterone, as well as a decrease in the activity of rats in the open field [4, 6], and in the subsequent postoperative period, the body's response to surgical stress is characterized by an increase in the activity of the sympathetic nervous system with an increase in total power in the period 2-4 days, with a peak on the third day, which coincides with the maximum changes in the cytoarchitecture of the pyramidal layer of the hippocampus in almost all of its subfields [7-9], as well as with the formation of a "plateau" on the graph of corticosterone concentration (Fig. 5).

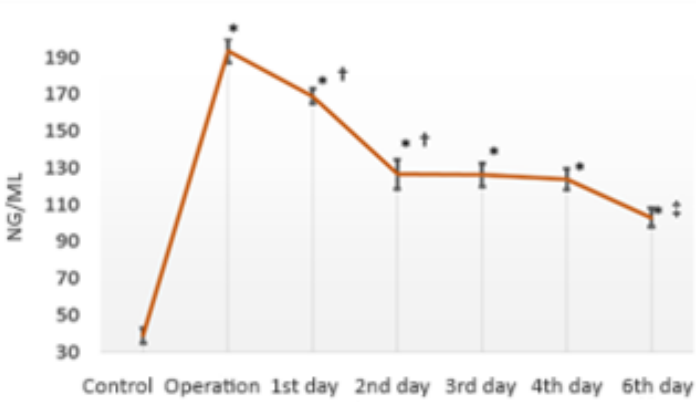

Figure 5. Dynamics of changes in the concentration of corticosterone in blood plasma in rats before and after the simulation of septoplasty. Note: * - significant differences between preoperative data (control) and postoperative data at p<0.001; † - significant difference between postoperative follow-up periods at p<0.001; ‡ – significant difference between postoperative follow-up periods at p<0.01.

6. Conclusions

The concentration of corticosterone in the blood plasma, SDNN/rMSSD and the total power of HRV most accurately characterize the developing responses of the body under conditions of surgical stress when modeling septoplasty in biological objects. Thus, modeling septoplasty in rats leads to the development of disadaptive processes on the first day, followed by normalization of adaptive processes in the period from the second to the fourth postoperative days.

Informed Consent Statement: Informed consent was obtained from all subjects involved in the study.

Conflicts of Interest: The authors declare no conflict of interest.

References

1. Pustovit OM, Nasedkin AN, Egorov VI, Isaev VM, Isaev EV, Morozov II. The impact of ultrasonic cavitation and photochromotherapy on the process of repair of the nasal mucosa after septoplasty and submucosal vasotomy of the inferior turbinates. Head and neck Russian Journal. 2018;6(2):20–26
2. Van Egmond MMHT, Rovers MM, Hannink G, Hendriks CTM, van Heerbeek N Septoplasty with or without concurrent turbinate surgery versus non-surgical management for nasal obstruction in adults with a deviated septum: a pragmatic, randomized controlled trial. The Lancet. 2019; 394(10195): 314-321
3. Siegel NS, Gliklich RE, Taghizadeh F, Chang Y Outcomes of septoplasty. Journal of Otolaryngology - Head & Neck Surgery. 2000; 122(2): 228–32
4. Kastyro IV, Reshetov IV, Popadyuk VI, Torshin VI, Ermakova NV, Karpukhina OV, Inozemtsev AN, Khamidulin GV, Shmaevsky PEE, Sardarov GG, Gordeev DV, Skopich AA Study of the physiological effects of a new model of septoplasty in rats. Head and neck. Russian Journal. 2020;8(2):33-38
5. Torshin V, Kastyro I, Kostyaeva M, Popadyuk V, Ermakova N, Surovtsev V, Gushchina Y, Kovalenko A The effect of destruction of the mucous membrane of the olfactory zone of the nasal septum on the cytoarchitectonics of the pyramidal layer of the hippocampus. Virchows Archiv. 2020; 477 (1): 340
6. Kastyro IV, Reshetov IV, Khamidulin GV, Shmaevsky PE, Karpukhina OV, Inozemtsev AN, Torshin VI, Ermakova NV, Popadyuk VI The Effect of Surgical Trauma in the Nasal Cavity on the Behavior in the Open Field and the Autonomic Nervous System of Rats Journal of Biochemistry and Biophysics. 2020; 492: 121–123.
7. Torshin VI, Kastyro IV, Kostyaeva MG, Eremina IZ, Ermakova NV, Khamidulin GV, Shevtsova SN, Tsaturova IA, Skopich AA, Popadyuk VI The influence of experimental modeling of septoplasty on the cytoarchitecture of the hippocampus in rats. Head and neck. Russian Journal. 2019;7(4):33–41.
8. IV Kastyro, MG Kostyaeva, VI Torshin, IZ Eremina, NV Ermakova, GV Khamidulin, TK Fatkhudinov, YuSh Gushchina, VV Surovtsev, GA Drozdova. Studying the effect of stress on morphological changes in the hippocampus during surgical interventions in the nasal area. Journal of Morphology. 2019, 156(4): 25-34
9. Kastyro IV, Reshetov IV, Khamidulin GV, Shilin SS, Torshin VI, Kostyaeva MG, Popadyuk VI, Yunusov TY, Shmaevsky PE, Shalamov KP, Kupryakova AD, Doroginskaya ES, Sedelnikova AD. Influence of Surgical Trauma in the Nasal Cavity on the Expression of p53 Protein in the Hippocampus of Rats. Journal of Biochemistry and Biophysics. 2021; 497:99–103.
10. Popadyuk VI, Ilyinskaya MV, Shevelev OA, Kastyro IV Intensity of acute pain and changes in heart rate variability during tonsillectomy. Effective pharmacotherapy. Journal of Pulmonology and otorhinolaryngology. 2017; 2(14): 14-18
11. Baevsky RM, Ivanov GG, Chireikin LV, Gavrilushkin AP, Dovgalevsky PYa, Kukushkin YuA, Mironova TF, Prilutsky DA, Semenov AV, Fedorov VF, Fleishman AN, Medvedev MM Analysis of heart rate variability using various electrocardiographic systems (part 1). Bulletin of Arrhythmology. 2002; 24:65-87
12. Selyatitskaya VG Adrenocortical system activity in alloxan-resistant and alloxan-susceptible Wistar rats / VG Selyatitskaya, NA Palchikova, NV Kuznetsova. Journal of Diabetes Mellitus. 2012; 2(2): 165–169.

13. Palchikova NA, Kuznetsova NV, Selyatitskaya VG Glucocorticoid function of the adrenal cortex of rats with streptozotocin diabetes in the dynamics of taking mifepristone per os. Fundamental research. 2014; 8-1: 100-104
14. Reyes del Paso GA, Langewitz W, Mulder LJM, Van Roon A, Duschek S The utility of low frequency heart rate variability as an index of sympathetic cardiac tone: a review with emphasis on a reanalysis of previous studies. Journal of Psychophysiology. 2013; 50: 477–87.
15. Koenig J, Thayer JF Sex differences in healthy human heart rate variability: a meta-analysis. Neuroscience & Biobehavioral Reviews. 2016; 64:288–310.
16. Karri J, Zhang L, Li S, Chen YT, Stampas A, Li S Heart Rate Variability: A Novel Modality for Diagnosing Neuropathic Pain after Spinal Cord Injury. Journal of Frontier Physiology 2017; 8:495.
17. Patural H, Pichot V, Flori S, Giraud A, Franco P, Pladys P, Beuchée A, Roche F, Barthelemy JC Autonomic maturation from birth to 2 years: normative values. Heliyon journal. 2019; 5:01300.
18. Silva CC, Bertollo M, Reichert FF, Boullosa DA, Nakamura FY Reliability of heart rate variability in children: influence of sex and body position during data collection. Journal of Pediatric Exercises. Sci. 2017; 29(2):228-236
19. Valentino RJ, Foote SL, Aston-Jones G Corticotropin-releasing factor activates noradrenergic neurons of the locus coeruleus. Journal of brain research. 1983; 2 (270): 363–367.
20. Gostyukhina AA, Samoshchina TA, Chaitsev KV, Gutor SS, Zhukova OB, Svetlik MV, Abdulkina NG, Saytsev AA Adaptive reactions of rats after light desynchronosis and physical fatigue. Journal of Bulletin of Siberian Medicine. 2018; 17 (3): 22–34.
21. Järvelin-Pasanen S, Sinikallio S, Tarvainen MP Heart rate variability and occupational stress – systematic review. Journal of Industrial Health. 2018; 56:500–511
22. Sztajzel J Heart rate variability: a noninvasive electrocardiographic method to measure the autonomic nervous system. Swiss Medical Weekly. 2004; 134:514–522
23. Desborough JP The response stress to trauma and surgery. The British Journal of Anaethesia. 2000; 85(1): 109-17.
24. Kang JH, Kim JK, Hong SH, Lee CH, Choi BY Heart Rate Variability for Quantification of Autonomic Dysfunction in Fibromyalgia. Annals of Rehabilitation Medicine. 2016; 40(2): 301–309
25. Pagani M, Lombardi F, Guzzetti S, Sandrone G, Rimoldi O, Malfatto G Power spectral density of heart rate variability as an index of sympatho-vagal interaction in normal and hypertensive subjects. Journal of Hypertension 1984; 2: 383–385;
26. Malliani A, Pagani M, Lombardi F, Cerutti S Cardiovascular neural regulation explored in the frequency domain. Journal of Circulation. 1991; 84:482-492

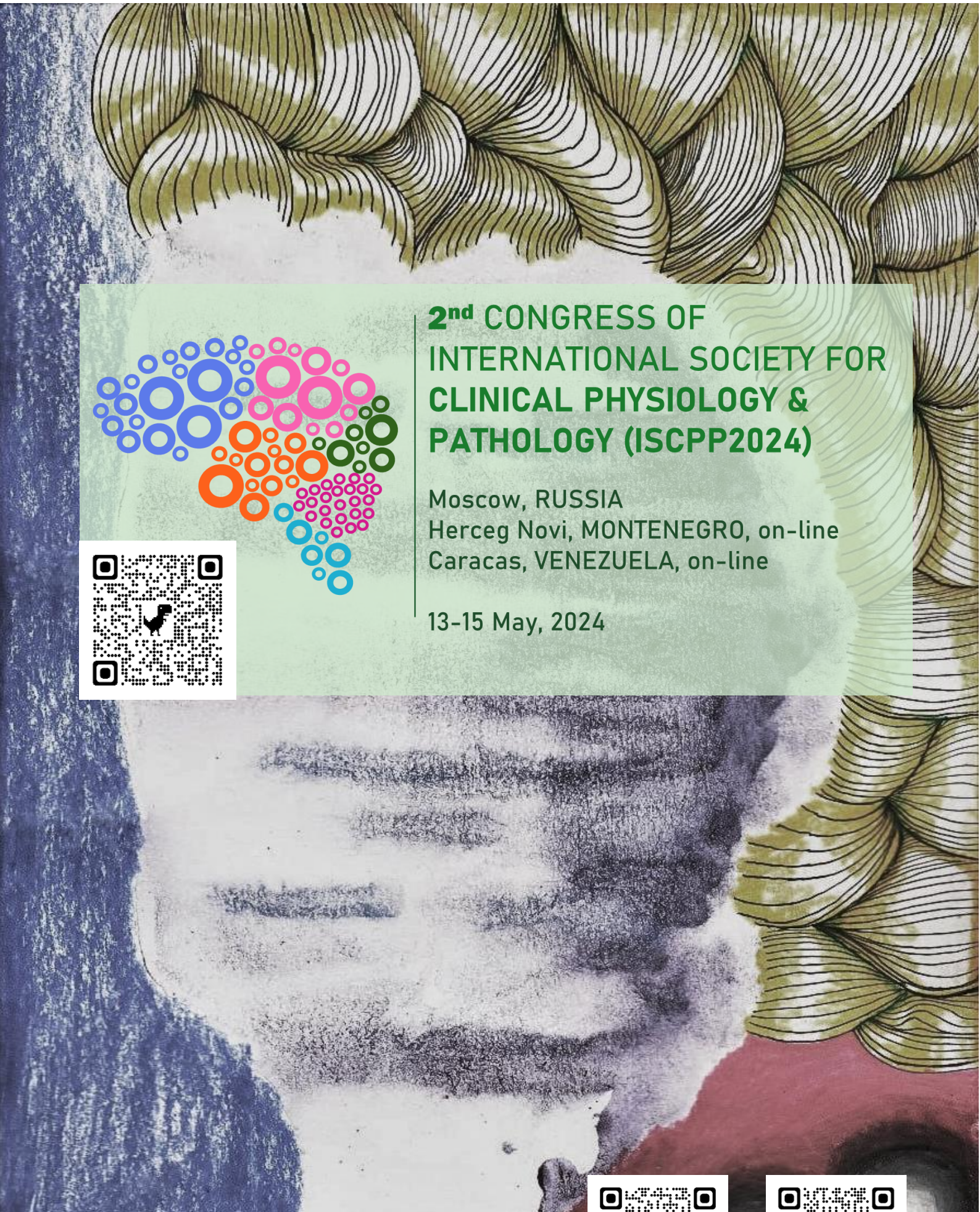
2nd CONGRESS OF
INTERNATIONAL SOCIETY FOR
CLINICAL PHYSIOLOGY &
PATHOLOGY (ISCPP2024)
Moscow, RUSSIA
Herceg Novi, MONTENEGRO, on-line
Caracas, VENEZUELA, on-line
13-15 May, 2024